Alma Mater Studiorum – Università di Bologna

DOTTORATO di RICERCA in

Biologia Cellulare e Molecolare

Ciclo XXXIII

Settore Concorsuale di Afferenza: 05/E2 - BIOLOGIA MOLECOLARE

Settore Scientifico Disciplinare: BIO/11 - BIOLOGIA MOLECOLARE

TITOLO TESI:

TAZ role in lung cancer: resistance to BET inhibitors and functional interaction with lncRNA

Presentata da: Giulia Gobbi

Coordinatore del Dottorato

Giovanni Capranico

Supervisore

Alessia Ciarrocchi

Co-supervisori

Davide Carlo Ambrosetti

Valentina Sancisi

Esame finale 2021

INDEX

2

ABSTRACT

Lung cancer is the main cause of cancer related mortality worldwide, with an overall five years survival of 17.4%. Despite the enormous progresses made in diagnosis and therapy, including the introduction of innovative drugs as target therapy and immunotherapy, the prognosis for patients remain poor. In most cases, the success of pharmacological treatment is impaired by drug resistance. Thus, the characterization of both response mechanisms to anti-cancer compounds and of the molecular mechanisms supporting lung cancer aggressiveness are crucial to ensure the most appropriate management for patients. In the first part of this thesis, we successfully characterized the molecular mechanism behind resistance of lung cancer cells to the Inhibitors of the Bromodomain and Extraterminal domain containing Proteins (BETi). In particular, through a CRISPR/Cas9 screening in non-small cell lung cancer cell line, we identified three Hippo Pathway members, LATS2, TAOK1 and NF2 as genes implicated in susceptibility to BETi. We observed that these genes confer sensitivity to these drugs, inhibiting TAZ effector activity by restraining its nuclear localization. Conversely, we observed that the overexpression of TAZ increases resistance to these drugs. TAZ and YAP are two transcriptional coactivators that, forming complexes with TEADs and SMADs transcription factors, enhance a gene expression program promoting pro-oncogenic cells features. Moreover, we also displayed that BETi downregulate the expression of both YAP, TAZ and TEADs in several cancer cell lines, including breast, thyroid, melanoma and prostate, implying a novel mechanism through which these drugs exert citotoxic anti-cancer effects.

In the second part of this work, we attempted to characterize the molecular crosstalk between the TAZ gene and its cognate antisense long-non coding RNA (lncRNA) TAZ-AS202 in lung tumorigenesis. LncRNAs are transcripts lacking protein-coding potential and with tissue and cell-specific expression patterns. These molecules play a role during cancer development and progression, holding the potential to become significant biomarkers and specific therapeutic targets. However, the landscape of lncRNAs and their specific role during lung tumorigenesis are far to be fully characterized. We showed that as for TAZ downregulation, silencing of TAZ-AS202 impairs NSCLC cells proliferation, migration and invasion ability, suggesting a pro-tumorigenic function for this lncRNA during lung tumorigenesis. TAZ-AS202 regulates TAZ main target genes without altering the expression or the localization of TAZ. This finding implies an uncovered functional cooperation between TAZ and TAZ-AS202 in the regulation of target genes. In addition, we found that the EPH-ephrin signaling receptor EPHB2 is a downstream effector significantly affected by both TAZ and TAZ-AS202 silencing.

Moreover, we assessed the role of EPHB2 in lung cancer cells. EPHB2 downregulation significantly attenuates cells proliferation, migration and invasion ability, suggesting that at least in part, TAZ-AS202 and TAZ pro-oncogenic activity in lung cancer depends on EPH-ephrin signaling final deregulation. Finally, we started to dissect the mechanism underlying the TAZ-AS202 regulatory activity on EPHB2 in lung cancer, which may involve the existence of an intermediate transcription factor and is the object of our ongoing research.

INTRODUCTION

Lung Cancer

Lung cancer represents the most frequent neoplastic disease diagnosed worldwide **(fig.1,2)**. It is responsible for 1.8 million deaths every year all over the world (*Teixtera Loiola de Alencar et al, 2020)*. This disease mostly affects older people, with rare cases in patients younger than 45. The incidence of lung cancer varies by geographic area, age, sex and tobacco

Figure 1

exposure; although 10-25% of lung cancer cases occur in patients who have never smoked. In addition, other risk factors are associated with lung cancer development, including air pollution, pulmonary diseases, carcinogenic chemicals and ionizing radiation exposure (*Teixtera Loiola de Alencar et al, 2020; Wong et al, 2017*). Lung cancer can be divided into two main histopathological subtypes: Non-Small Cell Lung Cancer (NSCLC), which account for about 80% of all cases, and Small Cell Lung Cancer (SCLC), which shows neuroendocrine differentiation and accounts for the remaining 20% of cases **(fig.2A)**. NSCLC can be further divided in three subgroups: Squamous Cell Carcinoma (SSC), Adenocarcinoma (AD) and Large Cell Carcinoma (LCC) **(fig.2B)**.
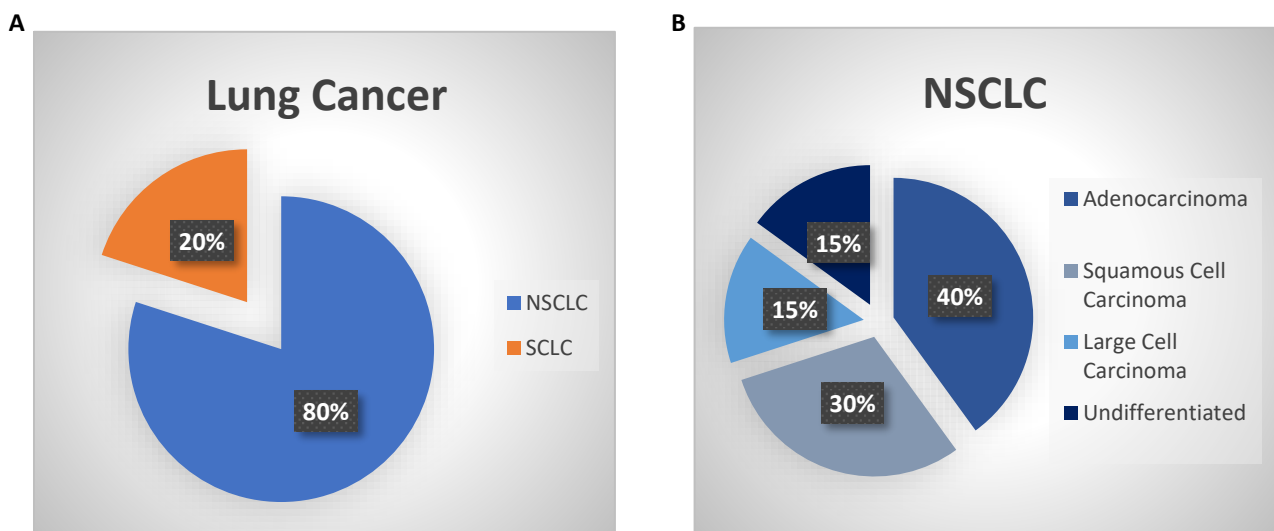
Figure 2

Figure 2: **A)** Frequencies of the two main subtypes of Lung Cancer on total cases. **B)** Schematic representation of the main subtypes of NSCLC: Adenocarcinoma represents the subtype with higher incidence in the population.

Tumour histotypes generally follow a proximal-to-distal distribution pattern moving from the trachea to the alveoli: SCC, SCLC and AD. It is thought that different tumour histotypes arise from distinct cells of origin, localised within a defined regional compartment and microenvironment *(Sutherland et al, 2010)*. In addition, different tumour histotypes are associated with specific molecular landscapes (*Zito Marino et al, 2019; Varella-Garcia, 2010)*. In the last years, the possibility to better describe patient's diseases and the advances in cancer genomics, have given the opportunity to understand driver molecular alterations responsible for tumour progression for each tumour histotype and to design tailored therapeutics in some cases.

Non-Small Cell Lung Cancer (NSCLC)

NSCLC represents 80% of all lung cancer cases. It is divided in three subgroups, of which AD represents the 40% of cases **(fig.2A-B)**. Molecular landscape of NSCLC is very heterogeneous, with genetic aberrations including mutations, gene fusions and copy number alterations (*Zito Marino et al, 2019; Varella-Garcia, 2010)***.** This subtype of lung cancer is less sensitive to chemotherapy than SCLC. However, several patients with NSCLC carry druggable driver molecular alterations, leading to the development of target therapy strategies for these patients. For example, patients who carry rearrangements involving ALK (Anaplastic Lymphoma Receptor Tyrosine Kinase) or ROS1 (ROS proto-oncogene 1), activating mutations in EGFR (Epidermal Growth Factor Receptor) or in BRAF (Serine/Threonine Protein Kisase B-Raf) show profound benefits with kinase-inhibitors therapy *(Zito Marino et al, 2019; Varella-Garcia, 2010; Rotow et al, 2017)*. In addition, the introduction of immunotherapy, inhibiting the immunosuppressive receptors CTLA-4 (Cytotoxic T-Lymphocyte Associated Protein 4) or PD-1 (Programmed Cell Death 1), has been a major advance for the treatment of this disease *(Lim et al, 2020)***.** 20-30% of patients with NSCLC carry activating mutations in KRAS (Kirsten Rat Sarcoma Viral Proto-Oncogene) *(Cancer Genome Atlas Network, 2014)*. KRAS aberrant activation leads to unrestrained signalling of pro-oncogenic downstream pathways, such as RAF/MAPK, PI3K/AKT and RAL-GEF/RAL. Until recently, patients with KRAS activating mutations had no therapeutic opportunities except chemotherapy. Today, small molecules inhibiting KRAS are in clinical trials *(McCormick et al, 2015; Hallin, J. et al, 2020)***.** However, patients not carrying targetable alterations or KRAS mutations are still those with less therapeutic opportunities, relying on standard chemotherapy. The evolution of target therapy and immunotherapy has profoundly changed the panorama of the treatment of lung cancer, considerably reducing the use of conventional cytotoxic chemotherapy. However, despite early remission of disease and

improvement of outcome, patient's prognosis remains poor, with an overall five years survival of 17,8%, mainly due to drug resistance (*Wong, M. et al, 2017*). Thus, developing novel therapeutic strategies and, simultaneously, defining molecular mechanisms underlying drug resistance are issues of great importance to improve management of lung cancer patients. Moreover, searching for novel biomarkers associated with NSCLC aggressiveness is still a major challenge and is fundamental to develop new tools useful to define patient's prognosis.

BET-proteins and BRD4

BET proteins (Mammalian Bromodomain and Extraterminal domain family) consist of four proteins named BRD2, BRD3, BRD4 and BRDT **(fig.3)** *(Basheer et al, 2015*). BRD2, BRD3 and BRD4 are ubiquitously expressed while BRDT is mainly expressed in testes *(Belkina et al, 2012)*.

Figure 3
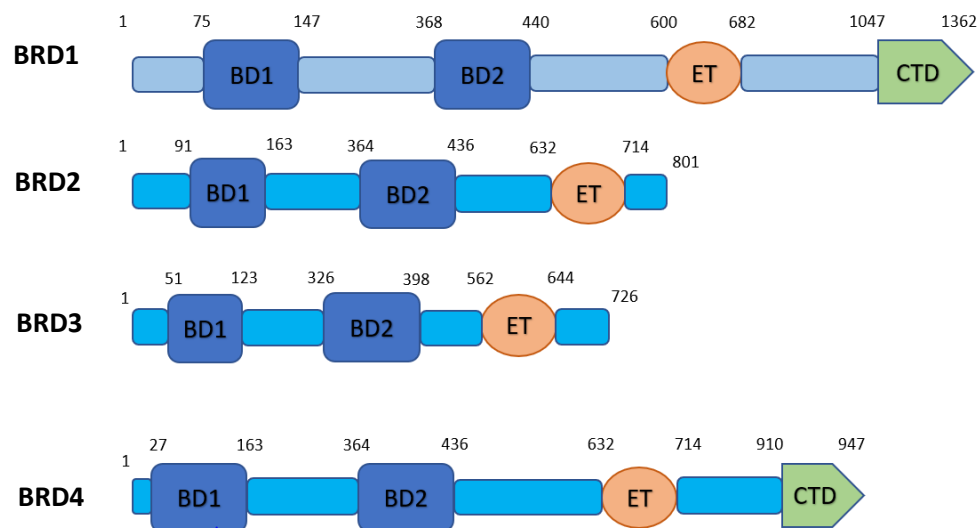
Figure 3: BET proteins structure. BRD4 and other members of BET bromodomain proteins are shown. The numbers indicate amino acids positions. BD: bromodomain; ET: Extraterminal domain; CTD: C-Terminal domain. *This figure is modified from Basheer et al, 2015.*

All proteins of this family contain two bromodomains (BD1 and BD2, BDs), interacting with acetylated peptides and a conserved extraterminal (ET) domain, enhancing protein-protein interactions **(fig.3)**. All these proteins can have overlapping or distinct functions in biological processes depending on context *(Belkina et al, 2012; Roberts T. C. et al, 2017; Xu Y & Vakoc C. R., 2017)*.

Bromodomain-containing protein 4 (BRD4), the best characterized BET protein **(fig.4)**, is a co-transcriptional activator which interacts with acetylated lysines on histones through its BDs *(Basheer F. et al, 2015)*. Acetylated histones, such as H3 acetylated on lysine 27 (H3K27Ac) or lysine 9 (H3K9Ac), are generally enriched on promoters and enhancers of transcribed genes, marking open chromatin *(Basheer F. et al, 2015; Igolkina AA. Et al, 2019)*. The presence of multiple acetylated residues contributes to BRD4 recruitment to enhancers and promoters of genes, enhancing coding and non-coding
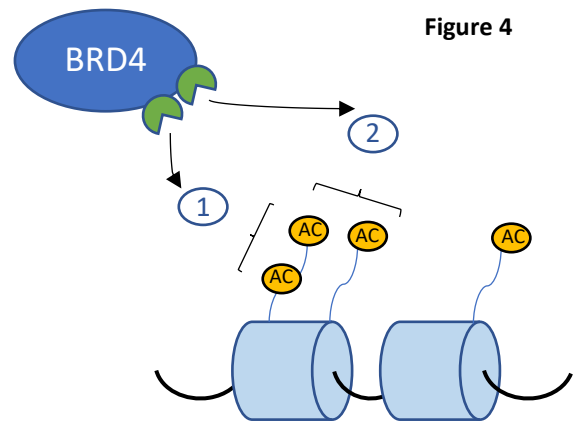
Figure 4

Figure 4: Schematic representation of BRD4 interaction with acetylated histones. 1 and 2 represent the two bromodomain of the protein. *This figure is modified from from Basheer F. et al, 2015*

genes transcription through well characterized molecular mechanisms **(fig.5)**. In the conventional model, promoters and enhancers are physically brought in contact by multi-protein complexes including BRD4, leading to interaction between enhancers-associated transcriptional factors and Transcriptional Starting Sites (TSS) of genes, stimulating transcription beginning. BRD4 is a key element in governing chromatin structure and in bringing together distant regulatory elements (*Wu, S.Y. & Chiang, C.M.,2007; Donati, B. et al, 2018).* BRD4 is also a crucial player in stimulating proficient transcription, working as an adaptor to recruit the elongation factor P-TEFb and Mediator complex, leading to RNA-Pol II phosphorylation on serine 2 and release from pausing near the TSS *(Patel, M. C. et al, 2013).* In addition, BRD4 itself has been shown to have kinase activity, directly phosphorylating RNA-Pol II on serine 2 *(Devaiah et al, 2012).* In 2014, another mechanism has been described, in which BRD4 functions as histone chaperon assisting the progression of the active transcriptional complexes within the gene body *(Kanno, T. et al, 2014).* All these mechanisms can cooperate to direct and enhance transcription of genes involved in pro-oncogenic pathways **(fig.5)**.

Figure 5
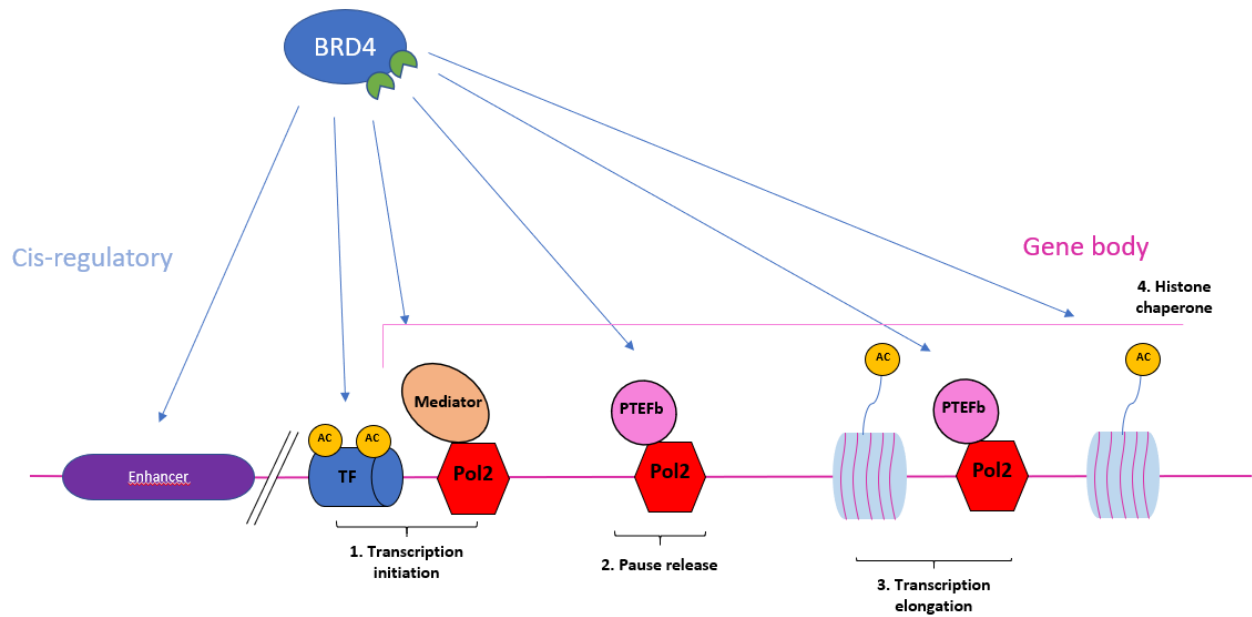
Figure 5: Scheme illustrating the multitude of BRD4 roles in the regulation of gene expression: BRD4 directly regulates transcription interacting with acetylated histones tails and physically bringing in contact promoters and enhancers of expressed genes. Moreover, BRD4 is involved in 1) Initiating transcription through the recruitment of transcription factors and mediator complex on promoter genes, 2) Releasing Pol2 from proximal promoter pausing, 3) elongating transcription and 4) chaperoning RNA Pol2 through hyperacetylated histone tails within gene body. The image is modified from *from Basheer F et al, 2015*

BRD4 activity is particularly relevant in cancer since it controls the expression of well-known oncogenes to which cancer cells are addicted, including BCL2, WNT5A, RUNX2, KIT, FOSL1 and MYC *(Donati, B. et al, 2018; Dawson, M. et al, 2011; Lockwood, W.W. et al, 2012; Loven, J. et al, 2013; Sancisi, V. et al, 2017).* This activity provided the rationale for the development of BET proteins inhibitors which, blocking the expression of key oncogenes, counteract cancer progression *(Donati B et al, 2018; Dowson, M et al, 2011; Lockwood W.W. et al, 2012; Loven, J et al, 2013; Zhao, Y. et al, 2016; Fu, L.L. et al, 2015*).

BET-Inhibitors

BET-Inhibitors (BETi) are epigenetic drugs, consisting in small molecules (including JQ1, OTX015, TEN-010 and CPI-0610) that compete with acetylated lysines on histones for the binding to BET proteins. These drugs cause BET proteins dissociation from chromatin, leading to target genes downregulation. It has been demonstrated that treatment with BETi induces cancer cells proliferation block, apoptosis and differentiation *(Shimamura, T. et al, 2013; Gao, Z et al, 2018)*, due to repression of key oncogenes **(fig.6).**

Figure 6
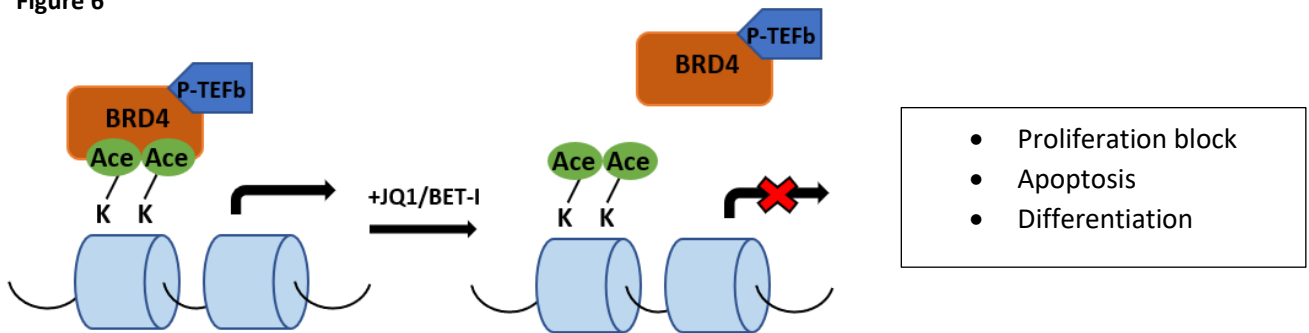
Figure 6: Image showing the molecular mechanism of BETi activity: BETi compete with acetylated histones for BRD4 binding. Treatment with BETi inhibits BRD4 interaction with acetylated histones tails and causes the consequent downregulation of target genes, leading to proliferation block, apoptosis and differentiation.

The promising efficacy of BETi on preclinical models provided the rationale to include these drugs in clinical trials for hematologic and solid neoplastic diseases, including lung cancer *(Xu, Y. & Vakoc, C.R. et al, 2017; Manzotti, G. et al, 2019).* Unfortunately, BETi showed limited efficacy as single-agent therapy in unselected groups of patients affected by solid tumors *(Postel-Vinay, S. et al, 2019)*. These findings indicate the need to unravel mechanisms of resistance to BETi, in order to identify predictive biomarkers of response that can help the selection of patients in future studies. Moreover, wider knowledge on BETi mechanism of action could lay the basis for the use of these drugs in combination with other anti-cancer compounds, with the aim to generate more durable patients' responses.

Hippo Pathway

Hippo Pathway is a universal regulator of organ size, tissue homeostasis and regeneration. It has been identified in *Drosophila* through genetic screenings for tumor suppressor genes *(Wu, S. et al, 2003);* however, most of recent studies focused attention on the role of this pathway in mammals **(fig.7)**. The core of Hippo pathway, in mammals, is a kinase cascade in which MST1/2 (Ste20-like Kinases-1/2), homologs of the Drosophila Hippo [Hpo]), binds to SAV1 (Salvador Homolog 1), forming an active complex that phosphorylates and activate LATS1/2 (Large Tumor Suppressor-1/2), homologs of Drosophila Warts [Wts]) *(Chan, E.H.Y.*

Figure 7

Hippo Pathway

Figure 7: Scheme representing Hippo Pathway core components in *Drosophila* (on the left) and in mammals (on the right). MST1/2 kinase (homolog of the *Drosophila* Hippo) bind to SAV1 and phosphorylates and activates LATS1/2 (homolog of the *Drosophila* Warts). Phosphorylated LATS1/2 interact with MOB1/A and phosphorylates the two final effectors YAP and TAZ (homologs of *Drosophila* Yorkie). phosphorylated YAP and TAZ are inactivated and accumulated in cytosol, with the consequent loss of their pro-oncogenic transcriptional activity.

et al, 2005). Activated LATS1/2 form a complex with MOB1A/B (Mob Kinase Activator 1A and 1B) and, in turn, phosphorylates the two final effectors of the Hippo Pathway: YAP (Yes-associated protein) and TAZ (transcriptional coactivator with PDZ-binding motif); two homologs of *Drosophila* Yorkie [Yki]), on specific serine (S) residues (S127 on YAP and S89 on YAP) **(fig.7)** *(Meng, Z et al, 2016; Zheng, Y. & Pan, D. 2019).* Phosphorylated YAP and TAZ are recognized by 14–3-3 proteins, sequestered within the cytoplasm and/or degraded by the proteasome, with consequent loss of transcription activating functions**.** Conversely, when Hippo Pathway is inactive, unphosphorylated YAP and TAZ entry in the nucleus and associate with specific transcription factors, activating and/or enhancing gene transcription *(Meng, Z et al, 2016; Zheng, Y. & Pan, D. 2019; Varelas, X. et al, 2008; Vassilev, A. et al, 2001).* LATS1/2, MST1/2, SAV1 and MOB1A/B represent the core of Hippo pathway; however, other proteins and signals participate in YAP/TAZ regulation. NF2 (Neurofibromin 2) is a plasma membrane associated protein, interacting with LATS1/2 and physically positioning LATS1/2 for being phosphorylated by MST1/2 *(Yin, F. et al, 2013).* TAOK genes (Thousand And One Amino Acid Protein Kinases) (TAOK1/2/3) phosphorylate and activate MST1/2 but also LATS1/2 through MST1/2 independent mechanisms *(Plouffe, S. W. et al, 2016).* Angiomotin family members AMOT (Angiomotin) and AMOTL1/2 (Angiomotin like 1 and 2) are able to bind and

activate NF2**,** which in turn positively regulates LATS1/2 *(Plouffe, S. W. et al, 2016; Li, Y. et al, 2015).* Angiomotin proteins also bind LATS1/2 and promote their kinase activity and YAP phosphorylation, functioning as scaffolds that connect LATS1/2 to both MST1 and YAP *(Li, Y. et al, 2015).* RASSF1A is another modulator of Hippo signalling, acting upstream of MST1/2 *(Plouffe, S. W. et al, 2016).*

YAP and TAZ

YAP and TAZ transcriptional cofactors are the two downstream effectors of Hippo pathway. Hippo signalling inactivation causes YAP and TAZ nuclear translocation and the activation of a specific gene expression program, controlling both normal tissues homeostasis and cancer initiation and progression. These two transcriptional cofactors lack DNA-binding domains, requiring the association with other transcriptional factors in the cell nucleus to direct and enhance transcription of specific genes **(fig.7)**.

Figure 8
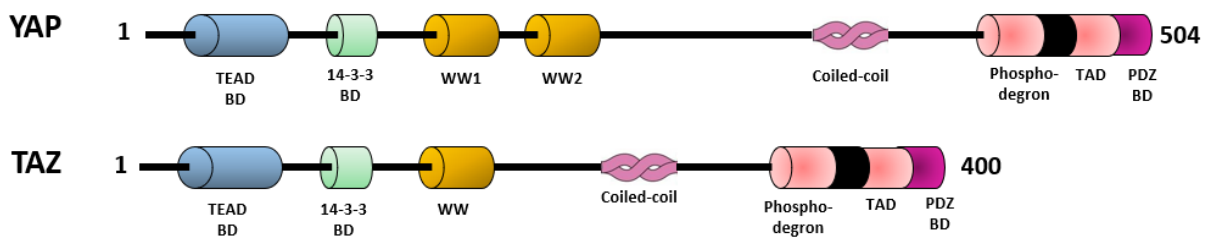
Figure 8: Scheme representing domains of the Hippo pathway effectors YAP and TAZ. Main regions include: TEADs binding domain (TEAD BD), 14-3-3 binding domain (14-3-3 BD), the WW domains (two for YAP and one for TAZ), the transcriptional activation domain (TAD) and the PDZ-binding domain.

Fig.8 reports the main functional domain of the two cofactors. WW domains are mediators of protein-protein interactions and are responsible of YAP/TAZ binding to a number of regulatory proteins and transcription factors, including LATS1/S, AMOTs, SMADs (Mothers Against DPP Homolog) and RUNXs (Runt-Related Transcription Factors). On the contrary, the interaction with transcription factors of the TEAD family (TEA domain transcription factors) is supported by the TEAD binding domain. The 14-3-3 binding domain comprises the serine that is the main target of LATS1/2 phosphorylation (S89 for TAZ and S127 for YAP) and mediates cytoplasmic retention through binding to proteins of 14-3-3 family. Both YAP and TAZ show a C-terminal phosphodegron (S381 for YAP and S311 for TAZ), mediating β-TrCP (beta-transducin repeat containing gene) recognition when phosphorylated and promoting proteasomal degradation. TAZ shows an additional N-terminal phosphodegron, comprising serines 58/62. Both proteins carry a coiled-coil domain, mediating heterodimerization between YAP and TAZ and a C-terminal transactivation domain, essential for transcription activation *(Reggiani et al, 2020).*

Besides TEADs and SMADs, other nuclear factors associate with YAP and TAZ and regulate their activity. For example, AP1 factor is known to interact with YAP/TAZ/TEAD complex to enhance the expression of target genes (*Zanconato, F. et al, 2015*). TBX5 (T-box transcription factor 5), member of T-box family of transcription factors, associates with β-catenin and YAP, thus resulting in survival and transformation of beta-catenin-active cancer cells (*Rosenbluh, J. at al, 2012*). On the contrary, association with other players induces YAP/TAZ inhibition. ARID1A (AT-rich interaction domain 1A) promotes the association between YAP/TAZ and the SWI/SNF complex. This interaction is regulated by cellular mechano-transduction and is predominant in cells with low mechanical signalling. At high levels of mechanical stress, ARID1A is sequestered by F-actin, in favour of an association between TEAD and YAP/TAZ (*Chang, L. et al, 2018*). TIAM1 (T Cell Lymphoma Invasion And Metastasis 1) suppresses the association between YAP/TAZ and TEADs, thus inhibiting YAP/TAZ pro-oncogenic program (*Diamantopoulou, Z. et al, 2017*). As emerging significant player, the VGLL4 protein (Vestigial Like Family Member 4) was shown to be a natural antagonist of YAP: VGLL4 competes with TEADs for YAP/TAZ binding, thus inhibiting YAP/TAZ/TEAD complex transcriptional activity (*Jiao, S. et al, 2014*).

YAP and TAZ are involved in various aspects of embryogenesis, physiology and control of organ growth, being considered as master regulators of processes involved in the correct development. During lung organogenesis, YAP and TAZ are crucial regulators of cell proliferation, differentiation and lineage specification. Homozygous YAP KO causes developmental arrest around E8.5, with yolk sac vasculogenesis defects and abnormalities in the embryonic axis, while conditional deficiency of YAP leads to defective development or homeostasis in various tissues. TAZ KO mouse are viable but show kidney disease and lung emphysema (*Morin-Kensicki, et al,2006; Hossain, Z. et al, 2007; Makita, R. et al, 2008; Lin, C. et al, 2017*). On the contrary, high levels of YAP/TAZ generally promote stemness and inhibit differentiation. During lung development, the epithelial expression of YAP and TAZ is sequentially required for correct organ formation (*Isago, H. et al, 2020*). In some organs, like heart, liver and intestine, increased expression of YAP/TAZ leads to increased organ size (*Varelas, X.; 2014; Gise, A. von et al, 2012; Camargo, F.D. et al, 2007*). On contrary, during heart development, loss of both TAZ and YAP impairs cardiomyocyte proliferation by increasing cells apoptosis (*Varelas, X., 2014*). In other organs, like pancreas, breast, salivary glands and kidney, the correct expression of YAP and TAZ and the correct balance between the two paralogues are required for normal differentiation (*Varelas, X., 2014; Chen, Q. et al, 2014*). Further, during osteogenesis, YAP and TAZ exert combinatorial roles by regulating bone formation, remodeling and matrix mechanical

properties and their KO causes skeletal defects *(Kegelman, C.D. et al, 2018)*. The role of YAP and TAZ has also been studied in nervous system, where YAP reduced levels impair the number of neuroepithelial cells, while increased YAP/TEAD activity drives the expansion of these cells *(Cao, X. et al, 2008)*.

Pathways converging on YAP/TAZ regulation

Besides Hippo signalling, multiple different proteins and pathways converge on YAP/TAZ final regulation; some of these directly controlling YAP/TAZ activity, while others controlling MST/LATS activation. Both YAP and TAZ show a tyrosine residue that can be phosphorylated by c-ABL (Abelson Murine Leukemia Viral Oncogene Homolog)**,** c-YES (YES Proto-Oncogene 1, Src Family Tyrosine Kinase) and SRC (SRC Proto-Oncogene, Non-Receptor Tyrosine Kinase) *(Jang, E. J. et al. 2012; Levy et al, 2008; Zaidi, S.K. et al, 2004)***.** Additionally, TAZ is phosphorylated by GSK3B (glycogen synthase kinase 3B) in specific serines *(Huang, W. et al 2012).* Furthermore, TAZ and YAP phosphorylation mediated by LATS1 and LATS2, allows subsequent CK1 (Casein Kinase 1) phosphorylation. GSK3B and CK1-dependent phosphorylation recruit β-TrPC to enhance TAZ and YAP degradation *(Liu, C.Y. et al, 2010; Zhao, B. et al, 2010).*

The complex interplay between YAP/TAZ and WNT-signalling has been extensively explored: WNT signal is able to inhibit GSK3B, thus resulting in TAZ and β−catenin increased levels and nuclear activity. In the absence of WNT, YAP and TAZ take part in the β-catenin destruction complex, stimulating β-catenin degradation and inhibiting its nuclear translocation. In the presence of WNT, YAP and TAZ are displaced from this complex and translocated into the nucleus where they activate WNT/YAP/TAZ downstream biological functions *(Azzolin, L. et al,2014).* Moreover, an alternative WNT-signalling converges on LATS1/2 to activate YAP and TAZ. This alternative WNT-signalling consists on Wnt-FZD/ROR-Ga12/13-Rho-Lats1/2-YAP/TAZ-TEAD *(Park, H.W. et al, 2015).*

YAP and TAZ are also important mediators of the biological effects observed in response to mechanical cues. The sensing and the translation of mechanical and cytoskeletal forces (cell shape changing, ECM elasticity and intracellular tension) into biochemical signals, involves the activation of genes and signalling cascades controlled by YAP and TAZ activity. It was shown that YAP and TAZ are nuclear and active under experimental mechanical conditions favouring high intracellular resisting forces and they are cytoplasmic and inactive under low contractile forces *(Dasgupta, I. & McCollum, D. 2019; Halder, G. et al, 2012)*. Furthermore, the activity and the localization of TAZ and YAP is also regulated by metabolic pathways as mevalonate pathway, glycolysis and nutrient-sensing pathways. Some of the intermediates of the mevalonate pathway generate protein prenylation,

facilitating protein attachment to cell membranes. Protein prenylation is an important mechanism governing YAP/TAZ regulation, bringing out mevalonate pathway as fundamental regulator of YAP/TAZ activity *(Sorrentino, G. et al, 2014; Koo, J.H. & Guan, K.L. et al, 2018).* In addition, the removal of glucose in culture medium has been shown to increase TAZ/YAP phosphorylation and cytoplasmic localization and glycolysis inhibition induced dramatic TAZ/YAP phosphorylation and inactivation. Finally, fatty acids, GPCR ligands, phospholipids, glucagon and epinephrine receptors are able to participate to TAZ and YAP activation (*Koo, J.H. & Guan, K.L. et al, 2018).*

In summary, multiple extra-cellular signalling and intra-cellular pathways converge on YAP and TAZ regulation, through the balance of their nucleo-cytoplasmic shuttling and the definition of their overall nuclear amount and transcriptional activity.

YAP and TAZ role in tumorigenesis

Recently, several works show that the aberrant activity of TAZ and YAP is associated with tumor initiation and progression, despite only rare mutations in upstream Hippo genes have been discovered (*Zanconato, F. et al, 2015; Zanconato, F. et al, 2016).* Increased activity of YAP and TAZ, has been associated with several cancer cells features, including stemness, aggressiveness, migration, metastasis potential and EMT *(Basu-Roy, U. et al, 2015; Li, J. et al, 2019; Shao, D. D. et al, 2014; Park, J. et al, 2019).* In particular, TAZ activity is required for the maintenance and self-renewal in breast and head and neck carcinoma, while in glioblastoma and osteosarcoma the stemness phenotype is sustained by YAP activation (*Basu-Roy, U. et al, 2015; Li J., Zhongwu L. et al, 2019*). The overexpression of TAZ and YAP is associated with poorer outcome and cell differentiation in hepatocellular and cholangiocarcinoma *(Patel, S.H. et al, 2017; Xu, M.Z. et al 2009)*. Both YAP and TAZ correlates with lung cancer metastasis and progression. In NSCLC patients, their expression is associated with tumor grade and metastasis, while, in xenograft models derived from NSCLC cell line A549, their downregulation attenuates tumor formation *(Lau, A.N. et al, 2014; Lo Sardo et al. 2018; Noguchi, S et al, 2014)*. Their aberrant expression is associated with lymph node and brain metastasis in NSCLC *(Su, L.L. et al, 2012; Hsu, P.C. et al, 2018)*. Moreover, SCLC cell lines with poor neuroendocrine differentiation, show relatively high TAZ and YAP expression and a non-adherent cell morphology *(Horie, M et al, 2016)*. These findings suggest that the potential evolution of drugs against YAP and TAZ may be a promising therapeutic choice to counteract cancer progression.

To date, several strategies have been pursued for the inhibition of TAZ and YAP activity. In 2012, verteporfin was identified as a small molecule able to disrupt the interaction between YAP and TEADs *(Liu-Chittenden, Y. et al, 2012; Wang, C. et al, 2016)*. Furthermore, peptides mimicking VGLL4 (Vestigial Like Family Member 4) functions have been proposed to antagonize YAP activity *(Jiao, S. et al, 2014)*. Similarly, in 2015, YAP-like peptides have been developed to disrupt YAP-TEAD complexes and to reduce tumor progression *(Zhou, Z. et al, 2015)*. Statins were shown to prevent TAZ/YAP nuclear accumulation through the inhibition of the enzyme of the mevalonate pathway HMG-CoA reductase *(Sorrentino, G. et al, 2014)*. Finally, given that TEADs activity depends on its palmitoylation, developing inhibitors of palmitoylation is a novel potential therapeutic strategy to counteract YAP/TAZ/TEADs program *(Chan, P. et al, 2016; Kim, N.G. & Gumbiner, B.M. et al, 2019)*.

Even if until recently YAP and TAZ were considered as functionally redundant in cellular functions, a great amount of literature is emerging considering YAP and TAZ as 'non identical twins', from embryogenesis to cancer development and progression. These studies highlight that structural differences, differential splicing regulation and post-translation modifications in YAP and TAZ, supporting the interaction with different transcriptional factors and the existance of differential regulatory mechanism, finally generating divergent transcriptional programs *(Reggiani, F. et al, 2020)*. These studies, still to be further explored, are of a great importance when considering YAP and TAZ as possible targets for the development of specific anti-cancer compounds and when considering YAP and TAZ as biomarkers for cancer progression and patient's prognosis.

YAP and TAZ and cancer drug resistance

The interest regarding YAP and TAZ role in tumorigenesis is also due to their participation to resistance to most anti-cancer drugs used in clinical practice, making them responsible, at least in part, of patient's therapy failure *(Reggiani et al, 2020)*. Mounting evidences indicate that signalling upstream of YAP and TAZ are important in the response to chemotherapy *(Ren, A. et al, 2008; Zhao, Y. et al,2014; Zhao, Y. & Yang, X., 2015)*. TAZ-TEAD complex is an important modulator of taxol resistance in breast cancer by positively regulating its main effectors Cyr61 (Cysteine Rich Angiogenic Inducer 61) and CTGF (Connective Tissue Growth Factor) and TAZ increased expression is responsible for doxorubicin resistance *(Bartucci, M. et al, 2015)*. TAZ is also implicated in taxol, gemcitabine and anti-tubulin drugs resistance in various cancer settings (*Zhao, Y. & Yang, X., 2015; Xu, W. et al, 2017; Zhan, T. et al, 2018*). YAP is involved in chemotherapy resistance as well. YAP

participates to taxol resistance in colorectal cancer, to 5-Fluorouracile (5FU) resistance in colon and esophageal carcinoma and to anti-tubulin drugs resistance (*Zhao, Y. et al,2014; Touil, Y. et al, 2014; Song, S. et al, 2015*). In addition, TAZ and YAP promote resistance to targeted therapy. TAZ is associated with EGFR-inhibitor (EGFRi) resistance in NSCLC and in TNBC (Triple negative breast cancer) *(Xu, W. et al, 2015; Guo, L. et al, 2016)*. YAP is associated with resistance to cetuximab in colorectal cancer *(Lee, K.W. et al, 2015)* and to EGFRi in NSCLC where its expression also associates with worst prognosis *(Lee, J.E. et al, 2016; Hsu, P.C. et al, 2016; Hong, S.A. et al, 2018; Lee, T.F. et al, 2018)*. In addition, YAP is associated with resistance to sorafenib in hepatocellular carcinoma *(Gao, J. et al, 2019)*, to PI3K/mTOR inhibitors and to cell cycle kinase WEE1-inhibitor in ovarian cancer *(Muranen, T. et al, 2016: Oku, Y. et al, 2018)*. Both YAP and TAZ participates to BRAF-inhibitors resistance in melanoma patients *(Lin, L. et al, 2015; Kim, M.H. et al, 2016),* to Cycline dependent kinase 4/6 (CDK4/6)-inhibitors resistance and Receptor Tyrosine-Protein Kinase ErbB-2 (HER2)-inhibitors resistance in breast cancer *(Li, Z. et al, 2018; Liu, L. et al, 2009)*. Finally, YAP and TAZ activity also participate to hormone therapy resistance *(Liu, J. et al, 2019; Guo, Y. et al, 2017)* in breast and prostate cancer.

Long non-coding RNAs

High-throughput genomic projects such as FANTOM and ENCODE revealed that about 75% of human genome is transcribed and over 50000 loci transcribe long non coding RNAs (lncRNAs), outnumbering coding transcripts *(Djebali S. et al, 2012; Iyer, M.K. et al, 2015)*. LncRNAs are RNA molecules longer than 200 nt that do not code for proteins. They comprise an heterogeneous class of intragenic and intergenic transcripts such as enhancer RNAs (eRNAs) and sense or antisense transcripts that may or not overlap with coding genes *(St Lauren, G. et al, 2015; Ulitsky, I. et al, 2016; Hon, C.C. et al, 2017)*. LncRNAs have been implicated in many biological processes, such as: 1) regulation of transcription *in cis* or *in trans*, 2) modulation of mRNA processing, post-transcriptional control, proteins activity regulation and localization, 3) organization of nuclear domains and chromatin dynamics, 4) regulation of miRNA activity *(Rinn, J.L. & Chang, H.Y.; 2012; Dykes, I.M. & Emanueli C.; 2017; Peng, W.X. et al, 2017).* Besides their role in physiological cellular processes, lncRNAs are abundantly expressed and their de-regulated expression is associated to tumorigenesis, aggressiveness, metastasis and tumor stage in a variety of cancer settings *(Vitiello, M. et al, 2015; Khandelwal, A. et al, 2015).* In addition, they show a specific tissue/cancer expression and can be detected also in blood and/or urine. Thus, lncRNAs can be considered as novel biomarkers to predict

tumor stage, metastasis, aggressiveness and patient's prognosis and, in future, may be considered also therapeutic targets for cancer treatment.

Natural Antisense Transcripts (NATs)

A particular class of lncRNAs are the Natural Antisense Transcripts (NATs). These lncRNAs are transcribed from the opposite DNA strand of protein coding genes and can be alternatively located within gene promoters, gene body or at the end of genes, thus resulting in a possible overlap between sense and antisense RNAs. NATs are abundantly present in the human genome and, although they may have also other functions, are known to regulate neighboring genes *in cis* through different mechanisms. In particular, transcription collision, RNA-DNA interactions, chromatin alteration, RNA-duplex formation, alternative splicing and termination, RNA transport and editing and protein translation regulation are the main mechanisms through which NATs modulate the expression of neighboring genes *in cis (Faghini, M.A. et al 2009).* For example, the lncRNA GAS6-AS1 is able to promote cell proliferation, migration and invasion both in vitro and in vivo controlling the expression of GAS6 (Growth Arrest Specific 6) neighboring gene both at transcriptional and translational level *(Zhang, P. et al, 2019).* The lncRNA FOXC2-AS1 forms an RNA-RNA duplex with its cognate FOXC2 (Forkhead Box C2) gene, necessary for FOXC2-AS1-mediated FOXC2 regulation *(Zhang, C.L. et al, 2017).* In lung cancer, the lncRNA FAM83A-AS1 promote cells proliferation and invasion through the regulation of FAM83A (Family With Sequence Similarity 83, Member G) cognate gene *(Shi, R. et al, 2019).* The lncRNA TMPO-AS1 is overexpressed in NSCLC cells and tissues and correlates with the expression of TMPO (Thymopoietin) cognate gene. TMPO-AS1 main function is to regulate the stability of TMPO RNA *(Qin, Z. et al, 2019).* The lncRNA AFAP1-AS1 is upregulated in NSCLC where promotes cells migration and proliferation through AFAP1 (Actin Filament Associated Protein 1) expression regulation *(He, J. et al, 2018).*

LncRNAs in Lung Cancer

The role of several lncRNAs has been characterized in NSCLC, even if a complete comprehension of the molecular mechanisms behind their functions is not available. They can act either as tumor suppressors or oncogenes and their dysregulation is associated with tumor cell growth, invasion, migration, apoptosis and metastasis *(Roth, A. & Diederichs, S. 2016).* In addition, given their role in pathophysiological pathways, they are gaining increasing attention as novel potential anti-cancer drugs targets *(Zhang, Y. & Tang, L.; 2018).*

The lncRNAs **HOTAIR** (HOX Transcript Antisense Intergenic RNA), **MALAT1** (Metastasis-Associated Lung Adenocarcinoma Transcript 1), **H19** and **PVT1** (Plasmacytoma Variant Translocation 1) are examples of important players in lung cancer, being all upregulated and promoting growth, invasion and proliferation of NSCLC cells.

HOTAIR has been reported to have increased expression in lung cancer tissues compared to adjacent normal tissues and its expression correlates with advanced pathological stage and lymph node metastasis *(Liu, X. et al, 2013)*. HOTAIR main function is to modulate the cancer epigenome, through binding with different histone modification complexes and, thus, changing the chromatin status to modify gene expression. HOTAIR-dependent reprogramming of gene expression leads to enhanced proliferation, aggressiveness, metastasis and drug resistance.

MALAT1 has been associated with high metastatic potential and poor NSCLC patient's prognosis *(Ji, P. et al, 2003).* This lncRNA is widely expressed in normal tissue but is upregulated in prostate, breast, lung, colon, liver and uterus tumors. MALAT1 overexpression promotes lung cancer metastasis, while its downregulation has the opposite effect *(Tang, Y. et al, 2018).* In addition, MALAT1 promotes EMT of lung adenocarcinoma cells by controlling SLUG expression by competing for mir-204 and MALAT1-induced EMT is required for efficient brain metastasis *(Li, J. et al, 2016; Shen, L. et al, 2015).*

H19 is upregulated during embryogenesis and downregulated in adult tissues. Like other players important during embryonic development, H19 is upregulated in cancer tissues, including lung, gastric, colorectal and breast cancer *(Peng, F. et al, 2017; Wu, K.F. et al, 2017; Cui, J. et al, 2015; Hashad, D. et al, 2016)*. In lung adenocarcinoma, H19 expression correlates with TNM stage and metastasis and patient's carrying H19 upregulation show worse cisplatin response *(Wang, Q. et al, 2017)*. There are several different molecular mechanisms through which H19 exerts its functions. In particular, the exon 1 of H19 is reported to generate two microRNA: miR-675-5p and miR-675-3p. Furthermore, H19 is able to regulate the expression of target genes by influencing methylation processes, through the recruitment of epigenetic regulatory factors on chromatin *(Alipoor, B. et al, 2020)*

**PVT1** is highly expressed in lung cancer tissue compared with normal tissues *(Huang, C. et al, 2016; Cui, D. et al, 2016)*. Silencing this lncRNA results in lung cancer cells proliferation block and enhanced apoptosis. Moreover, Increased PVT1 expression has been associated with increased tumor size and poor overall survival in lung cancer patients. Two molecular mechanisms explaining PVT1 activity

have been described: 1) PVT1 binds EZH2, thus repressing the transcription of the onco-suppressor Hippo pathway protein LATS2 *(Wan, L. et al, 2016)* 2) PVT1 works as a sponge for miR-195, enhancing proliferation and reducing apoptosis and radio-sensitivity *(Wu, D. et al, 2017)*.

The established key roles of many lncRNAs in physiology and cancer, highlights the importance of characterizing novel lncRNAs that may be implicated in the regulation of relevant pathways in tumorigenesis.

EPH-Ephrin Signalling

EPH-ephrin signalling is a short distance cell-cell communication system generating a bidirectional signal in two cells upon binding between an EPH-receptor-expressing cell and an ephrin-ligand-expressing cell. There are two subfamilies of EPH receptors: EPHA and EPHB receptors, which are both implicated in disease and cancer *(Xi, H.Q. et al, 2012)*. In the human genome, there are 9 EPHA receptors which bind 5 ephrin-A ligands and 5 EPHB receptors, which bind 3 ephrin-B ligands. Ephrin ligands are divided in glycosylphosphatidylinositol (GPI)-linked ephrin-A and transmembrane ephrin-B classes, based on their modality of association to cell membrane and on differential affinity
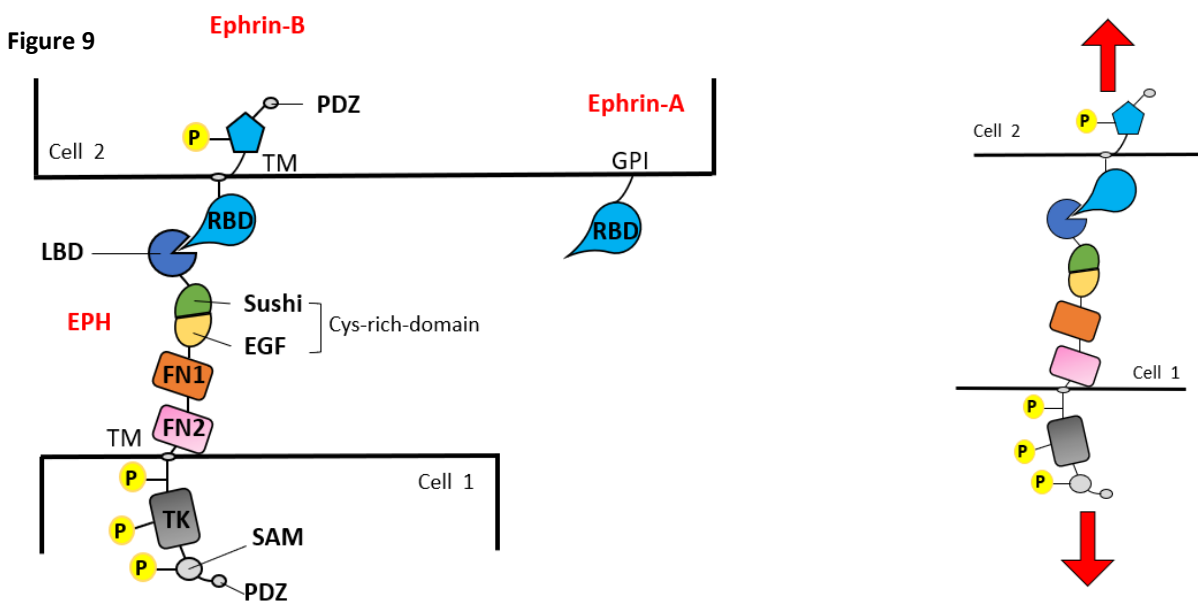
Figure 9: **A)** Image representing the structural domain of EPH receptors and ephrin ligands and their positioning on cell surface. Eph-ephrin signaling relies on specific functional domains present in Ephs and ephrins proteins. Eph receptors are composed of a ligand-binding domain (LBD), which binds the receptor-binding domain (RBD) of ephrins. The LBD domain is linked to a Cys-rich domain, formed by a Sushi and an Epidermal-growth factor (EGF)-like domain and two fibronectin (FN1 and FN2) domains. Moreover, the EPH receptor comprises a trasmembrane region (TM) and am intracellular region, formed by a Tyr kinase domain (TK), a sterile alpha motif (SAM) and a PDZ binding domain. Ephrins are divided into A and B classes: class A is linked to the membrane via a glycosylphosphatidylinositol (GPI) linkage, whereas B class has a transmembrane domain and an intracellular PDZ binding domain. **B)** EPH-ephrin signaling can occur in various modes, depending on context and on the direction of the signal. In the figure, is reported the classical model of EPHB/ephrin B bi-directional signaling, where EPH-ephrin binding results in the phosphorylation of the intracellular domain of both EPH receptor and ephrin ligand, resulting in the activation of a response in both cells and in the final repulsion of cells. *These images are modified from Kania, A. & Klein, R., 2016.*

for the EPHA or EPHB classes of receptors *(Pasquale E.B. et al, 2010; Campbell T.N. et al, 2008)* (**fig. 9A-B**).

In the classic model of EPHB/ephrinB interaction, transmembrane or membrane-associated ephrins act as ligands for EPH receptors located on the membrane of neighbouring cells (**fig. 9B**). To elicit robust Eph receptor signaling, ephrins and receptors are presented as clusters on cells membranes *(Davis, S. et al, 1994)*. Upon binding, the kinase activity of EPH receptor is activated, resulting in the autophosphorylation of EPH juxtamembrane tyrosine residues and the activation of forward signaling. On the other cell, the phosphorylation of the intracellular domain of ephrin ligand by intracellular kinases is the event that initiates the reverse signaling. Once intracellular signaling is initiated, ephrins and EPH receptors dissociate, through proteolytic cleavage or complexes internalization by endocytotic vesicles *(Zimmer, M. et al, 2003; Wilkinson, D.G., 2003; Lin, K.T. et al, 2008)*. EPH-ephrin signal transduction comprises the activation of intracellular proteins, including Src family kinase, Vav2, Vav3, Nck1, Nck2 and PI3K. In turn, these effectors are coupled with Rho GTPase such as Rac1 and RhoA which can modulate and rearrange actin cytoskeleton, thus resulting in cell repulsion *(Kania, A. & Klein, R.; 2016)*. The EPH and ephrin families exert a fundamental role during embryogenesis, allowing processes as neurogenesis, synaptogenesis, axon guidance, tissue separation and boundary formation, blood and lymphatic vessel development and organ size determination. They also control processes important during adulthood, as cell-cell adhesion, cell proliferation and cell migration *(Kania, A. & Klein, R.; 2016)*. In addition, multiple EPH receptors and ephrin ligands are deregulated in cancer tissues and tumor microenvironment, influencing tumor properties by the enhancement of aberrant cell-cell communication within cells and between tumor compartments *(Castano, J. et al, 2008; Surawska, H. et al, 2004; Chen, J. et al, 2015; Ireton, R.C. & Chen, J. et al, 2005; Noren, N.K. et al, 2007; Gao, Q. et al, 2014; Sato, S. et al, 2019; Zhao, C. et al, 2017)*. Different EPH receptors and ephrins show contrasting behavior in cancers, displaying both anti – and pro-oncogenic properties. While the pro-oncogenic role of EPHA receptors has been established, being overexpressed in melanoma, glioma, prostate, breast, ovarian, lung, esophageal, gastric, cervical and bladder cancer *(Ireton, R.C. & Cheng; 2005; Day, B.W. et al, 2013; Vail, M.E. et al, 2014)*, a double tumor-promoting and suppressive role has been reported for EPHB receptors, depending on cancer context and, sometimes, on different stage of the same cancer *(Solanas, G & Batlle, E., 2011)*. For example, EPHB2 expression suppresses tumor growth in prostate cancer *(Huusko, P. et al, 2004)* and its downregulation correlates with poor prognosis in colorectal cancer patients *(Guo, D.L. et al, 2006; Jubb, A.M. et al, 2005; Cortina C. et al, 2007)*. On the contrary, in lung cancer, EPHB2 expression is associated with worse prognosis *(Zhao, C. et al, 2017)*, even if a

complete understanding of the molecular mechanism of EPHB2 regulation and activity in different settings remains elusive. Despite this complexity, the location of EPH receptors on cell surface make these proteins promising candidates for therapeutic intervention in cancer and their molecular structure make them accessible to be targeted by various molecules *(Janes, P.W. et al, 2020)*. To date, clinical trials with molecules against EPHA and molecules targeting all EPH receptors are available for glioblastoma, glioma and different solid tumors *(http://www.clinicaltrial.gov)* However, the dissection of the signals regulating EPH receptors activation and their specific role in different cancer setting remain a major challenge to ensure the most appropriate management for patients.

PRELIMINARY DATA

Genome Scale CRISPR/Cas9 screening on A549 Lung Cancer cell line

Given the recent interest in BETi anti-cancer therapy, our laboratory previously performed a genome-scale CRISPR/Cas9 knockout screening in A549 NSCLC cell line with the aim of characterizing genes responsible for resistance and/or susceptibility to BETi treatment in lung cancer. A549 cells, previously engineered with stably expressing Cas9 (**fig.10A**), were infected with GeCKOv2 library *(Sanjana NE et al, 2014)* and treated with the pan-BETi JQ1 or vehicle (MOCK) and DNA was collected at three different time points (5, 9 and 14 days) (**fig.10B**). The frequency of each sgRNA in the GeCKOv2 library was assessed by amplification and deep sequencing of the library. The library is divided in two semi-libraries and each gene is targeted by 3 different sgRNAs per semi-libraries. With this method, we followed the contribution of 19050 genes and 1864 miRNAs in modulating JQ1 response in A549 lung cancer cell line. The sgRNAs we found depleted after JQ1 treatment are expected to target genes important for JQ1 resistance and the sgRNAs we found enriched after JQ1 treatment are expected to target genes important for JQ1 susceptibility. As seen in **fig.10C**, sgRNAs targeting 889 genes were enriched, whereas sgRNAs targeting 1134 genes were depleted in all MOCK samples, identifying genes that modulate proliferation in this cell line. SgRNAs targeting 952 genes were enriched, whereas sgRNAs targeting 682 genes were depleted in all JQ1-treated samples, indicating genes modulating JQ1 response. Intriguingly, the BTP/POZ domain protein SPOP was found to be among the 20 top hits of enriched genes at 9 and 14 days after JQ1 treatment. SPOP has been recently associated with JQ1 sensitivity in prostate and ovarian carcinoma *(Dai, X. et al, 2017; Janouskova H. et al, 2017)*, confirming the validity of the screening performed. Among the 20 top hits of genes enriched at 5, 9 and 14 days of JQ1 treatment, we found the sgRNAs targeting four genes belonging to the Hippo Pathway, LATS2, TAOK1, NF2 and AMOTL2 **(fig.10D-E)**, suggesting the involvement of Hippo Pathway in mediating BETi sensitivity in lung cancer. Interestingly, these four genes were found also enriched in MOCK samples, but their enrichment resulted higher in JQ1 treated samples, indicating that Hippo Pathway plays important role both in restraining cells proliferation and in mediating JQ1 sensitivity. These preliminary data suggest a relevant role for Hippo Pathway in lung cancer progression and in BETi response.

Figure 10
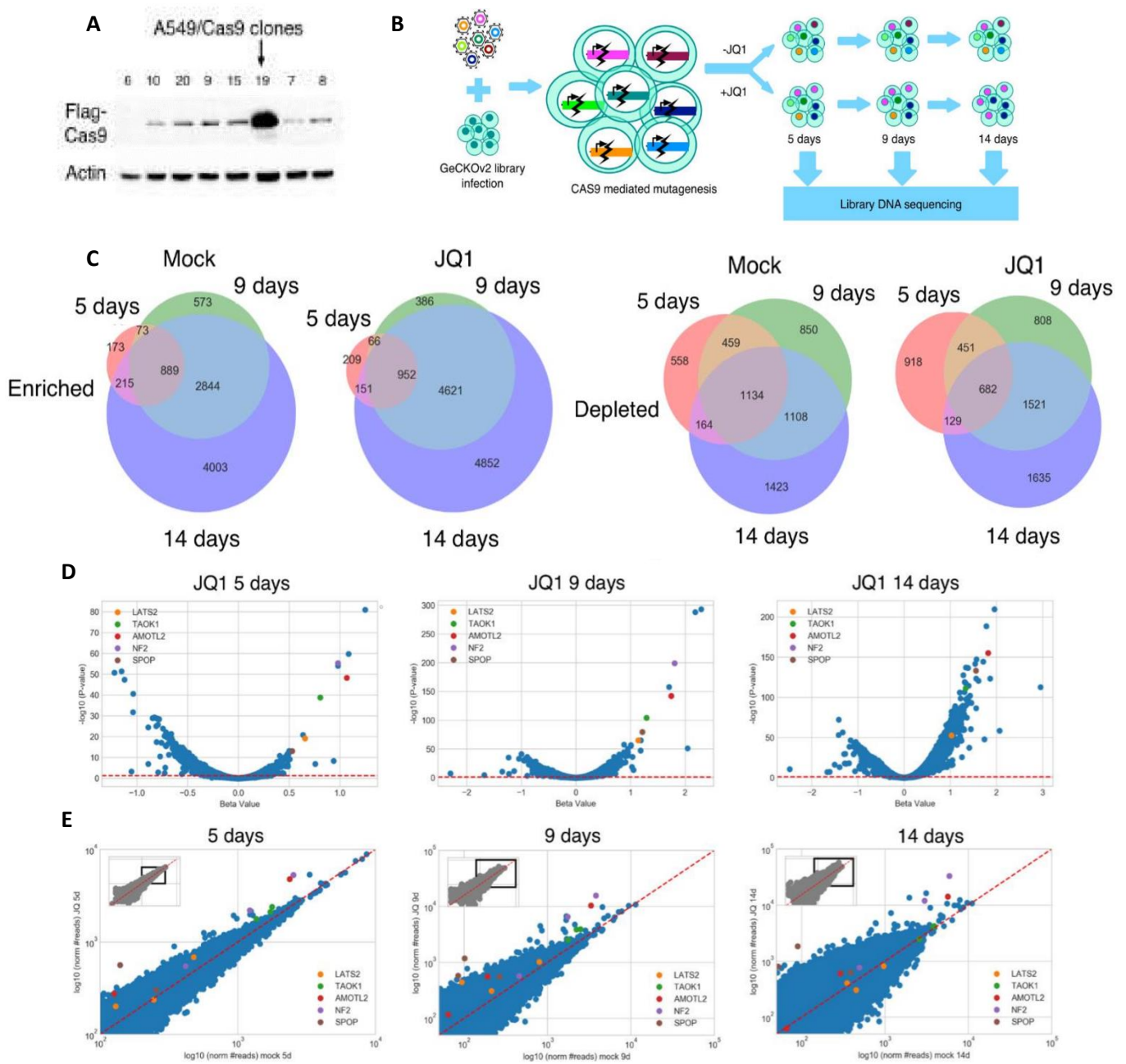
Figure 10: A) Western blot showing different A549/Cas9 clones with different levels of Cas9 expression. For the screening and the following experiments A549/Cas9 #19 was chosen. **B)** Graphic showing an overview of CRISPR/Cas9 screening. **C)** Venn diagrams showing the number of genes correspondent to enriched or depleted sgRNAs at each time point in library A. Volcano plot showing beta-value and FDR adjusted p-value distributions at the three different time points. **D)** Volcano plot showing beta-value and FDR adjusted p-value distributions at the three different time points. **E)** Scatter plot analysis showing normalized read counts (log scale) of JQ1 treated or DMSO treated samples (MOCK) at the three different time points. The sgRNAs targeting the selected enriched genes are highlighted with different colours. *These figures are from Gobbi et al, 2019.*

LncRNA TAZ-AS202 and TAZ-AS203

While TAZ is not required for normal tissue homeostasis in adults, numerous studies highlighted its pivotal role in lung tumor formation, survival, stemness, progression, metastasis and resistance to various anti-cancer compounds. As previously described, TAZ over-expression has been detected in about 66% of lung cancer patients. However, few mutations are present on TAZ or Hippo pathway genes, suggesting that other mechanisms regulate its expression and activity. We noticed that TAZ genomic locus comprises two uncharacterized antisense lncRNAs named TAZ-AS202 (1700 nt) and TAZ-AS203 (980 nt) (Gene ID:100128025, Transcript ID: ENST00000479752.1 and ENST00000495094.1 respectively) that share with the TAZ gene the same promoter region and are transcribed in antisense orientation (**fig.11**). Transcription of TAZ-AS203 initiates in the region of TAZ reference transcript exon 2, producing an RNA molecule partially overlapping with TAZ, whereas TAZ-AS202 does not overlap with TAZ reference transcript.

Figure 11
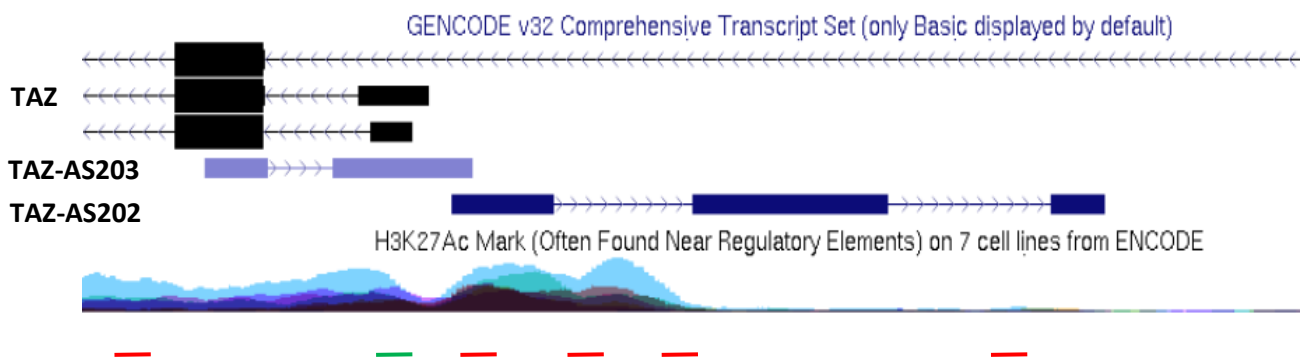
Figure 11: The image represents TAZ genomic locus obtained from Genome Browser. In black are reported the different annotated isoforms of the TAZ gene. In light blue is reported the lncRNA TAZ-AS203, 980 nt long and transcribed in antisense orientation compared to the TAZ gene. In dark blue is reported the lncRNA TAZ-AS202, 1700 nt long and transcribed in antisense orientation compared to the TAZ gene. The lines in red represent putative TEADs binding sites while the line in green represent a putative SMAD3 binding site obtained from JASPAR database.

To date, no literature is available concerning the role of TAZ-AS202 and TAZ-AS203 in physiology and cancers, except for one paper regarding TAZ-AS202 in head-neck squamous cell carcinoma *(Li, J. et al, 2019)*, linking the overexpression of TAZ-AS202 with TAZ overexpression and poor overall survival in patients. However, the biological function of these TAZ-associated lncRNAs remains elusive in lung cancer. Given the relevant role for NATs in the regulation of neighbouring gene *in cis*, our first hypothesis was that TAZ-AS202 and TAZ-AS203 may regulate the expression of TAZ in lung cancer and may be part of the TAZ pro-oncogenic program.

AIMS OF THE PROJECT

- Drug-resistance has been described as the main cause of therapeutic failure and tumor progression. This project aims to clarify the effect of the Hippo pathway members LATS2, TAOK1, NF2 and AMOTL2 in lung cancer response to anti-cancer drugs BETi.

- Given the established role of TAZ in lung tumorigenesis, the full characterization of the molecular mechanisms governing its expression and activity represents a major challenge. The presence of two uncharacterized lncRNAs that share with the TAZ gene the same promoter region, suggests that these molecules may take part in lung cancer progression through TAZ regulation. The second part of the project aims to characterize the role of TAZ-AS202 and TAZ-AS203 in lung cancer and to dissect the possible crosstalk with TAZ.

RESULTS:

Knockout of LATS2, TAOK1 and NF2 confers resistance to JQ1

The CRISPR/Cas9 screening described in the Preliminary Data section identified the Hippo pathway members LATS2, TAOK1, NF2 and AMOTL2 as susceptibility genes for JQ1. First, we validated the Hippo pathway genes as important for JQ1 susceptibility, generating single knockout (KO) of LATS2, TAOK1, NF2 and AMOTL2 in A549 cells stably expressing Cas9 and evaluating the response to JQ1 treatment. For each gene, we individually cloned three sgRNAs sequences derived from GeCKOv2 semi-library A in LentiGuide-Puro plasmid (from Addgene). We also cloned sgRNAs targeting SPOP as positive control and a non-targeting sgRNA (CT) as negative control. The viral surnatant for each sgRNA was infected in A549/Cas9 clone #19 cells **(fig.10A Preliminary data).** The Cas9-mediated mutagenesis of each locus was verified through '*ALTR genome editing detection kit*' (from IDT) on individual pools of transduced A549/Cas9 cells **(fig.12 and table1)**. We also evaluated the extent of the genetic modification within off-target sites through next generation sequencing of the 9 off-target sites showing the highest scores for each sgRNA. This analysis showed that in most of cases, off-targets sites were not modified, confirming the specificity of the following results **(table2).**

Figure 12
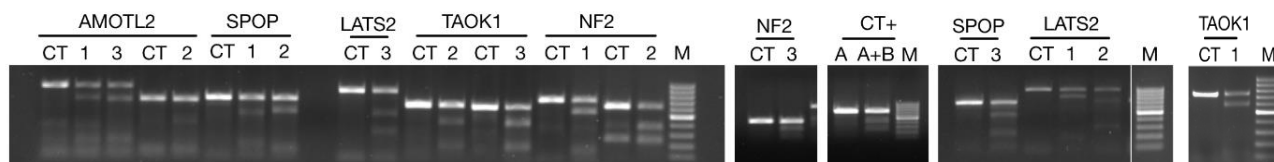
Figure 12: Agarose gel runs showing Alt-R mismatch analysis in A549/Cas9 cells infected with the respective sgRNAs. As control (CT), A549/Cas9 cells were infected with a non-targeting sgRNA. Positive control to check nuclease activity (CT+) was provided by the manufacturer of the kit. M is the molecular weight marker in the range between 100 bp and 1000 bp. *This figure is from Gobbi et al, 2019.*

Table 1

Gene	sgRNA	Code	sgRNA sequence	PCR lenght (bp)	Dig. Fragm. (bp)	Dig. % (Alt-R) A549
AMOTL2	1	Gecko_A01819	ACTGTCCATCTTGTTCCGCA	868	670/198	32
AMOTL2	2	Gecko_A01820	GCCGCAGCCGCGAAAACAGA	664	406/258	11
AMOTL2	3	Gecko_A01821	GGAATCTGCAAATCGCCGCC	868	210/658	37
SPOP	1	Gecko_A46762	CAAGCTTACCCTCTTCTGCG	708	193/515	24
SPOP	2	Gecko_A46763	CCAGTAACAGGTAAAGTGAC	708	545/163	26
SPOP	3	Gecko_A46764	GTCATCAGGGAGAAGCCCGT	708	232/476	16
LATS2	1	Gecko_A26066	CACGTTGAGGCTGTTCCGCG	994	189/805	14
LATS2	2	Gecko_A26067	GTAGGACGCAAACGAATCGC	994	711/283	20
LATS2	3	Gecko_A26068	GGATGTCCTGAACCGGAATC	835	515/320	25
TAOK1	1	Gecko_A48305	TCTGCTTCGGATTTACTAGA	796	144/652	35
TAOK1	2	Gecko_A48306	ATTTACGTGAACACACAGCA	630	209/421	14
TAOK1	3	Gecko_A48307	ATCATATTGTCCTTCATCCA	614	193/421	27
NF2	1	Gecko_A31760	CCTGGCTTCTTACGCCGTCC	707	554/153	28
NF2	2	Gecko_A31761	AAACATCTCGTACAGTGACA	621	389/232	37
NF2	3	Gecko_A31762	CTTATTAACACGAAGCTTTG	451	297/154	14

Table 1: Table showing the sequence of each sgRNA used for generating the knockout of SPOP LATS2, TAOK1, NF2 and AMOTL2 *(sgRNA sequence)*, the number of bp of the full-length product expected from PCR reaction *(PCR length bp)*, the bp length of the fragments expected upon endonuclease T7 digestion *(Dig. Fragm. bp)* and the percentage of digestion *(Dig. % Alt-R A549)* considered as percentage of indel generation. *This table is from Gobbi et al, 2019.*

Table 2

Gene	Guide ID	OFF Target Coordinate	Mutation Frequency (%)
AMOTL2	A01819	chr19:-17439148	6.3
		chr8:-12947975	0
		chr18:-46287784	0
		chr1:-45962143	0
		chr6:-151243325	0
		chr1:+149901448	0
		chr1:-880520	0
		chr21:+47552227	0
		chr4:+25417034	0
	A01820	chr1:+214787236	0
		chr3:-13663238	0
		chr6:+38138582	0
		chr1:+45672259	0
		chr3:-39149844	0
		chr15:+65675447	0
		chr16:-11362794	0
		chr3:-156392423	0
		chr14:+92789518	0
	A01821	chr6:-11044831	0
		chr4:-55991872	0
		chr9:+139913672	0
		chr22:-23522479	0
		chr15:-42693898	0
		chr13:+113622712	0
		chr13:-105527464	0
		chr2:+1810442	0
		chr1:-2236779	1.2

Gene	Guide ID	OFF Target Coordinate	Mutation Frequency (%)
SPOP	A46762	chr5:+79647089	0
		chr19:+38851246	0
		chr2:+179448323	0
		chrX:+134421086	0
		chr1:-181059669	0
		chr9:+37784707	0
		chr19:+36430287	0
		chr8:+141572752	0
		chr18:+77809260	0
	A46763	chr3:+51694252	0
		chr17:+19174700	0
		chr3:+16216518	0.6
		chr14:+63882019	0
		chr8:+27291075	0
		chr7:+47915926	0
		chr2:+74759066	0
		chr13:-51937456	0
		chr3:-42299648	0
	A46764	chr16:+30456874	0
		chr18:-74700922	0
		chr18:+72775205	0
		chr2:+37459464	0
		chr17:-78188535	0
		chrX:-153762671	0
		chr5:+149681903	0
		chrX:-153068625	0
		chr1:-15812391	0

Gene	Guide ID	OFF Target Coordinate	Mutation Frequency (%)
LATS2	A26066	chr17:-47075293	0
		chr1:-15420692	0
		chr7:+99017466	0
		chr6:+46097754	0
		chr15:+33954409	0
		chr9:+139408959	0
		chr2:+44058975	0
		chr8:+144893463	0
	A26067	chr6:+35100840	0
		chr4:+165865733	0
		chr5:+170058504	0
		chr11:+131356747	0
		chr8:-15115633	0
		chr2:+178704870	0
		chr12:-60407820	0
		chr1:+106102887	0
		chr6:+128684140	0
	A26068	chr10:-124402686	0
		chr1:-162722914	0
		chr19:-4676729	0
		chr17:-22023736	0
		chr20:+55933724	0
		chr7:-142375413	0
		chrX:+55208051	0
		chr9:+131687436	0

Gene	Guide ID	OFF Target Coordinate	Mutation Frequency (%)
TAOK1	A48305	chr12:-118677026	0
		chr2:-26536849	0
		chr22:-41527526	0
		chr7:+35942631	0
		chr6:+62978647	0
		chr8:+56480674	0
		chr2:-125324686	0
		chr19:-21932681	0
		chr19:+21585381	0
	A48306	chr5:+137292259	0
		chr11:+66975002	0
		chr12:-51834579	0
		chr9:+80944340	0
		chr14:+74983639	0
		chr3:+87311173	0
		chr3:-190345288	0.5
		chr22:-19223344	0
		chrX:-18659346	0
	A48307	chr1:+197447486	0
		chr12:+118671523	1.2
		chr16:-29990756	0
		chr17:+10608639	0
		chr17:-72517676	0
		chr19:+14829015	0
		chr19:+39075716	0
		chr19:+49316932	0
		chr21:-33694131	0

Gene	Guide ID	OFF Target Coordinate	Mutation Frequency (%)
WWTR1	Brunello_#2	chr9:+129642754	0
		chr13:-73301843	0
		chr8:+144378553	0
		chr7:+148921358	0
		chr2:-106682131	0
		chr19:-58867566	0
		chrX:+44732881	26.0
		chr3:+122296706	0
		chr17:-42455797	0
	Brunello_#3	chr2:+66660680	0
		chr19:+47113085	0
		chr2:+31751284	0
		chr10:+72619124	0
		chr10:+60145259	0
		chr17:-27417608	0
		chr15:-51150433	0
		chr21:+32594154	0
		chr2:+9903417	0
	Brunello_#4	chr19:-7625956	0
		chr1:+71512151	0
		chr1:-200883987	0
		chr1:-145897304	0
		chr1:-147439005	0
		chr6:+26204973	0
		chr6:-26285598	0
		chr16:-11119459	0

Gene	Guide ID	OFF Target Coordinate	Mutation Frequency (%)
NF2	A31760	chr15:+90198631	0
		chr19:+1433880	0
		chr10:-62634870	0
		chr12:+48143682	0
		chr1:+151678872	0
		chr7:-76111910	0
		chr1:-120465287	0
		chr19:-55954177	2.9
		chr1:+155402994	0
	A31761	chr1:+21936113	0
		chr2:-59289847	0
		chr14:-101005389	0
		chr16:-30037215	0
		chr5:-139574265	0
		chr5:-149360341	0
		chr20:-18167974	0
		chr14:-94039066	0
		chr5:-78301090	0
	A31762	chrX:+117053569	0
		chr17:-28758714	0
		chr19:-22498637	0
		chr15:-44951310	0
		chr3:-105377274	0
		chr8:-72968440	0
		chr11:+108186744	0
		chr4:+123610105	0
		chr2:-141215305	0

Table 2: Frequency of off-target cleavage upon specific sgRNA infection. Genomic coordinate for each off-target site is reported. For indel evaluation, exclusively mutations with a coverage of at least 2000X and a frequency higher than 0,5% were evaluated. See Materials and Methods section for further information. *This table is from Gobbi et al, 2019.*

Next, we assessed the downregulation of LATS2, TAOK1, NF2, AMOTL2 and SPOP at protein level, upon knockout generation, through western blot. Our results confirmed that the pools of infected cells contained a good proportion of knockout cells **(fig.13).**
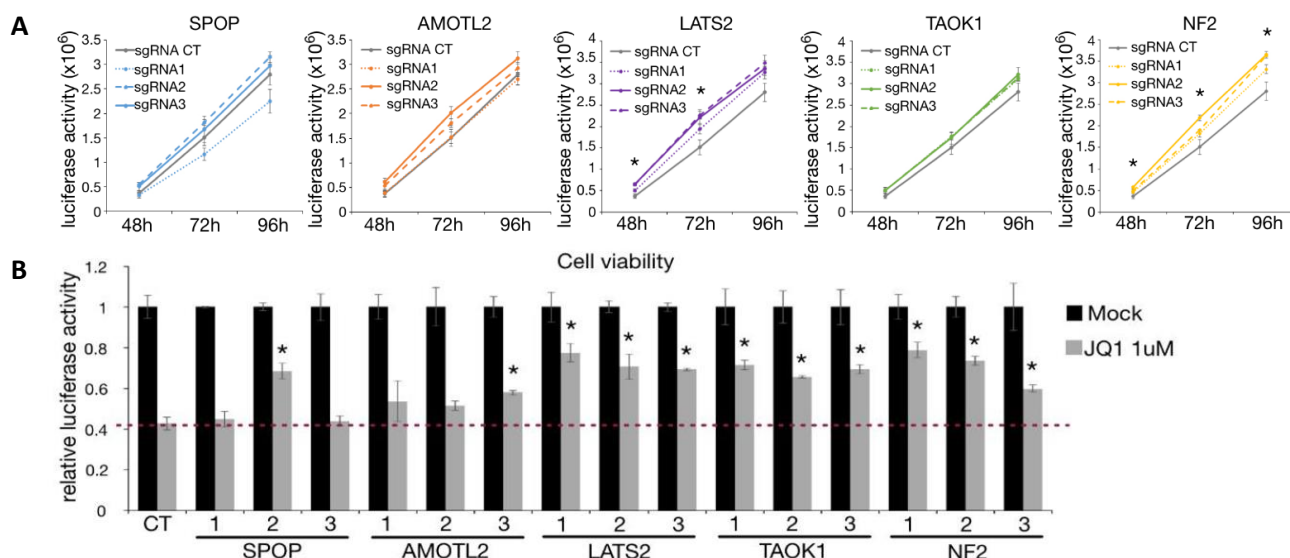
Figure 13
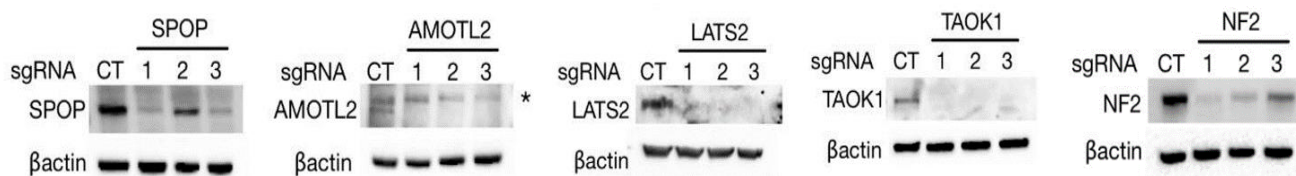
Figure 13: Western blot of A549 cells with specific antibodies showing the expression of SPOP, AMOTL2, LATS2, TAOK1 and NF2 in the corresponding knockout pools, compared to cells infected with a non-targeting sgRNA (CT). The star (*) in AMOTL2 western blot indicates an unspecific band. *These figures are from Gobbi et al, 2019.*

As seen in the **fig.13**, each sgRNA generated a significative downregulation of the respective protein, but with variable efficiency, probably due to different efficiencies of sgRNAs used for KO generation. First, we used these knockout pools to verify the proliferation rate compared to the CT. As seen in **fig.14A**, the knockout of Hippo genes induced a slightly higher proliferation rate. In contrast, SPOP knockout showed a proliferation rate comparable to the CT. Next, we verified if the knockout of Hippo genes confers resistance to JQ1. To this end, we evaluated the viability of knockout cells and CT cells in presence of 1μM JQ1 compared to DMSO treated cells (MOCK). As seen in **figure 14B**, the KO cells for LATS2, TAOK1 and NF2, obtained with all three sgRNAs, showed a significant increment of cell viability in comparison to control, upon treatment with 1μM JQ1. On the contrary, only the cells infected with one out of three sgRNAs for SPOP and AMOTL2 showed increased resistance to JQ1 (**fig.14B**).
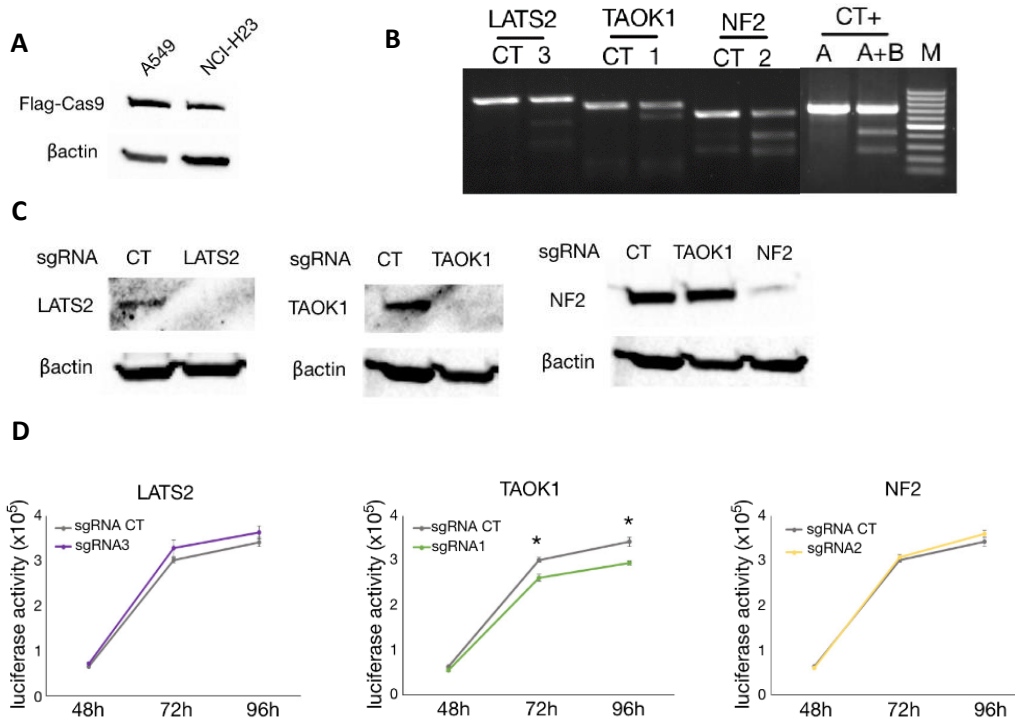
Figure 14

Figure 14: A) Viability assay showing cell proliferation of A549 KO for the indicated genes or infected with a non-targeting sgRNA (CT), measured with RealTime Glo MT assay. **B)** Assay showing cell viability of A549 KO cells for the indicated genes and cells infected with non-targeting sgRNA (CT), measured by RealTime-Glo MT Assay upon 1uM JQ1 treatment for 48 hours, compared to DMSO-treated samples (MOCK). Data are expressed as mean +/- SEM. N=3 * p<0.05. *These figures are from Gobbi et al, 2019.*

For this reason, we focused our subsequent analyses on LATS2, TAOK1 and NF2. For further experiments, we selected only one sgRNA per gene to obtain the knockout, choosing the sgRNA that showed the higher indel generation efficiency: sgRNA #3 for LATS2, sgRNA #1 for TAOK1 and sgRNA #2 for NF2 **(table1)**.

To strengthen our analysis, we generated the KO of the selected genes also in NCI-H23 cells, a second NSCLC cell line harbouring a genetic background similar to A549. First, we generated NCI-H23 pool stably expressing the Cas9 enzyme and we confirmed Cas9 expression by western blot analysis. **(fig.15A)**. Then, we infected NCI-H23/Cas9 with the selected sgRNA for each gene. After NCI-H23/Cas9 KO pools generation, we verified genetic alteration, protein down-regulation and the rate of proliferation in comparison with CT pool **(fig. 15B-D).**
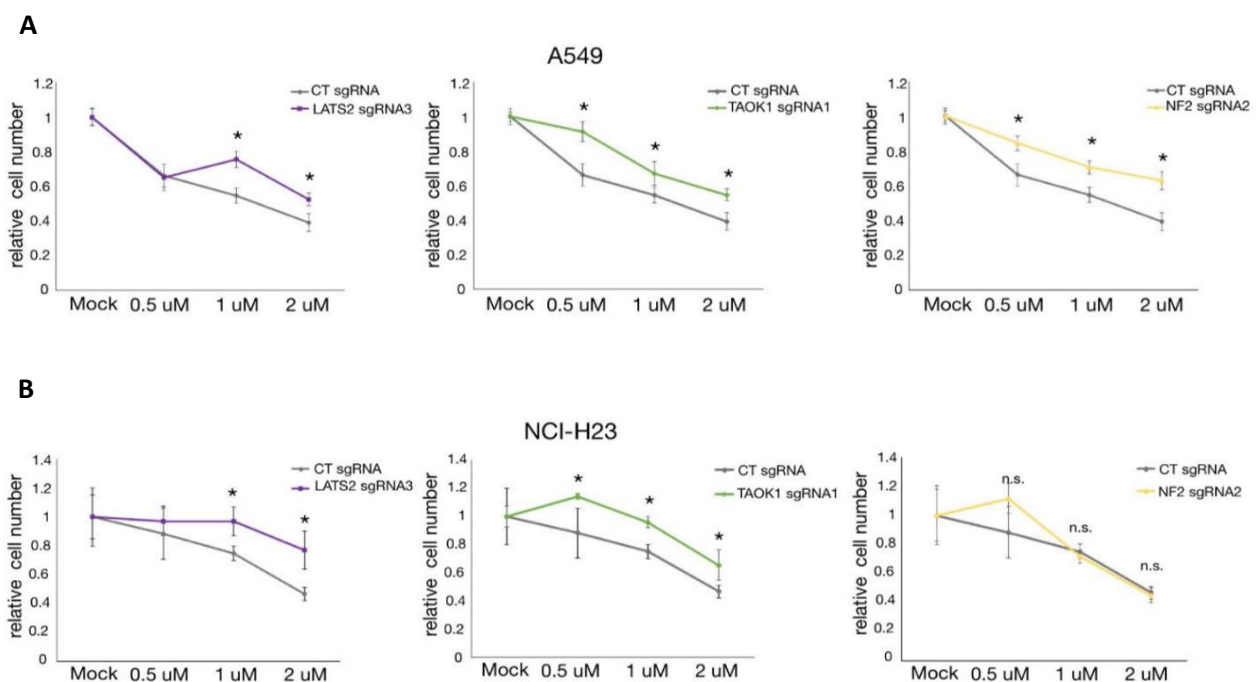
Figure 15

Figure 15: A) Western blot showing Cas9 protein expression in NCI-H23/Cas9 pool. A549/Cas9 clone #19 was used as positive control. **B)** Agarose gel showing Alt-R mismatch analysis in NCI-H23/Cas9 cells infected with the respective sgRNAs. As control (CT), NCI-H23/Cas9 cells were infected with a non-targeting sgRNA. Positive control to check nuclease activity (CT+) was provided by the manufacturer of the kit. M is the molecular weight marker in the range between 100 bp and 1000 bp. **C)** Western blot analysis of NCI-H23 knockout cells with the specific antibody showing the downregulation of the respective protein. **D)** Viability assay showing proliferation of NCI-H23 cells KO for the indicated genes and cells infected with a non-targeting sgRNA (CT), measured with RealTime Glo MT assay. Data are expressed as mean +/- SEM. N=3 * p<0.05. *These figures are from Gobbi et al, 2019.*

To further validate the results obtained by cell viability assay, we performed cell growth analysis, through manual cell counting on both A549 and NCI-H23 KO pools treated with different concentrations of JQ1 (0.5-1-2 μM) or with DMSO as a control (MOCK). This analysis confirmed the increased resistance to JQ1 in the KO cells for all three genes in A549 cells and for LATS2 and TAOK1 in NCI-H23 cells (**fig.16A-B**). In addition, we evaluated the effect of JQ1 on the ability to form colonies. As seen in **fig.17**, the KO of Hippo genes conferred an increased capacity of cells to form colonies upon treatment with different concentrations of JQ1.

All together, these findings demonstrate that Hippo pathway, and in particular its members LATS2, NF2 and TAOK1, is required for susceptibility to BETi in NSCLC.

Figure 16

Figure 16: A) JQ1 sensitivity of A549 KO cells compared to CT, measured by Trypan blue count of viable cells after 72 hours of JQ1 treatment. **B)** JQ1 sensitivity of NCI-H23 KO cells compared to CT, measured by Trypan blue count of viable cells after 72 hours of JQ1 treatment. Cells were treated with three different concentrations of JQ1. For each cell line, values were normalized to MOCK-treated sample and statistical significance was calculated between JQ1-treated CT cells and JQ1-treated KO cells. Data are expressed as mean ± SEM. N = 5, *p < 0.05. *These figures are from Gobbi et al, 2019.*

Figure 17
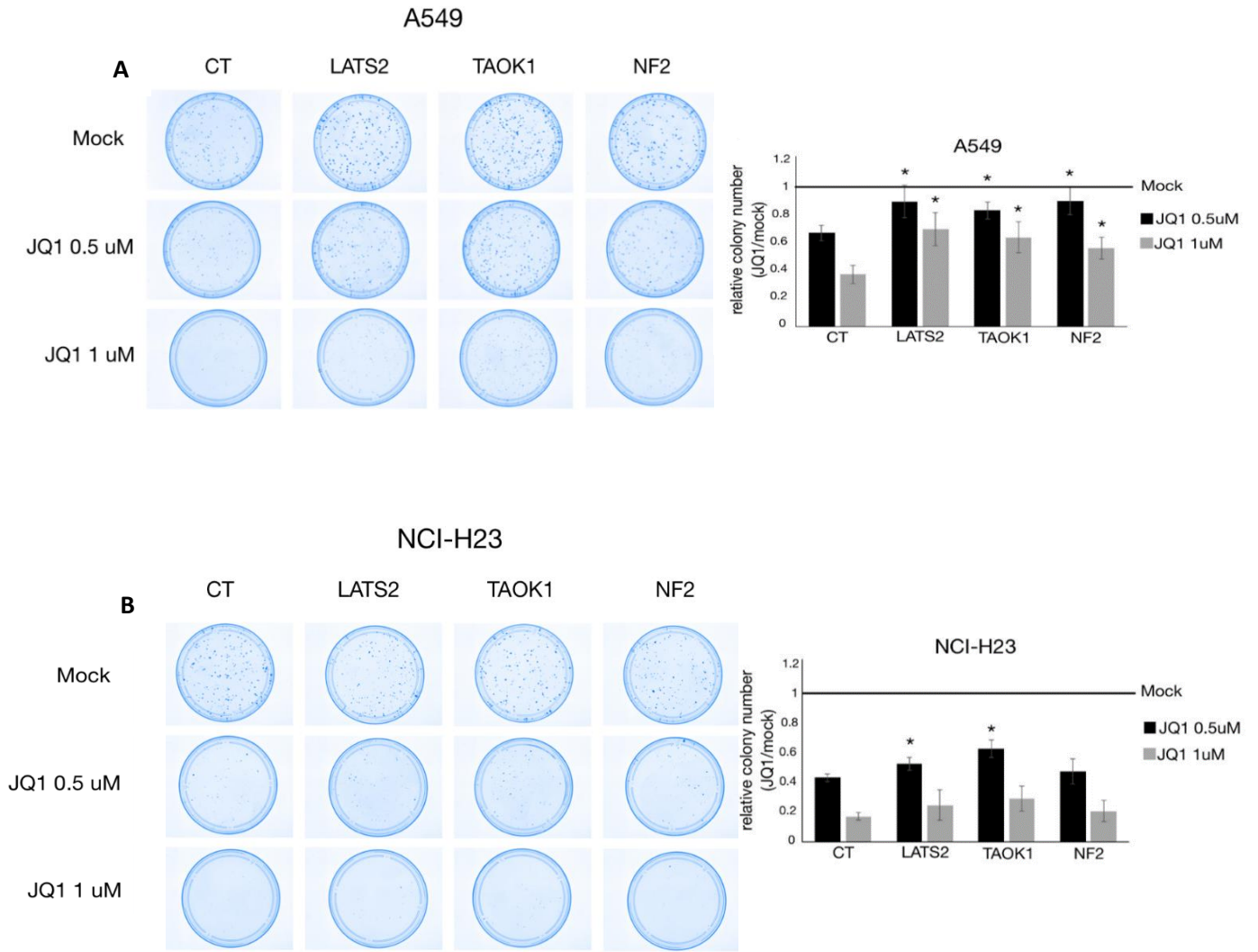
Figure 17: A-B) JQ1 sensitivity of A549 and NCI-H23 KO cells compared with CT, measured by colony number formation in JQ1-treated samples relative to MOCK. On the left are reported pictures of cell dishes showing colonies of A549 or NCI-H23 KO or CT cells formed upon JQ1 or MOCK treatment. On the right, graphs showing the number of colonies formed upon JQ1 treatment expressed as the ratio of MOCK. Statistical significance was calculated comparing Hippo KO cells with CT cells for each drug concentration. Data are expressed as mean ± SEM. $N = 3$, $*p < 0.05$. *These figures are from Gobbi et al, 2019.*

Knockout of LATS2, TAOK1 and NF2 increases YAP/TAZ activity enhancing TAZ nuclear accumulation

Hippo pathway main biological function is to regulate the activity of transcriptional co-factors YAP and TAZ in response to a number of intra-cellular and extra-cellular stimuli. In particular, LATS2 is one of the two main kinases phosphorylating YAP and TAZ, thus enhancing interaction with 14-3-3 proteins, cytoplasmic retention and degradation. TAOK1 is an upstream kinase that can phosphorylate MST1/2, which in turn phosphorylate LATS1/2. NF2 is a plasma membrane associated protein which interacts with LATS1/2, physically positioning LATS1/2 for being phosphorylated by MST1/2 *(Yin, F. et al, 2013)*. Given the role of these proteins, we reasoned that BETi increased resistance in KO pools might be due to a different final balance in YAP and/or TAZ activity. To investigate this hypothesis, we verified the effect of each KO on YAP and/or TAZ total protein levels and/or localization. As seen in **fig. 18A-B**, neither LATS2, TAOK1 nor NF2 KO increased YAP and/or TAZ total protein levels in A549 cells. Conversely, immunofluorescence analysis and nuclear/cytosol fractionation experiments showed the nuclear relocation of TAZ in all three KO pools (**fig.18C, 19A, 19C**). We also observed a statistically not significant slight re-localization of YAP (**fig.18D, 19B, 19D**).

Figure 18:
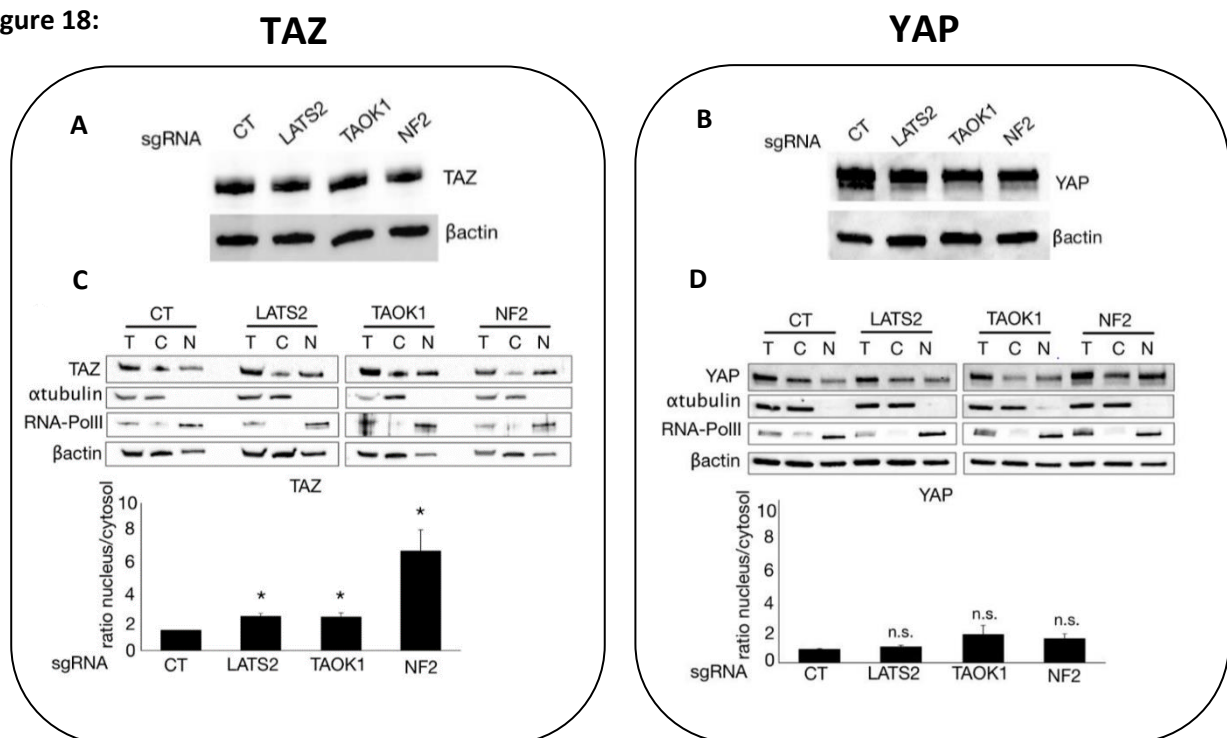
Figure 18: A, B) Western blot in Hippo genes KO A549 cells, with antibodies recognizing TAZ or YAP. **C, D)** Western blot with anti-TAZ or anti-YAP antibodies on separated nucleus and cytosol fractions of KO A549 cells or CT. T, C and N indicate total, cytosolic and nuclear extract, respectively. Anti-tubulin and anti-RNA-Pol II antibodies were used to check cross contamination between cytosolic and nuclear fraction. The intensity of each band in each fraction was quantified and normalized on β-actin. In the graph, the ratio between nuclear and cytosolic proteins is represented. Data are expressed as mean +/- SEM. N=3 *P<0.05. *These figures are from Gobbi et al, 2019.*

Figure 19
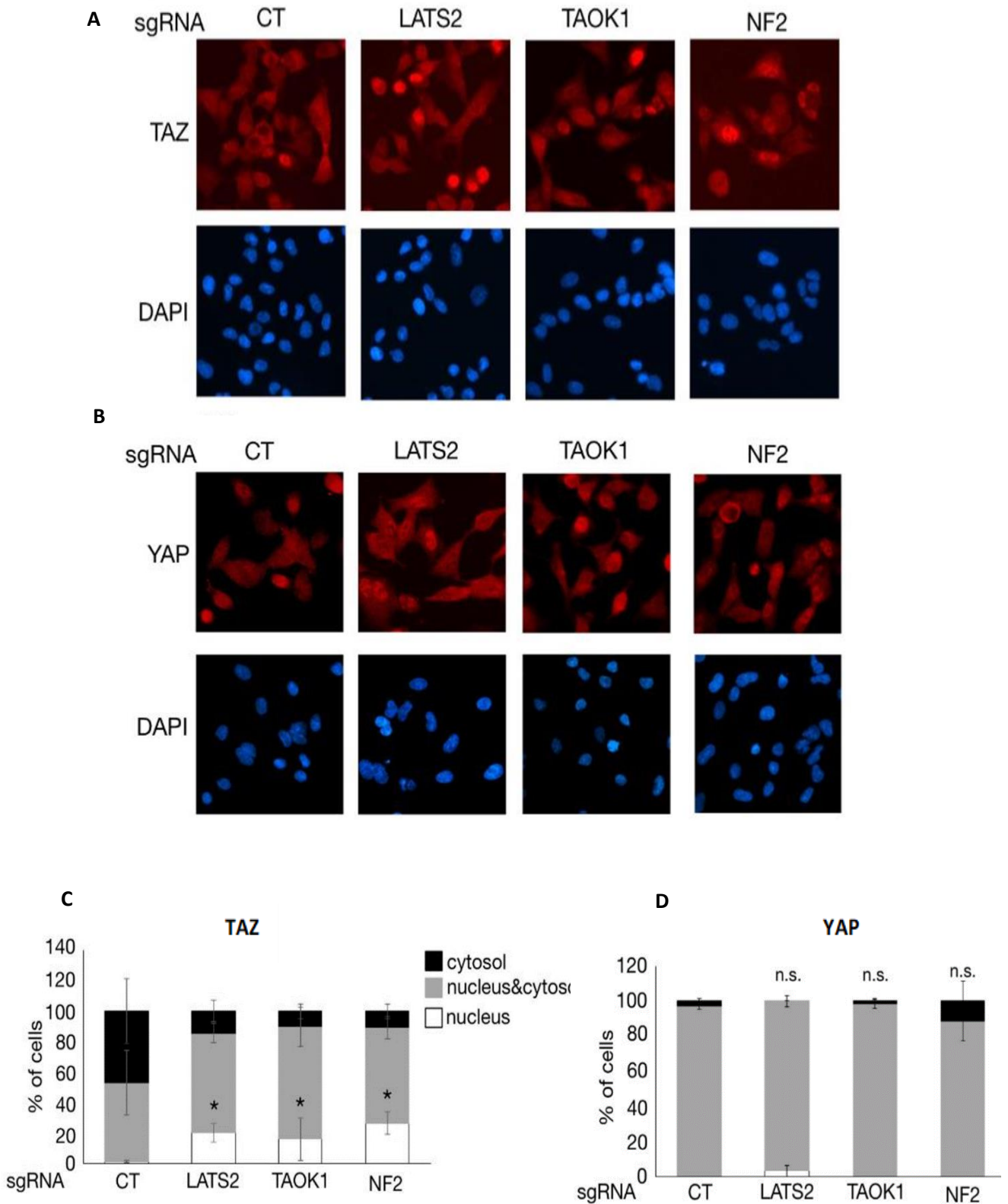
**Figure 19: A, B)** Immunofluorescence showing TAZ and YAP (in red) sub-cellular localization in A549 KO or CT cells. DAPI staining (in blue) was used to highlight nuclei. **C, D)** The percentages of cells showing TAZ and YAP localization in nuclei, cytosol or both is reported in the graphs. At least 200 cells were counted for each sample. Data are expressed as mean +/- SEM. N=3 *P<0.05. *These figures are from Gobbi et al, 2019.*

These data demonstrated that in our cancer model, TAZ re-localization is the main consequence of LATS2, TAOK1 or NF2 KO. In accordance, TAZ co-transcriptional activity, assessed using a reporter plasmid containing 8X TEAD binding sites, was significantly higher in all knockout pools, compared to CT **(fig. 20A)**. In addition, we also verified the expression of the main TAZ target genes (CTGF, ANKRD1, AXL, CYR61) in all KO pools in comparison to CT. As seen in figure, CTGF, ANKRD1, AXL and CYR61 mRNA levels are higher in all KO pools **(fig. 20B).**

All together, these data demonstrate that the inactivation of LATS2, TAOK1 or NF2 induces the relocation of TAZ to the nucleus and, consequently, the enhancement of its co-transcriptional activity.
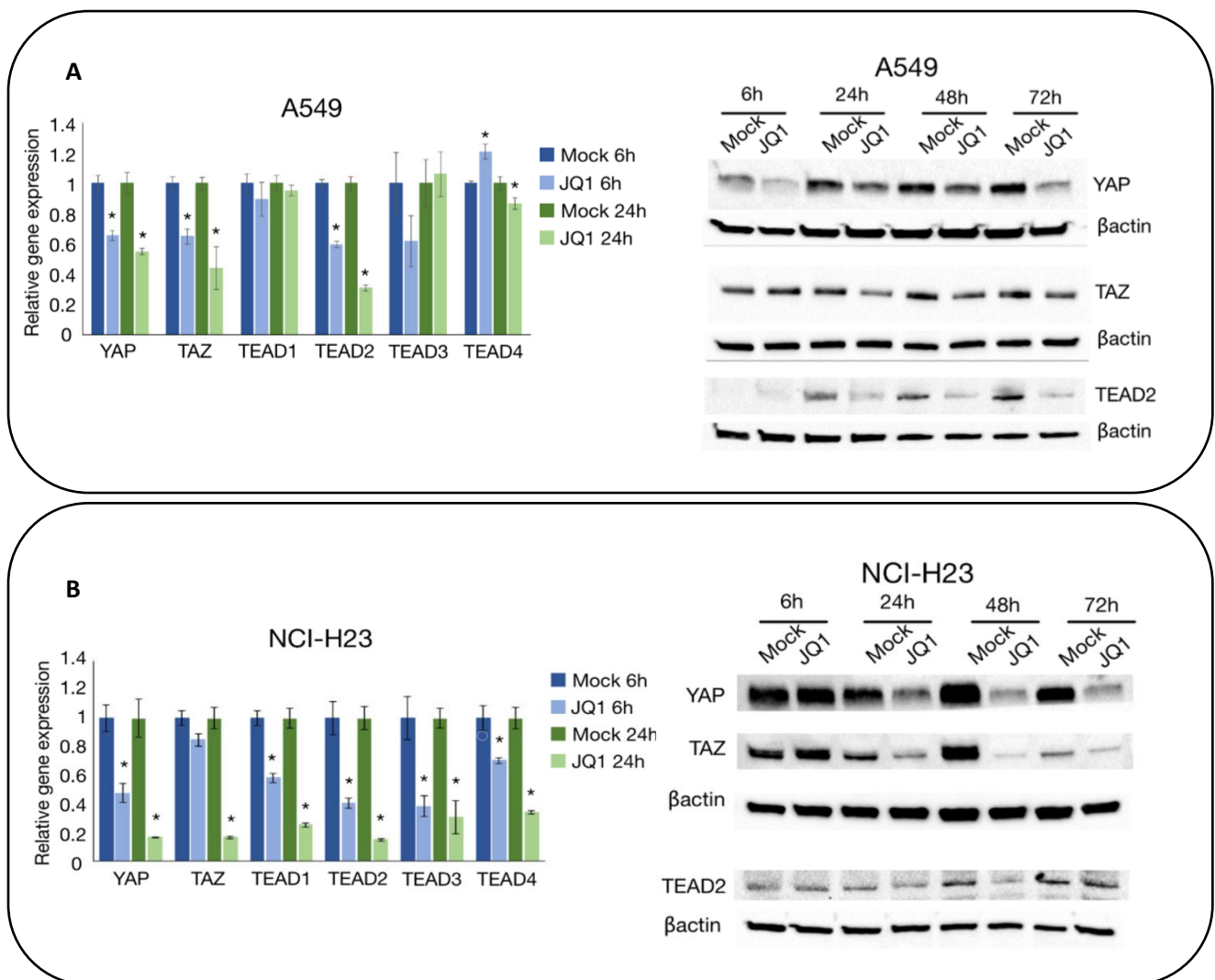
Figure 20:
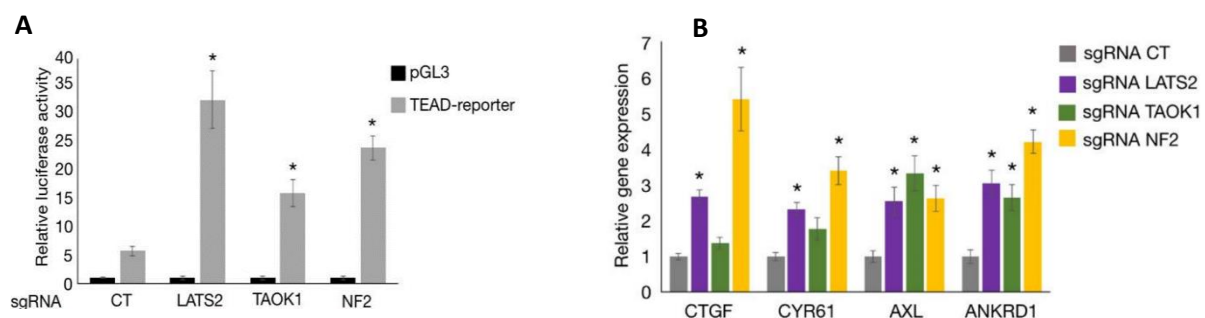
Figure 20: A) Luciferase assay of a reporter plasmid containing 8 binding sites for TEAD factors transfected in Hippo KO or CT cells. Data are expressed as mean +/- SEM. N=3 *P<0.05. **B)** RT-qPCR showing expression levels of the indicated YAP/TAZ target genes in KO A549 cells or CT. Data are expressed as mean +/- SEM. N=3 *P<0.05. *These figures are from Gobbi et al, 2019.*

YAP, TAZ and TEADs are BRD4 target genes and downregulated by JQ1

The main anti-cancer effect of BETi is exerted through the down-regulation of oncogenes to which cancer cells are addicted, leading to proliferation block, apoptosis and differentiation. One of the best characterized effect of BETi is the downregulation of c-MYC in multiple myeloma cells, leading to the block of cell proliferation *(Jakob Loven et al, 2013).* In addition to c-MYC, many other pro-oncogenic genes have been shown to be under the control of BRD4 and down-regulated by BETi treatment, including RUNX2, FOSL2, FOSL1, BCL2, WNT5A, RUNX2 and KIT. Given that YAP, TAZ and their transcriptional partners TEADs are known oncogenes being involved in tumor initiation, progression and metastasis formation in a variety of tumors, we hypothesized that YAP, TAZ and TEADs could be targets of BRD4 and down-regulated upon JQ1 treatment. Thus, we treated A549

and NCI-H23 cells with JQ1 or MOCK and we collected RNA and protein extracts at different time points after treatment. As seen in the **fig.21A-B**, treatment with JQ1 caused an early and strong downregulation of YAP and TAZ at RNA and protein level in both cell lines, suggesting that these genes may be under the direct transcriptional control of BET proteins. Similarly, TEAD2 expression is strongly downregulated in both cell lines, while the other TEAD family members are consistently downregulated only in NCI-H23 cells.

Figure 21:

Figure 21: **A)** On the left, RT-qPCR showing mRNA level of YAP, TAZ and TEADs in A549 cells after 6 or 24 hours of JQ1 treatment. Data are expressed as mean +/- SEM. N=3 *P<0.05. On the right, western blot analysis showing YAP, TAZ and TEAD2 protein levels in A549 cells after 6,24,48 or 72 hours of JQ1 treatment. **B)** On the left, RT-qPCR showing mRNA level of YAP, TAZ and TEAD in NCI-H23 cells after 6 or 24 hours of JQ1 treatment. Data are expressed as mean +/- SEM. N=3 *P<0.05. On the right, western blot analysis showing YAP, TAZ and TEAD2 levels in NCI-H23 cells upon 6,24,48 or 72 hours of JQ1 treatment. *These figures are from Gobbi et al, 2019.*

Moreover, since YAP/TAZ/TEADs transcriptional complex is implicated in different tumors development and progression, we reasoned that the downregulation of the components of this complex could be a new and still not elucidated mechanism of anti-cancer activity of BETi. To explore this hypothesis, we measured the expression of TAZ, YAP and TEAD2 upon JQ1 treatment in a panel of cell lines deriving from different tumors: breast carcinoma (MDA-MB231 and MCF7), thyroid papillary carcinoma (TPC1 and BCPAP), prostate carcinoma (DU-145 and LNCAP) and melanoma (A375 and SK-MEL28). As shown in **fig.22A-B**, treatment with JQ1 caused a reduction in mRNA and protein levels of YAP, TAZ and TEAD2 in most cell lines, confirming our hypothesis.
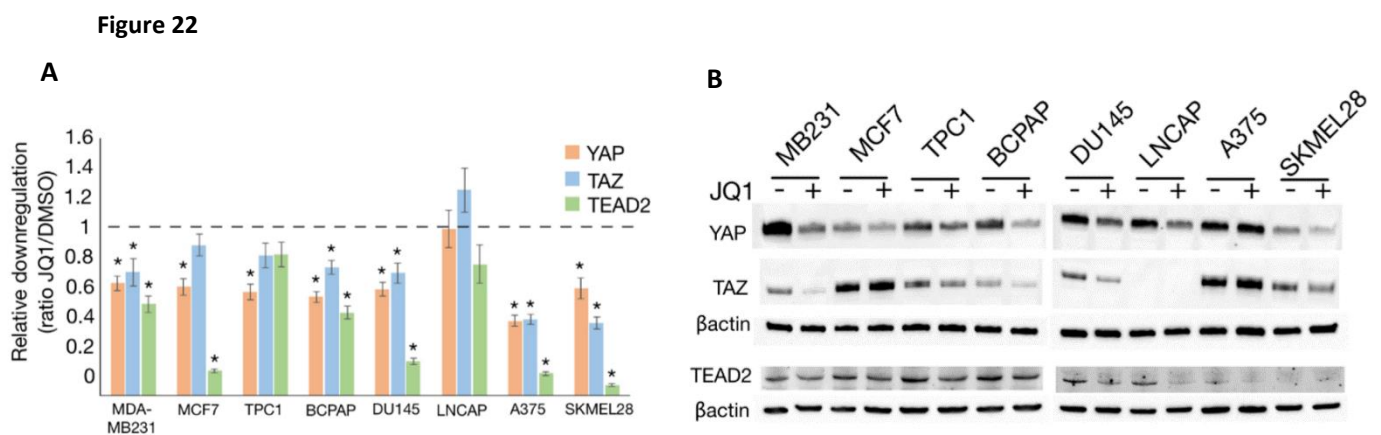
Figure 22

Figure 22: A) On the left, RT-qPCR showing YAP, TAZ and TEAD2 mRNA levels in a panel of cancer cell lines upon 1μM JQ1 treatment. For each cell line, expression level was relative to MOCK-treated cells. Data are expressed as mean +/- SEM. N=3 *P<0.05. **B)** On the right, western blot showing YAP, TAZ and TEAD2 protein levels in a panel of cancer cell lines upon 1μM JQ1 treatment. *These figures are from Gobbi et al, 2019.*

Next, to assess whether BRD4 is directly involved in TAZ, YAP and TEAD2 transcription regulation, we verified the binding of BRD4 on YAP, TAZ and TEAD2 promoters through Chromatin Immunoprecipitation (ChIP) experiments. As seen in **fig.23A**, we observed a significative binding of BRD4 in the promoter regions of these genes. Moreover, we observed a decrease in BRD4 binding upon JQ1 treatment, whereas acetylated histone marks in the same regions do not decrease (**fig.23B**). These findings suggest that the main mechanism leading to TAZ, YAP and TEAD2 downregulation upon JQ1 treatment is the detachment of BRD4 from their regulatory regions. To confirm the direct role of BRD4 in YAP, TAZ and TEAD2 regulation, we knocked-down BRD4 through siRNA transfection. As expected, BRD4 down-regulation caused a marked decrease of YAP, TAZ and TEAD2 mRNA levels (**fig.23C**).

Figure 23
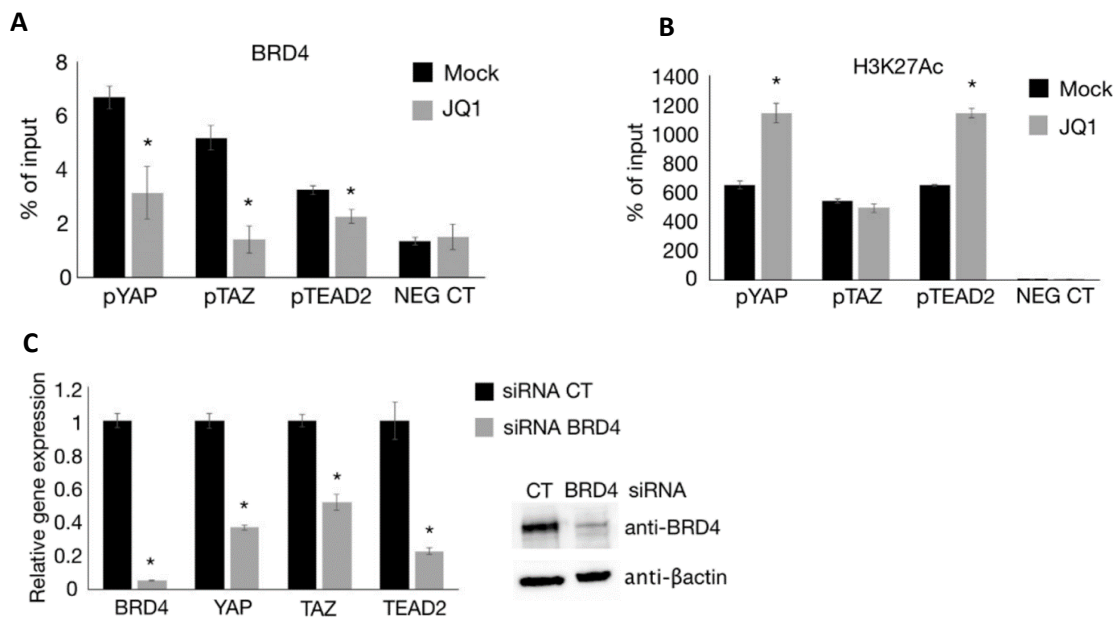
Figure 23: ChIP showing BRD4 **A)** or H3K27Ac **B)** binding on YAP, TAZ and TEAD2 promoters (pYAP, pTAZ and pTEAD2) on A549 cells treated with 1μM JQ1 or DMSO (MOCK) for 24 hours. An unrelated intergenic region was used as negative control (NEG CT). Values are represented as percentage of input. Data are expressed as mean +/- SEM. N=3 *P<0.05. **C)** RT-qPCR showing BRD4, YAP, TAZ and TEAD2 mRNA levels upon siRNA against BRD4 treatment. Western blot with anti-BRD4 antibodies is shown in the inset to confirm BRD4 downregulation at protein level upon siRNA transfection. *These figures are from Gobbi et al, 2019.*

Moreover, we observed a significant downregulation of CTGF, CYR61, AXL and ANKDR1, the main YAP/TAZ target genes, upon JQ1 treatment in both A549 and NCI-H23 cell lines (**fig.24A-B**).

Figure 24
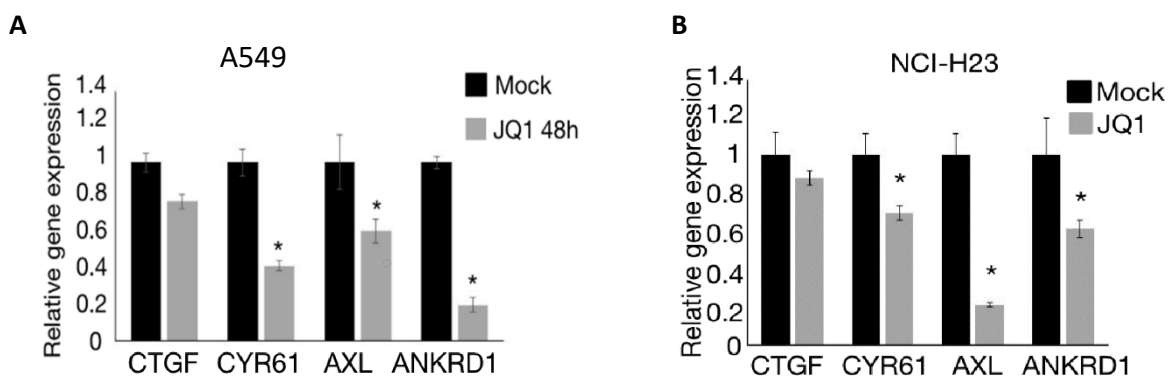
Figure 24: RT-qPCR showing mRNA expression of YAP/TAZ/TEAD main target genes (CTGF, CYR61, AXL, ANKDR1) upon 1μM JQ1 treatment for 48 hours compared to MOCK treated samples in **A)** A549 and **B)** NCI-H23 cells. *These figures are from Gobbi et al, 2019.*

Taken together, these data demonstrate that BRD4 directly regulates YAP, TAZ and TEAD2 through its binding on their promoter regions and suggest that the down-regulation of these genes upon JQ1 treatment is part of anti-cancer effect of BETi in several cancer models.

Hippo genes knockout confers BETi resistance by promoting TAZ nuclear localization and activity

Until now, we demonstrated that there are two different mechanisms that regulate YAP/TAZ activity in our cell models of NSCLC (**fig.25**). In the first (**fig.25A**), BRD4 directly binds to YAP and TAZ promoters, enhancing YAP and TAZ at transcriptional levels. BETi prevents BRD4 binding on their DNA promoter regions, thus resulting in YAP and TAZ transcriptional downregulation. In the second (**fig.25B**), TAZ is post-translationally regulated by Hippo proteins LATS2, NF2 and TAOK1, which restrict its nuclear accumulation. The KO of LATS2, TAOK1 or NF2 induces TAZ nuclear re-localization and enhances its transcriptional activity and pro-oncogenic function.

Figure 25
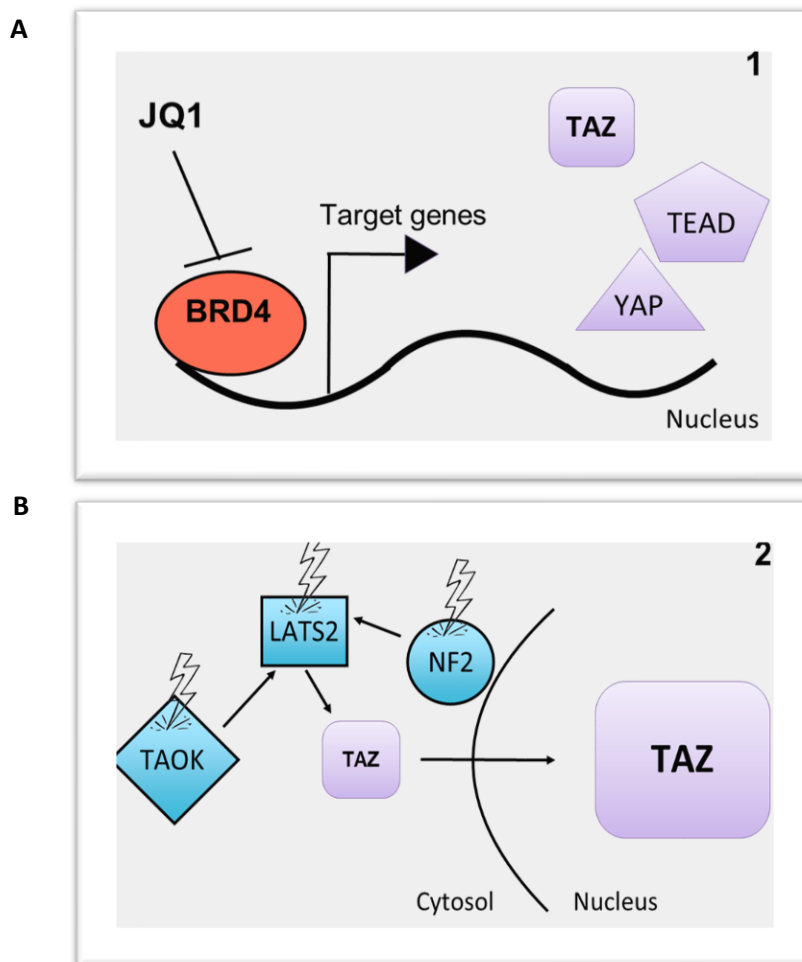
Figure 25: In the scheme are reported the two mechanisms regulating TAZ activity in our NSCLC models. In the first **A)**, TAZ is activated at transcriptional level, through BRD4 binding on its promoter region. In the second mechanism **B)**, Hippo pathway genes TAOK1, LATS2 and NF2 restrict TAZ nuclear localization. When these genes are inactive, TAZ is more nuclear and its activity is enhanced.

To further explore the interplay between these two mechanisms, we treated KO pools for LATS2, NF2 or TAOK1 with JQ1 or MOCK and we evaluated the effect on YAP and TAZ expression and activity. As expected, treatment with JQ1 determined a down-regulation of YAP, TAZ and TEAD2 both in KO and in CT cells at the same level, demonstrating that the KO of LATS2, TAOK1 and NF2

do not interfere with BETi mediated down-regulation of these genes (**fig.26A**). The same results were obtained through Western blot analysis for YAP, TAZ and TEAD2 proteins (**fig.26B**). On the contrary, the expression levels of YAP/TAZ main target genes remained higher in KO pools compared to CT upon JQ1 treatment (**fig.26C-F**). These results can be explained by the fact that in KO pools, TAZ is mainly located in the nucleus and, consequently, more active, even if its total amount is downregulated by JQ1 treatment. Overall, these results demonstrate that BRD4 transcriptionally regulates YAP and TAZ levels independently from Hippo pathway and that KO of Hippo pathway genes LATS2, TAOK1 and NF2 promote resistance to JQ1 by enhancing TAZ nuclear localization and activity.

Figure 26
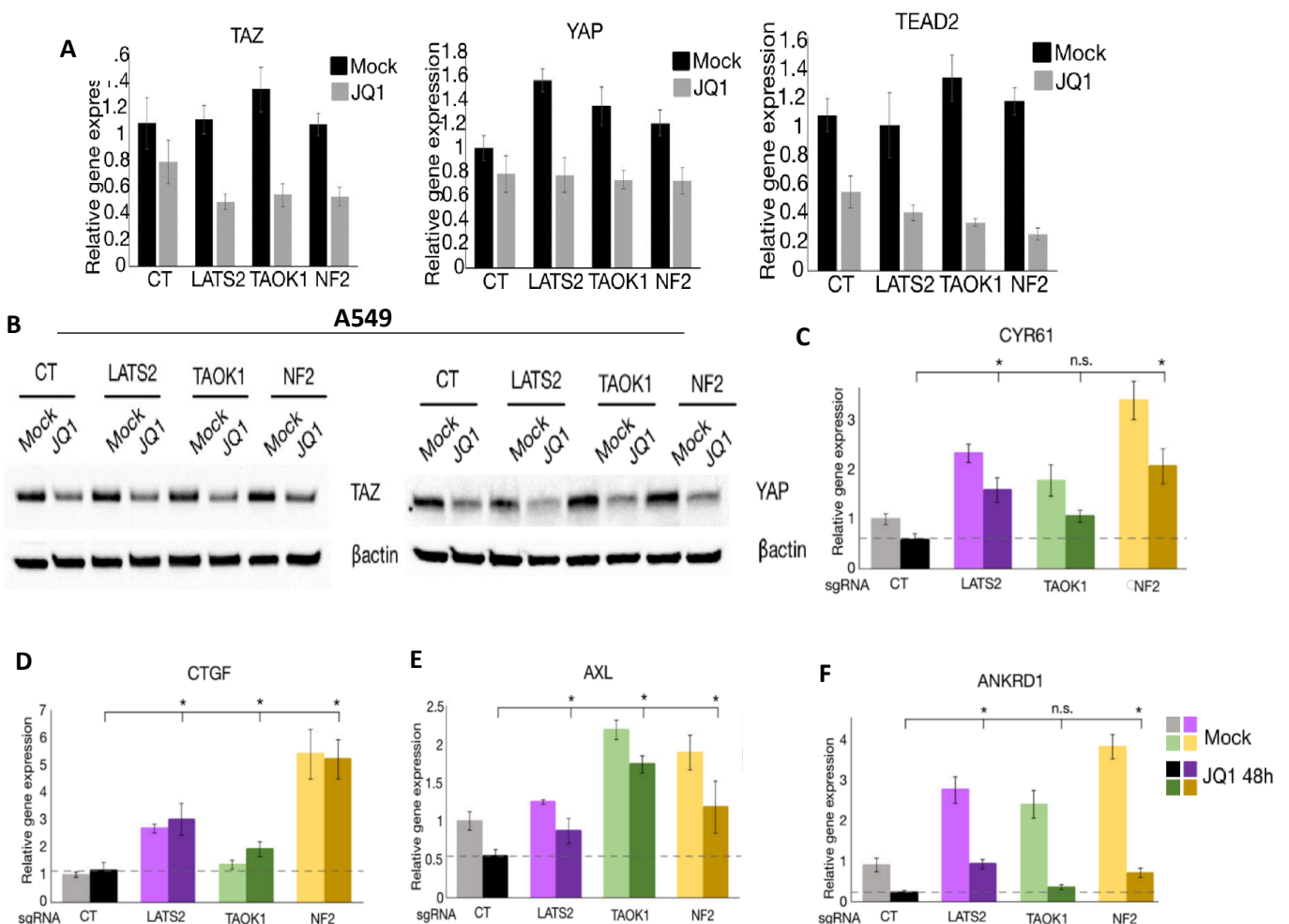
Figure 26: A) RT-qPCR showing mRNA expression of YAP, TAZ and TEAD2 in A549 cells upon 1μM JQ1 treatment for 48 hours in the indicated KO pools compared to MOCK-treated cells. B) Western blot analysis showing YAP and TAZ protein levels in A549 cells upon 1μM JQ1 treatment for 48 hours compared to MOCK-treated cells. C, D, E, F) RT-qPCR showing mRNA levels of TAZ/YAP target genes (ANKDR1, CTGF, AXL and CYR61) upon 1μM JQ1 treatment for 48 hours compared to MOCK-treated cells. Expression values were normalized to MOCK-treated CT cells. Statistical significance was calculated between JQ1-treated CT cells and JQ1-treated KO cells. Data are expressed as mean +/- SEM. N=3 *P<0.05. *These figures are from Gobbi et al, 2019.*

TAZ knockout increases JQ1 sensitivity

Based on previously reported data, we hypothesized that TAZ and/or YAP activity could be involved in the mechanism modulating BETi response in lung cancer. To confirm this hypothesis, we knocked out either YAP or TAZ in A549 cells to evaluate the effect on JQ1 response. We used CRISPR/Cas9 technology to obtain TAZ and YAP knockout, choosing three sgRNAs for TAZ and three sgRNAs for YAP (**table3**). The Cas9-mediated editing in the specific locus was assessed with *ALTR genome editing detection kit* (**fig.27A-B** and **table3**). The downregulation of the proteins was assessed through Western blot analysis (**fig.27C-D**). First, we evaluated proliferation rate and JQ1 response in knockout pools compared to CT through viability assay. TAZ knockout generates a decrease in cell proliferation rate, while the YAP KO pools show a proliferation rate comparable to CT (**fig.27E** and **27H**). First, we measured JQ1 sensitivity in KO pools through cell viability assay. As expected, TAZ KO significantly increases JQ1 sensitivity, while YAP KO shows a JQ1 sensitivity comparable to CT (**fig.27F-G,27I-J**). This suggests that, in our cancer model, TAZ, but not YAP, is an important regulator of both cell proliferation and JQ1 response. For the following experiments, we choose the best targeting sgRNA: sgRNA #3 for TAZ KO and sgRNA #1 for YAP KO. Growth curves by manual cell counting confirmed that TAZ KO increases JQ1 sensitivity while YAP KO shows result comparable to CT (**fig.27G, 27J**).

Table3:

Gene	sgRNA	Code	sgRNA sequence	PCR lenght (bp)	Dig. Fragm. (bp)	Dig. % (Alt-R) A549
WWTR1 (TAZ)	1	Brunello_#2	ACGCGGGCGACGAGTGCGAG	740	442/298	39
WWTR1 (TAZ)	2	Brunello_#3	AGGCTTACCGAGATTTGGCT	799	466/333	21
WWTR1 (TAZ)	3	Brunello_#4	ATCCGAAGCCTAGCTCGTGG	740	537/203	N/a
YAP1	1	Gecko_A54630	CCAAGGCTTGACCCTCGTTT	896	641/255	32
YAP1	2	Gecko_A54631	TGGGGGCTGTGACGTTCATC	830	516/314	6
YAP1	3	Gecko_A54632	GCAGTCGCATCTGTTGCTGC	587	88/499	17

Table 3: Table showing the sequence of each sgRNA used for generating the KO of TAZ and YAP *(sgRNA sequence)*, the number of bp of the full-length product expected from PCR reaction *(PCR length bp)*, the bp length of the fragments expected upon endonuclease T7 digestion *(Dig. Fragm. bp)* and the percentage of digestion *(Dig. % Alt-R A549)* considered as percentage of indel generation. *This table is from Gobbi et al, 2019.*

Figure 27:
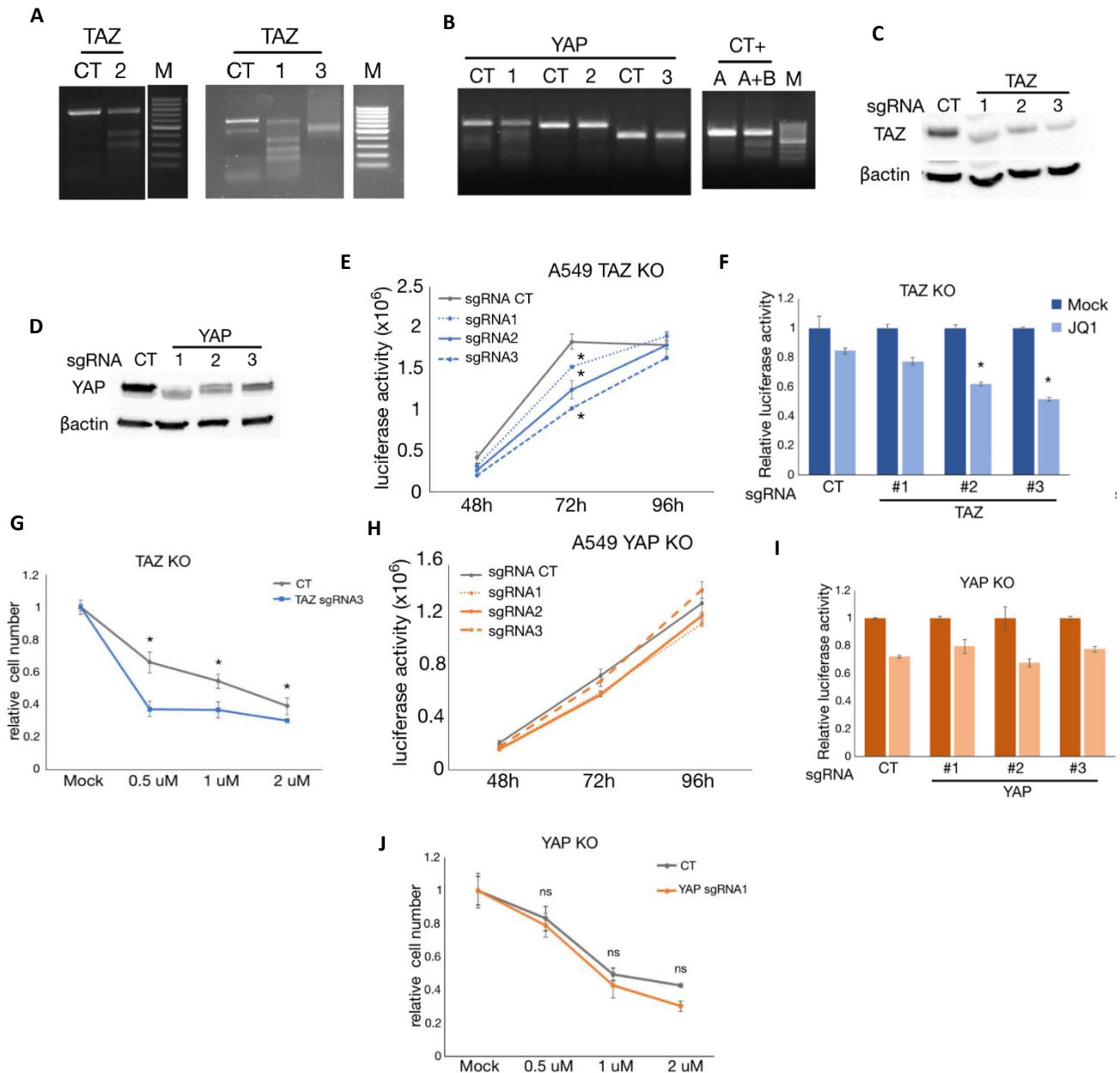
Figure 27: **A, B)** Agarose gel runs showing Alt-R mismatch analysis in A549/Cas9 cells infected with the sgRNA against TAZ **A)** or YAP **B)**. As control (CT), A549/Cas9 cells were infected with a non-targeting sgRNA. Positive control to check nuclease activity (CT+) was provided by the manufacturer of the kit. M is the molecular weight marker in the range between 100 bp and 1000 bp. **C, D)** Western blot with anti TAZ **C)** or anti-YAP **D)** antibody showing TAZ and YAP downregulation upon infection with specific sgRNAs. **E, H)** Cell viability assay measuring the rate of proliferation of TAZ **E)** and YAP **H)** A549 KO cells compared to cells infected with a non-targeting sgRNA, measured by RealTime Glo MT assay. **F, I)** JQ1 sensitivity of TAZ **F)** and YAP **I)** A549 KO cells measured by RealTime Glo MT assay after 72 hours of treatment with 1 μM JQ1. For each cell line, values were normalized to MOCK-treated sample and statistical significance was calculated between JQ1-treated CT cells and JQ1-treated KO cells. Data are expressed as mean +/- SEM. N=3 *P<0.05. **G, J)** JQ1 sensitivity of TAZ **G)** and YAP **J)** A549 KO cells measured by Trypan blue count of viable cells, choosing the sgRNA #3 for TAZ and sgRNA #1 for YAP. Cells were treated with three different concentration of JQ1 (0.5-1 and 2 μM) and were counted 72 hours after JQ1 treatment. For each cell line, values were normalized to MOCK-treated sample and statistical significance was calculated between JQ1-treated CT cells and JQ1-treated KO cells. Data are expressed as mean +/- SEM. N=5 * p<0.05. *These figures are from Gobbi et al, 2019.*

All these experiments were repeated also in NCI-H23 and NCI-H1975 cell lines choosing sgRNA #3 for TAZ KO and sgRNA #1 for YAP KO, confirming that TAZ knockout increases JQ1 sensitivity (fig.28A-G).

Figure 28:
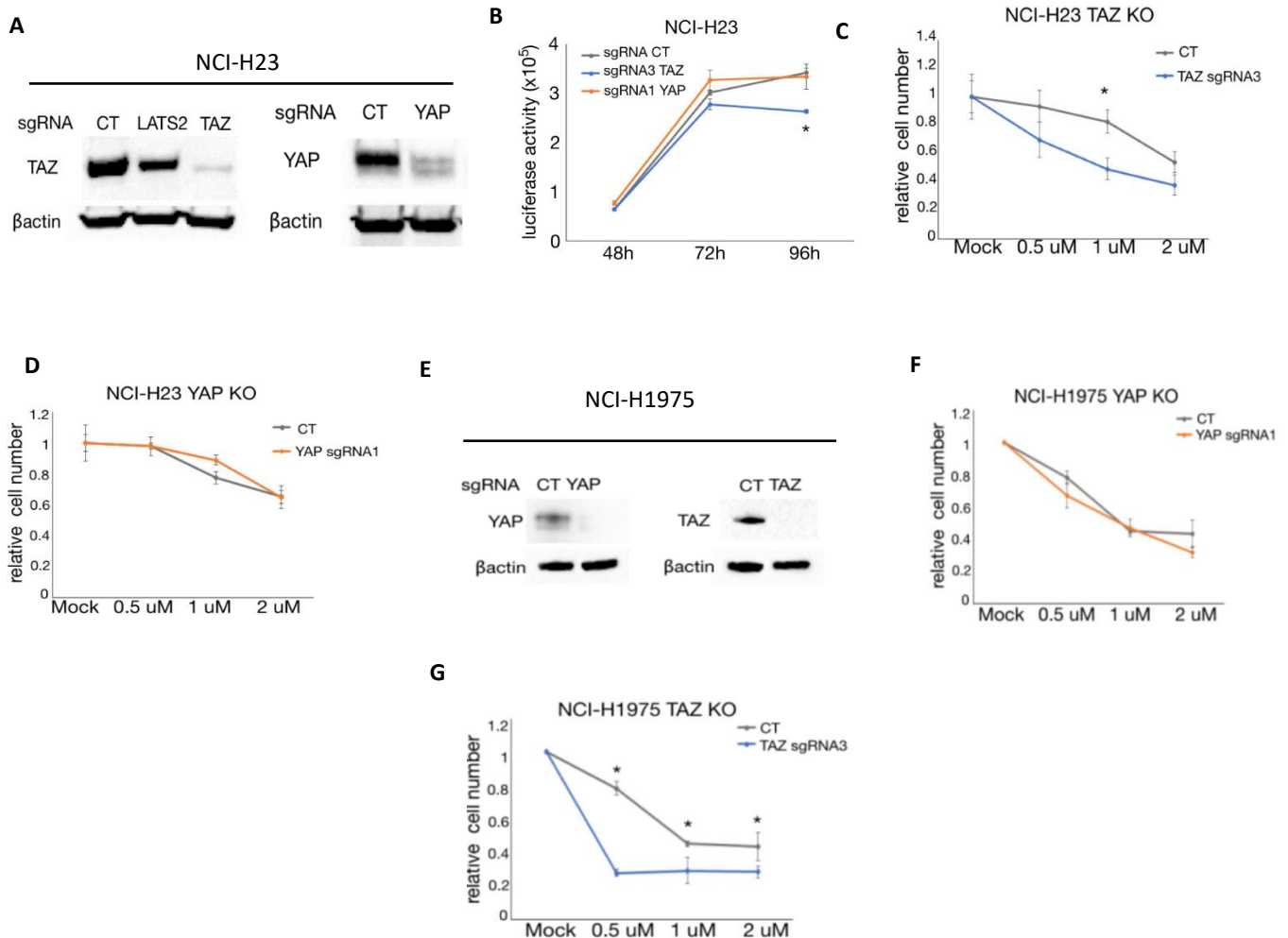
Figure 28: A) Western blot with anti-TAZ and anti-YAP antibodies showing YAP and TAZ downregulation in NCI-H23 KO cells. **B)** Cell viability assay measuring the rate of proliferation of YAP and TAZ KO NCI-H23 cells compared to control measured by RealTime Glo MT assay. **C, D)** JQ1 sensitivity in **C)** TAZ and **D)** YAP KO NCI-H23 cells measured by Trypan blue count of viable cells. Cells were treated with three different concentration of JQ1 (0.5-1 and 2 μM) and were counted 72 hours after JQ1 treatment. For each cell line, values were normalized to MOCK-treated sample and statistical significance was calculated between JQ1-treated CT cells and JQ1-treated KO cells. Data are expressed as mean +/- SEM. N=5 * p<0.05. **E)** Western blot with anti-TAZ and anti-YAP antibodies showing YAP and TAZ downregulation in NCI-H1975 KO cells. **F, G)** JQ1 sensitivity in **F)** YAP and **G)** TAZ KO NCI-H1975 cells measured with Trypan blue count of viable cells. Cells were treated with three different concentrations of JQ1 (0.5-1 and 2 μM) and were counted 72 hours after JQ1 treatment. For each cell line, values were normalized to MOCK-treated sample and statistical significance was calculated between JQ1-treated CT cells and JQ1-treated KO cells. Data are expressed as mean +/- SEM. N=5 mean +/- SEM. *These figures are from Gobbi et al, 2019.*

Together, these data demonstrate that, in NSCLC models, TAZ, but not YAP, is responsible for JQ1 resistance. TAZ down-regulation or increased TAZ cytosolic localization makes cells more sensible to BETi anti-cancer treatment.

In support of the evidence of a non-overlapping function for TAZ and YAP, we observed a differential effect of the two paralogues on target genes expression, as CTGF is downregulated only upon YAP KO, whereas AXL is downregulated only upon TAZ KO (**fig.29**). This means that in our cancer model, YAP and TAZ have non-overlapping functions and, being only TAZ expression and activity important for modulation of JQ1 response.

Figure 29:
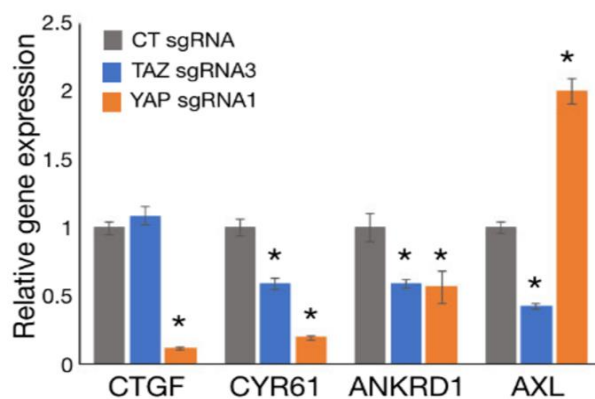
Figure 29: RT-qPCR showing mRNA levels of CTGF, CYR61, ANKRD1 and AXL in TAZ or YAP KO pools compared to CT in A549 cells. Data are expressed as mean +/- SEM. N=3 *P<0.05. YAP and TAZ have both overlapping and non-overlapping function. *These figures are from Gobbi et al, 2019.*

TAZ over-expression promotes BETi resistance

We observed that TAZ knockout sensitized cells to BETi treatment. To confirm that TAZ activity increases BETi resistance, we over-expressed TAZ in A549, NCI-H23 and NCI-H1975 cell lines. To this end, we generated stable cells expressing TAZ under the control of a constitutive promoter **(fig.30A, 30I, 30K)**. As expected, the over-expression of TAZ generated an increase in the rate of proliferation of A549 cells compared to empty-vector containing cells **(fig.30B)**. Moreover, TAZ overexpression increased the activity of TEAD reporter plasmid and increased expression of TAZ target genes in A549 cell line **(fig.30C-D)**. Importantly, TAZ over-expression determined JQ1 increased resistance, measured by cell counting, cell viability assay and colony forming assay in A549 and by cell counting in NCI-H23 and H1975 cell lines **(fig.30E-L).**

Figure 30
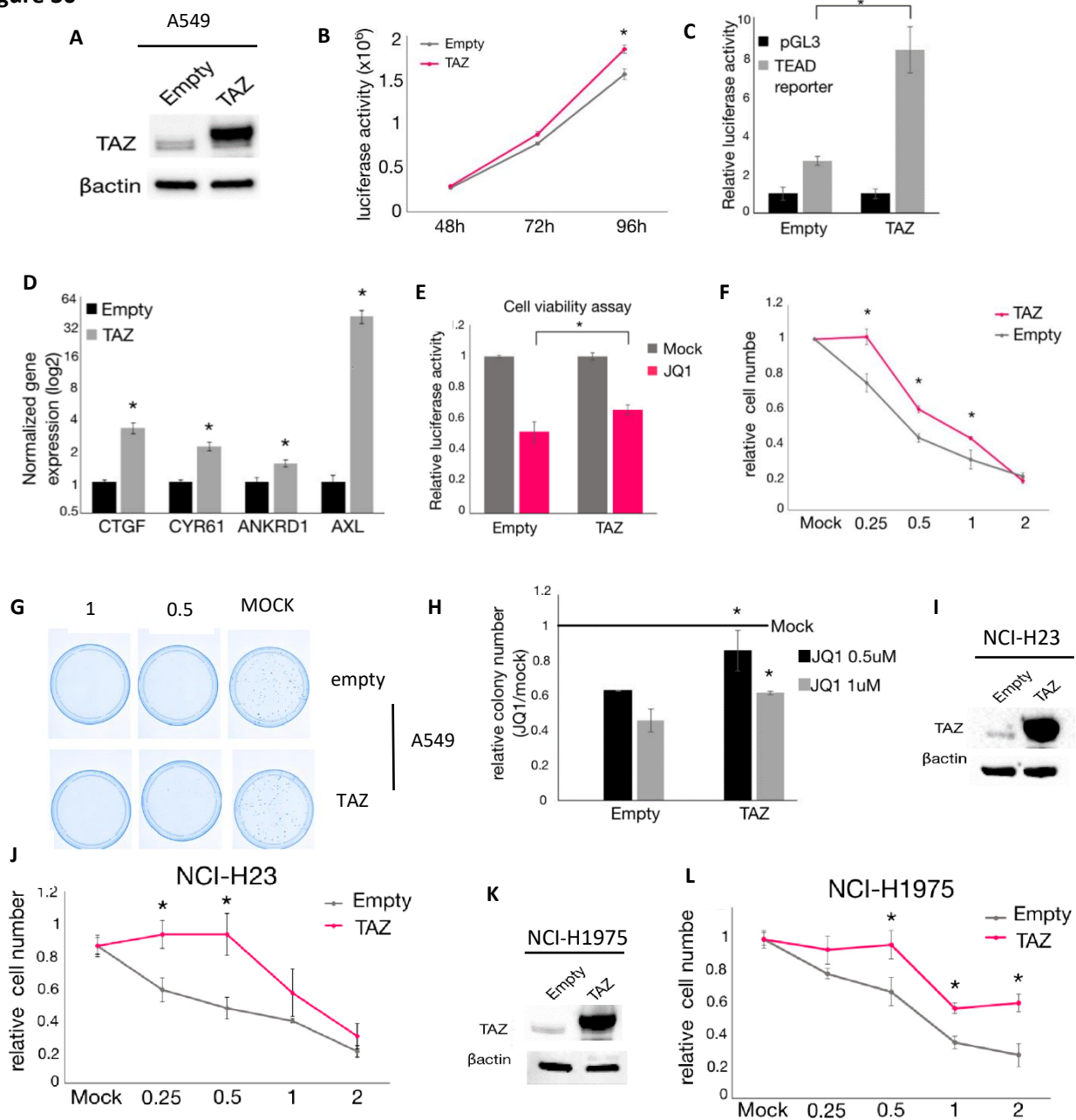
Figure 30: **A)** Western blot with anti-TAZ antibodies showing TAZ protein level in A549 cells infected with an expression vector for TAZ compared to cells infected with an empty vector. **B)** Viability assay measuring proliferation of A549 cells overexpressing TAZ compared to control, measured with RealTime Glo MT assay **C)** Luciferase assay of a reporter construct containing 8 binding sites for TEAD factors transfected in TAZ overexpressing or empty vector-containing cells. Data are expressed as mean +/- SEM. N=3 *P<0.05. **D)** RT-qPCR showing mRNA levels of YAP/TAZ target genes in TAZ overexpressing or empty vector-containing cells. Data are expressed as mean +/- SEM. N=3 *P<0.05. **E, F)** JQ1 sensitivity in A549 TAZ-overexpressing or empty vector-containing cells measured with **E)** RealTime Glo MT Assay and **F)** Trypan blue count of viable cells 72 hours after treatment with 1μM JQ1 in A549 cells. For each cell line, values were normalized to MOCK-treated sample and statistical significance was calculated between JQ1-treated CT cells and JQ1-treated KO cells. Data are expressed as mean +/- SEM. N=3 *P<0.05 **G)** Pictures of cell dishes showing colonies of TAZ-overexpressing A549 compared to empty vector containing cells upon JQ1 or MOCK treatment. **H)** JQ1 sensitivity of TAZ-overexpressing A549 compared to empty-vector containing cells measured by colony forming potential in JQ1 treated samples compared to MOCK treated samples. Data are expressed as mean +/- SEM. N=3 * p<0.05. **I, K)** Western blot with anti-TAZ antibodies showing TAZ protein level in NCI-H23 and NCI-H1975 cells infected with an expression vector for TAZ compared to cells infected with an empty vector. **J, L)** JQ1 sensitivity in NCI-H23 and NCI-H1975 TAZ-overexpressing or empty vector-containing cells measured with Trypan blue count of viable cells 72 hours after treatment with different concentration of JQ1 (0.25-0.5-1 and 2 μM). For each cell line, values were normalized to MOCK-treated sample and statistical significance was calculated between JQ1-treated empty vector cells and JQ1-treated TAZ overexpressing cells. Data are expressed as mean +/- SEM. N=3 * p<0.05. *These figures are from Gobbi et al, 2019.*

Finally, to further confirm TAZ involvement in JQ1 resistance, we generated A549 and NCI-H23 JQ1-resistant cell lines by treating them with progressively increased doses of JQ1. We performed growth curves by cell counting to confirm the increased JQ1-resistance (**fig.31A-D**). In accordance with our data, A549 and NCI-H23 resistant cells show higher TAZ protein levels compared to parental cell lines.

Figure 31
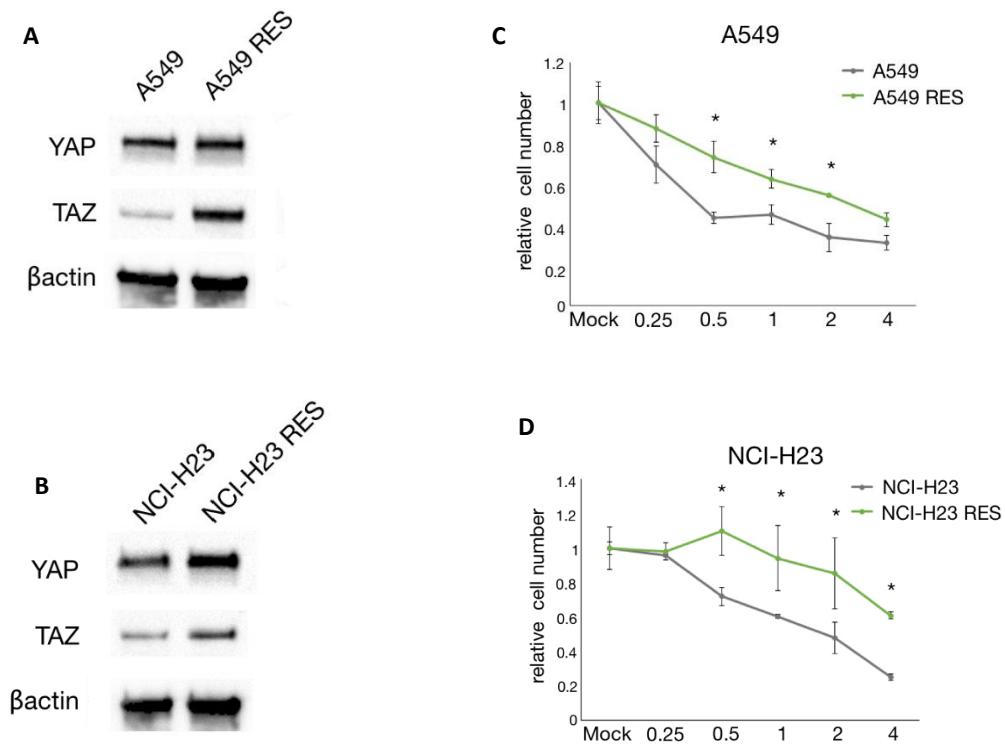
Figure 31: A, B) Western blot with anti-TAZ and anti-YAP antibody showing TAZ and YAP protein levels in A549 and NCI-23 resistant cells compared to non-resistant cell lines. **C, D)** JQ1 sensitivity of A549 and NCI-H23 resistant cells compared to non-resistant cells, measured with Trypan Blue count of viable cells after 72 hours of JQ1 treatment with different drug concentrations. For each cell line, values were normalized to MOCK-treated sample and statistical significance was calculated between JQ1-treated RES and normal cells. Data are expressed as mean +/- SEM. N=3 * $p<0.05$. *These figures are from Gobbi et al, 2019.*

NSCLC patients carry alterations in Hippo Pathway genes

Our data demonstrated that in NSCLC cell models, inactivating alterations in LATS2, TAOK1 and NF2 or aberrant TAZ expression confer resistance to BETi treatment. Our findings suggest that lung cancer patients carrying alterations in Hippo pathway genes, might respond less to BETi treatment. These genes could be considered as novel molecular biomarkers used to predict BETi response and to select patient with the best chance to positively respond to these drugs. Unfortunately, we did not have access to patients treated with BETi to verify this concept. However, we verified the presence and frequency of molecular alterations in Hippo pathway genes in the TCGA *(The Cancer Genome Atlas)* cohort of NSCLC patients. We reported in **fig.32A-B** the frequency of point mutations, copy number variations and gene expression alterations for LATS2, TAOK1, NF2, TEADs, YAP and TAZ in a cohort of 408 NSCLC patients, comprising 178 lung squamous cell carcinoma and 230 lung adenocarcinoma cases. Strikingly, we found that at least one molecular alteration in the selected genes is present in 50% of adenocarcinoma patients and 71% of squamous cell carcinoma patients. We found that TAZ alterations, mainly amplification and mRNA up-regulation, are very frequent in squamous cell carcinoma patients, being present in 44% of patients. These data are in line with other studies which report that upregulation of YAP and TAZ are frequent events in lung cancer development *(Wang, Y., 2010; Xie, M., 2010)*. Moreover, alterations in LATS2 and NF2 have already been described to be oncogenic in various cancer settings. Next, we verified if alterations in YAP and/or TAZ could impact patient's prognosis. As seen in the **fig.32C-D**, high TAZ expression or amplification correlates with a significant worse prognosis in lung adenocarcinoma patients. On the contrary, YAP high expression or amplification does not impact patient's survival. These data confirm that YAP and TAZ play non-overlapping roles in lung tumorigenesis and support our *in vitro* results, indicating that TAZ plays a pivotal role in lung cancer progression and drug resistance.

Figure 32

A

Lung adenocarcinoma
Altered 116/230 (50%) samples
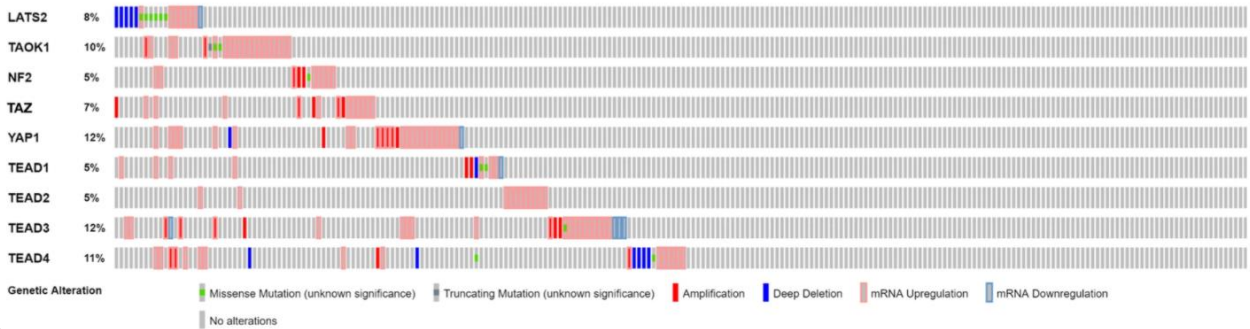
B

Lung squamous cell carcinoma
Altered 127/178 (71%) samples
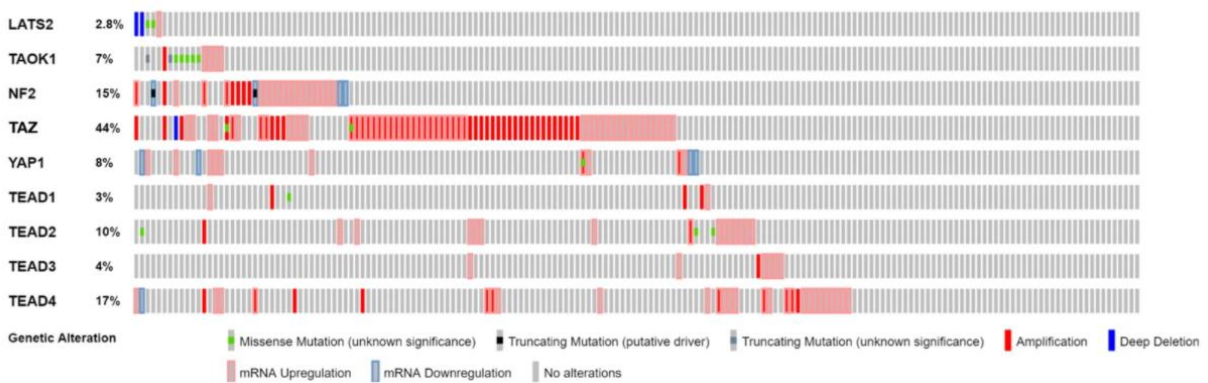
C

Lung adenocarcinoma
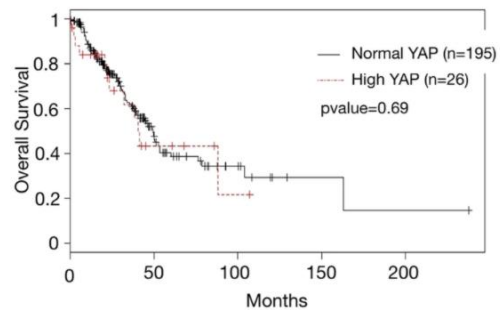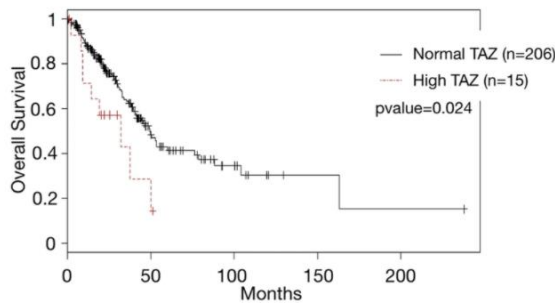
D

Lung squamous cell carcinoma
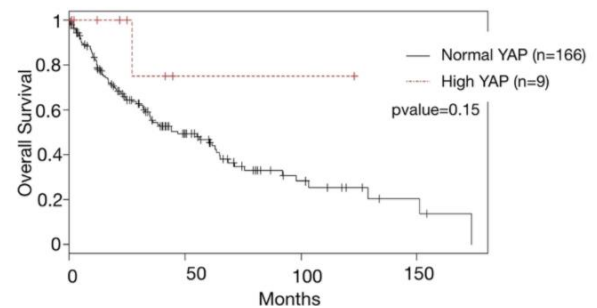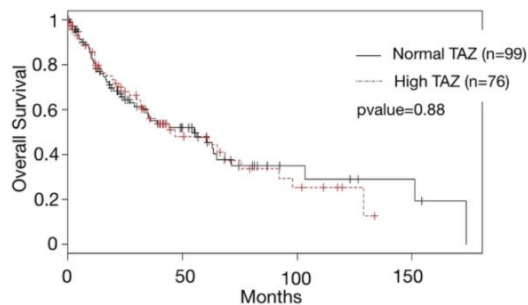
Figure 32: A, B) Oncoprint scheme from TCGA analysis showing the type and the frequency of Hippo pathway genes alterations in NSCLC patients. Oncoprint shown in panel A was obtained from Adenocarcinoma patient's cohort while Oncoprint shown in panel B from Squamous Cell Carcinoma patient's cohort. Graphs are modified from cBioportal (www.cBioportal.org). **C, D)** Kaplan-Meier overall survival curves comparing lung Adenocarcinoma or lung Squamous Cell Carcinoma patient's carrying amplification or upregulation of TAZ (High TAZ) or YAP (High YAP) with all other patients with the same disease (Normal TAZ and Normal YAP). *These figures are from Gobbi et al, 2019.*

Silencing TAZ-AS202, but not TAZ-AS203, inhibits NSCLC cells proliferation, migration and invasion

NATs are antisense lncRNAs with established molecular functions in various patho-physiological processes, including tumor development. The main mechanism behind their participation in cancer progression and/or suppression is the regulation of *in cis* neighboring genes through various mechanisms. TAZ-AS202 and TAZ-AS203 are two NATs that share with the TAZ gene the same promoter region. TAZ-AS203 initiates in the region of TAZ reference transcript exon two, while TAZ-AS202 initiates upstream TAZ promoter, producing an RNA that does not overlap with the TAZ transcript (**fig.10, Preliminary Data**). Their possible interplay with TAZ and their role in lung cancer have never been characterized. First, we explored the role of TAZ-AS202 and TAZ-AS203 in lung cancer, investigating their biological function in NSCLC cell lines. To this end, we transfected A549, NCI-H23 and H1299 cells with siRNAs against TAZ-AS202 and TAZ-AS203, using siRNA against TAZ as positive control and a control non-targeting siRNA as negative control. As seen in **figure 33A- C**, we obtained a significative downregulation of the specific targets. Strikingly, as for TAZ silencing, TAZ-AS202 downregulation causes a significative inhibition of cell proliferation, measured by cell counting, in both A549 and H1299 cells **(fig.33D,33F)**. NCI-H23 cells show a decreased proliferation only in TAZ downregulated condition **(fig.33E)**. Moreover, wound-healing assay was used to evaluate cell migration. TAZ-AS202 silencing significantly restrained the capacity of A549 and NCI-H23 to migrate **(fig.34A-B)**. A minor effect was seen in H1299 cells **(fig.34C)**. Strikingly, in A549 cells, the effect of TAZ-AS202 silencing on cell migration is greater than the effect of TAZ, suggesting a more essential role for this lncRNA in regulating the ability of cells to migrate. On the contrary, upon TAZ-AS203 silencing, we observed an increment in cell proliferation and a slight increase in motility only in NCI-H1299 cells. These observations indicate that TAZ-AS202 and TAZ-AS203 have different roles in regulating cell features and suggest that TAZ-AS202 has a prominent pro-oncogenic role in our cell models of NSCLC. For these reasons, we decided to continue our analysis focusing on TAZ-AS202. Invasion assay was conducted to evaluate the effect of TAZ-AS202 silencing on the invasive ability of A549 cells, using TAZ silencing as positive control. The results demonstrate that the ability of A549 cells to invade through Matrigel matrix was significantly decreased upon both TAZ and TAZ-AS202 silencing **(fig.35A-C).**
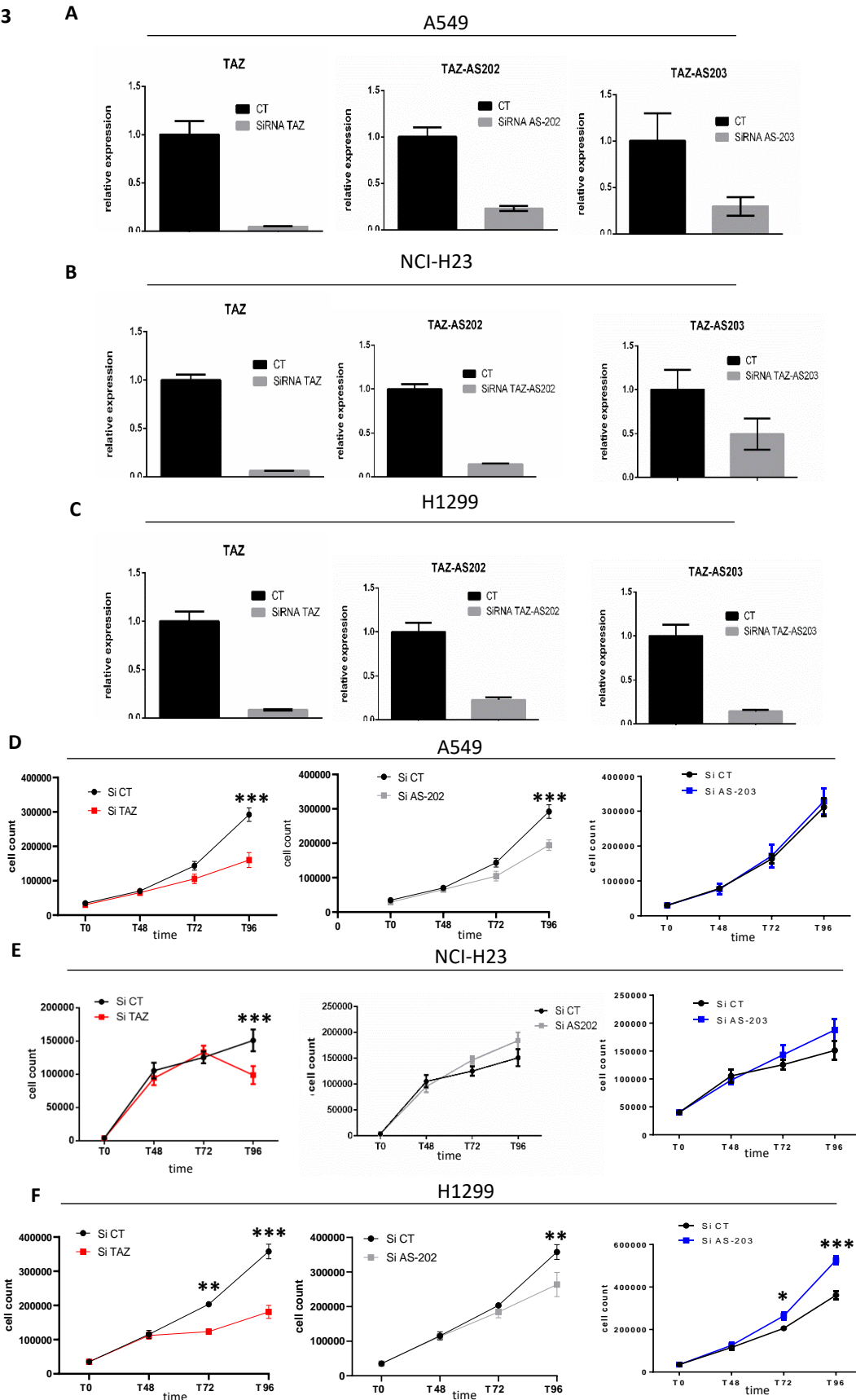
Figure 33: A, B, C) RT-qPCR showing expression levels of TAZ, TAZ-AS202 and TAZ-AS203 RNA in **A)** A549, **B)** NCI-H23 and **C)** NCI-H1299 control cells and cells treated with siRNA against TAZ, TAZ-AS202 and TAZ-AS203 for 48 hours. Data are expressed as mean +/- SEM. **D, E, F)** Growth curves in **D)** A549, **E)** NCI-H23 and **F)** NCI-H1299 cells measured by Trypan blue count of viable cells after 48 hours, 72 hours and 96 hours of siRNA transfection against TAZ, TAZ-AS202 and TAZ-AS203 compared to control cells. Statistical significance was calculated between siRNA treated cells and CT cells. Data are expressed as mean ± SEM. N = 6, *p < 0.05, **p< 0.01, ***p<0.001.

Figure 34
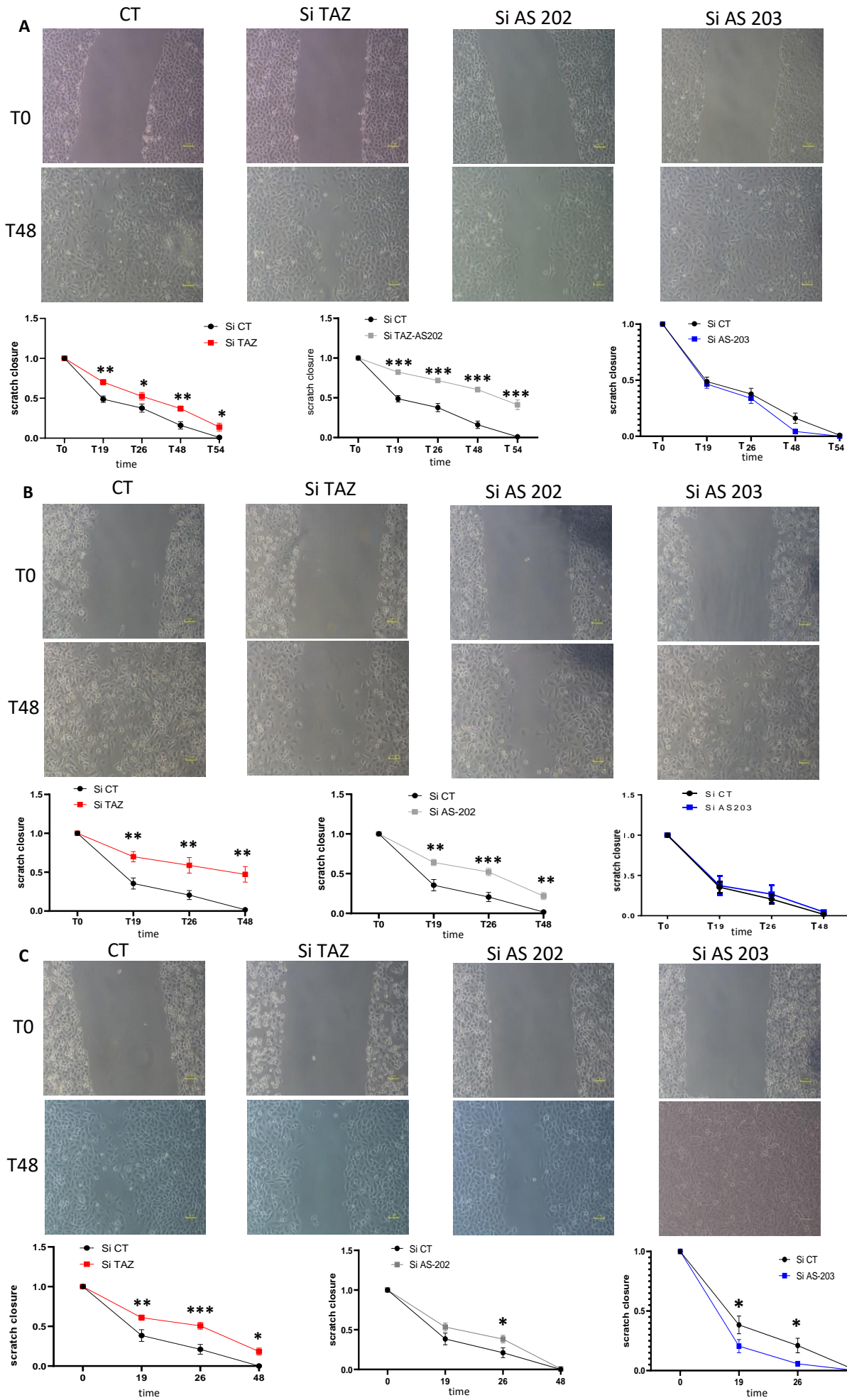
Figure 34: A, B, C) Migration assay. Migration ability in **A)** A549, **B)** NCI-H23 and **C)** NCI-H1299 cells transfected with siRNA against TAZ, TAZ-AS202 and TAZ-AS203 compared to control cells measured by scratch wound healing assay. The photos represent the wound closure 48 hours from the scratch, comparing CT treated cells with siRNA treated cells. In the graphs: wound closure ratio. The area of the scratch was measured at different time point from the scratch (T0) using ImageJ software. The area of each time point was normalized to the area of T0 and statistical significance was calculated between CT treated cells and siRNA treated cells. Data are expressed as mean ± SEM. N = 6, *p < 0.05, **p< 0.01, ***p<0.001.

Figure 35
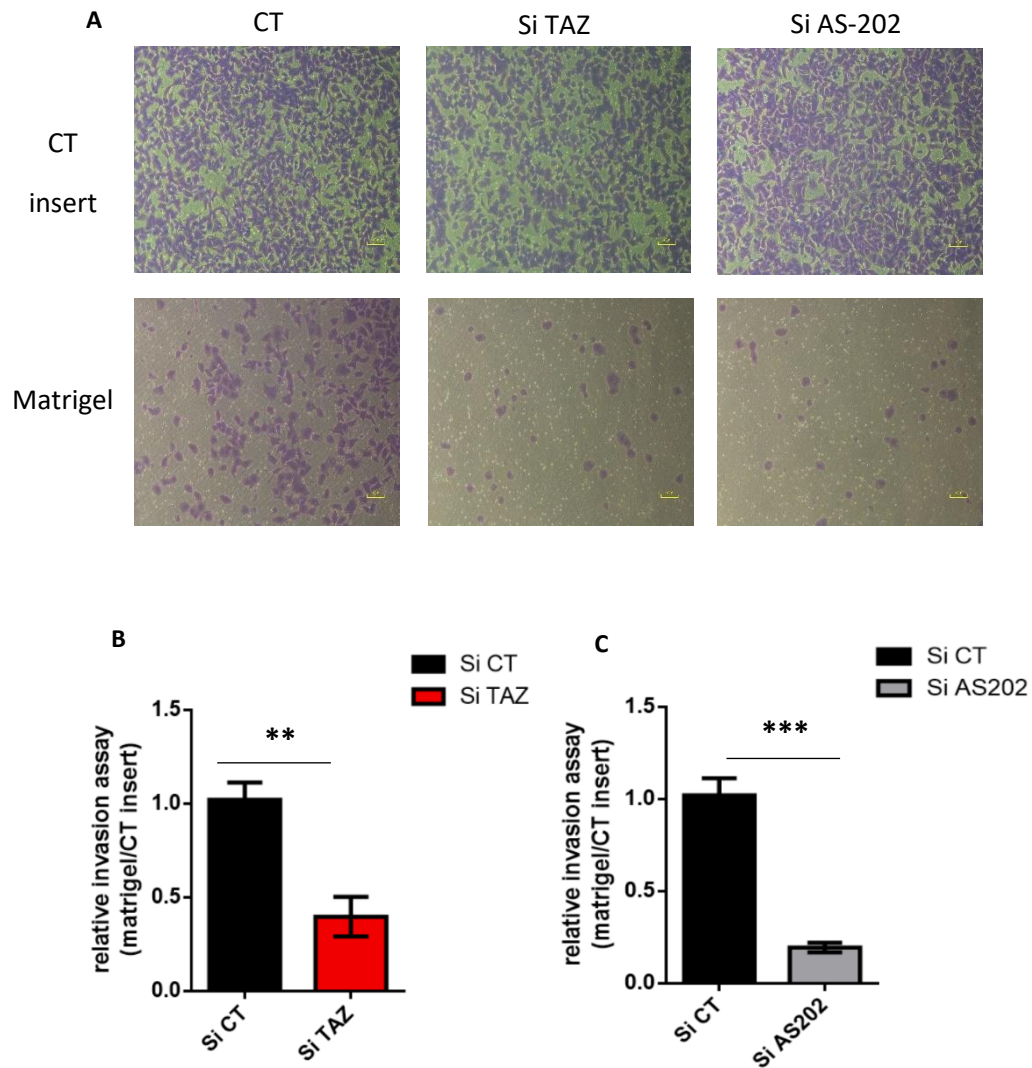
Figure 35: Invasion ability of A549 cells. **A)** Cells were transfected with siRNA against TAZ, TAZ-AS202 or control. Images of invading cells were taken 72h from transfection. **B, C)** Graph showing the rate of invasion. Cells were counted using ImageJ software and the number of cells for each condition was normalized on the number of cells in the control insert conditions. Data are expressed as mean ± SEM. N = 6, *p < 0.05, **p< 0.01, ***p<0.001.

TAZ-AS202 is both nuclear and cytosolic in NSCLC cells

The molecular mechanism behind lncRNAs function is tightly linked to their sub-cellular localization. To gain some insights into TAZ-AS202 mechanism of action, we examined the localization of this lncRNA in sub-cellular compartments (**fig.36**). We used anti-PolII and anti-tubulin antibodies to check cross-contamination of proteins between nucleus and cytosol, respectively (**fig.36B,36E**). Next, we performed RT-qPCR to verify the localization of U1 and KCNQ1OT1 as controls for RNAs localized mainly in nucleus or chromatin-associated, respectively (**fig.36C,36F**). We also verified the subcellular localization of OIP5-AS1. OIP5-AS1 is a lncRNA localized both in cytosol, acting as a miRNAs sponge, and in nucleus, interacting with EZH2 to repress the expression of genes (*Soudeh Ghafouri-Fard et al, 2021; Yunlei Bai et al, 2019*). RT-qPCR shows that TAZ-AS202 localization is similar to OIP5-AS1 in both A549 and NCI-H23, suggesting a possible double role for this lncRNA, or, alternatively, its possible ability to shuttle between the two subcellular compartments (**fig.36A,36D**).

Figure 36
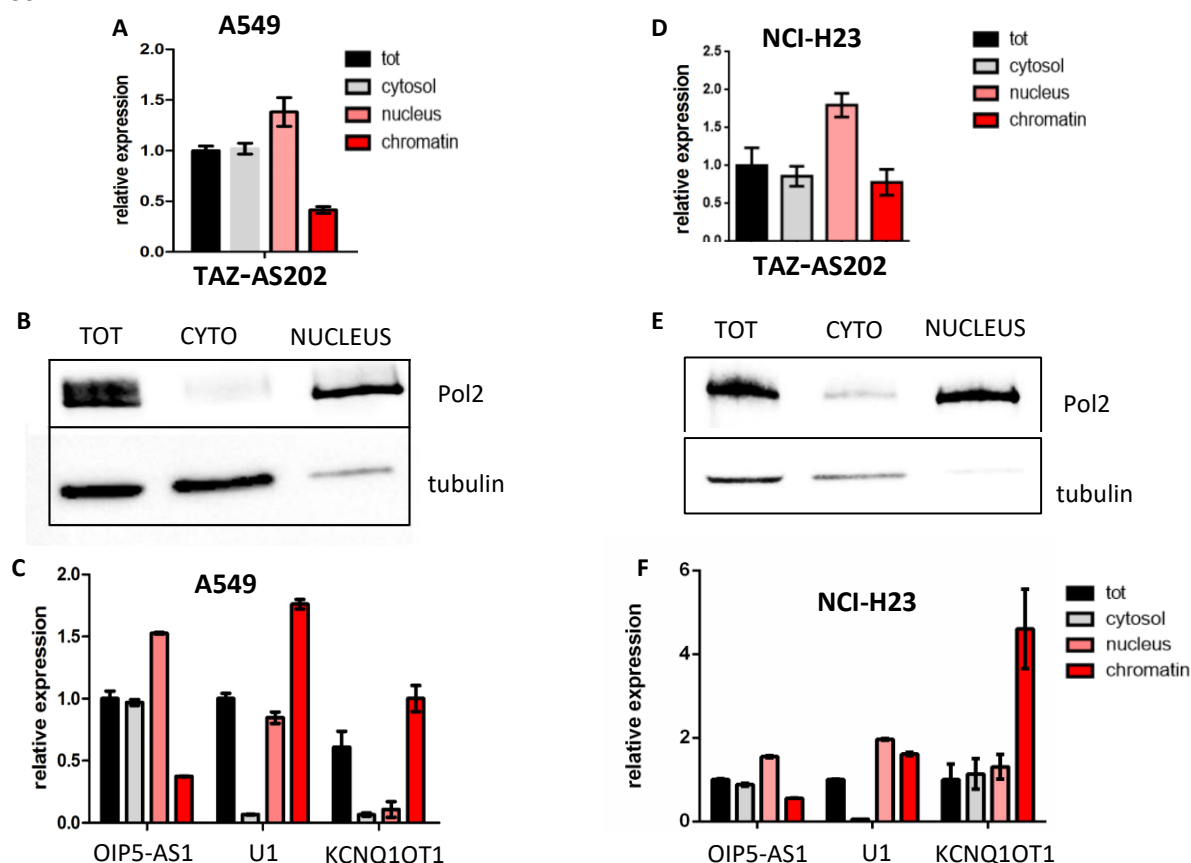
Figure 36: A) RT-qPCR showing TAZ-AS202 subcellular localization in A549 cells upon nucleus/cytosolic fractioning experiments. Data are expressed as mean +/- SEM **B)** Western blot with anti-Pol II or anti-tubulin antibodies on separated nucleus and cytosol fractions of A549 cells, used to check cross contamination between cytosolic and nuclear fractions. **C)** RT-qPCR on A549 cells showing subcellular localization of OIP5-AS1, U1 and KCNQ1OT1, used to check RNA cross-contamination between cytosol, nucleus and chromatin fractions, respectively. Data are expressed as mean +/- SEM **D)** RT-qPCR showing TAZ-AS202 subcellular localization in NCI-H23 cells upon nucleus/cytosolic fractioning experiments. Data are expressed as mean +/- SEM. **E)** Western blot with anti-Pol II or anti-tubulin antibodies on separated nucleus and cytosol fractions of NCI-H23 cells, used to check cross contamination between cytosolic and nuclear fraction. **F)** RT-qPCR on NCI-H23 cells showing subcellular localization of OIP5-AS1, U1 and KCNQ1OT1, used to check RNA cross-contamination between cytosol, nucleus and chromatin fractions, respectively. Data are expressed as mean +/- SEM.

__A functional interplay between TAZ and TAZ-AS202 controls TAZ-AS202 expression and TAZ activity in NSCLC cells__

We observed that TAZ-AS202 silencing is associated with decreased proliferation, motility and invasion capacity in NSCLC cells, similarly to TAZ downregulation. A growing amount of evidence on the biology of NATs supports their role in regulating the expression and/or the activity of neighbouring genes *in cis* through various mechanisms *(Faghihi, M.A. et al, 2009)*. Furthermore, we observed that TAZ-AS202 expression correlates with TAZ expression in a panel of cancer cells lines (**fig.37A**). Thus, our first hypothesis was that TAZ-AS202 may regulate TAZ expression or activity and be part of TAZ pro-oncogenic program. To verify this hypothesis, we downregulated TAZ-AS202 expression through siRNA transfection and we measured TAZ mRNA and protein levels, phosphorylation and nucleus/cytoplasmic localization in comparison to control cells (**fig.37B-C,37F**). Strikingly, no differences were observed in TAZ, implying a different mechanism behind lncRNA function. Moreover, TAZ-AS202 silencing does not change either YAP mRNA, protein level, phosphorylation or nucleus/cytoplasmic localization (**fig.37D-F**). Intriguingly, the expression of YAP/TAZ/TEAD main target genes was significantly downregulated upon TAZ-AS202 silencing (**fig.37G**), suggesting a cooperation between YAP/TAZ and TAZ-AS202 in the regulation of common target genes through a still unknown mechanism. Supporting the interplay between TAZ and its cognate lncRNA, we also observed that TAZ silencing significantly downregulates the expression of TAZ-AS202 (**fig.37H**). This result suggests that TAZ may direct the expression of TAZ-AS202 transcript by binding on its own promoter. This hypothesis is supported by the presence of 5 binding sites for TEAD and one for SMAD3 on the promoter region shared between TAZ and TAZ-AS202 (**fig.11, Preliminary Data**)

Figure 37
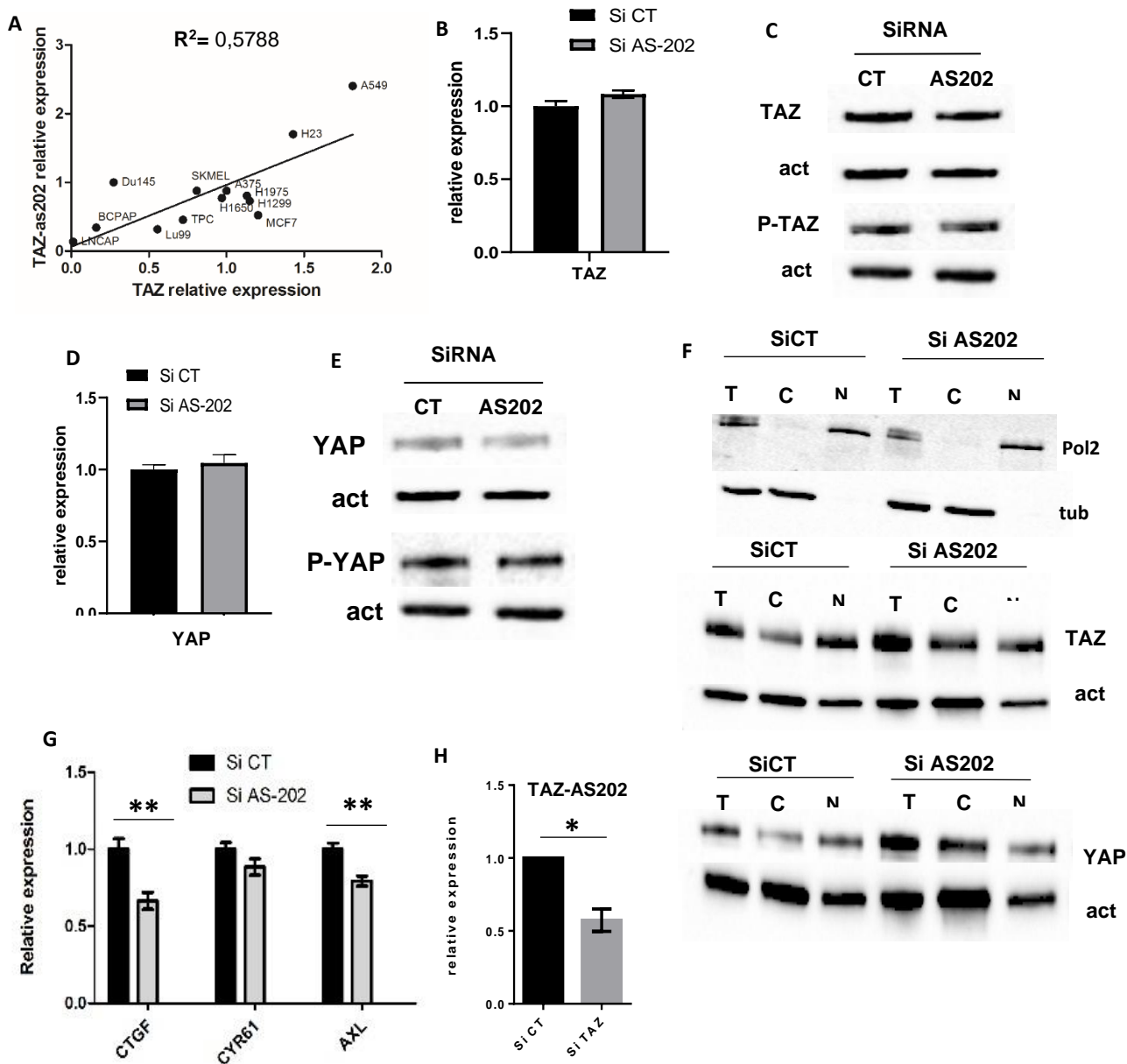
Figure 37: **A)** Graph showing positive correlation between TAZ-AS202 and TAZ expression in cancer cell lines. **B, D)** RT-qPCR showing TAZ and YAP mRNA levels upon transfection with siRNA against TAZ-AS202 for 48 hours compared to control cells. Data are expressed as mean +/- SEM. **C, E)** Western blot showing TAZ, phosphorylated-TAZ (P-TAZ), YAP and phosphorylated-YAP (P-YAP) protein levels after 48 hours transfection of siRNA against TAZ-AS202 compared to control cells. **F)** Western blot with anti-TAZ or anti-YAP antibodies on separated nucleus and cytosol fractions of A549 cells upon transfection with siRNA against TAZ-AS202 for 48 hours compared to control cells. Anti-tubulin and anti-RNA-Pol II antibodies were used to check cross contamination between cytosolic and nuclear fraction. T, C and N are total fraction, cytosolic fraction and nuclear fraction, respectively. **G)** RT-qPCR showing the expression level of YAP/TAZ main target genes (CTGF, CYR61 and AXL) on A549 cells upon transfection with siRNA against TAZ-AS202 for 48 hours compared to control cells. Statistical significance was calculated between SiRNA-treated cells compared to control cells. Data are expressed as mean +/- SEM. N=3 *p < 0.05, **p< 0.01, ***p<0.001. **H)** RT-qPCR showing TAZ-AS202 RNA expression upon transfection with siRNA against TAZ for 48 hours. Statistical significance was calculated between SiRNA treated cells compared to control cells. Data are expressed as mean +/- SEM. N=3 *p < 0.05, **p< 0.01, ***p<0.001.

RNA-sequencing identifies TAZ-AS202-dependent transcriptional program

In the attempt to define TAZ and TAZ-AS202-dependent programs in NSCLC and to characterize which genes and pathways may explain the pro-oncogenic function of TAZ-AS202, transcriptome analysis was performed by RNA-sequencing (RNA-seq) on two independent biological replicates, upon transfection with siRNA against TAZ, TAZ-AS202 or a CT siRNA for 48 hours in A549 cells. The scheme of RNA-seq analysis pipeline is reported in the Materials and Methods section. Principal Component Analysis (PCA) plot revealed a clear separation between the three siRNA-treated conditions, displaying a good distribution of variance (**fig.38A**). Once completed the quality checks, we proceeded with the analysis of differentially expressed genes (DEGs). We identified 1673 genes upregulated and 1662 genes downregulated upon TAZ silencing compared to control cells, resulting in a total of 3335 deregulated genes. We identified 487 genes upregulated and 695 genes downregulated upon TAZ-AS202 silencing compared to control cells, resulting in a total of 1182 deregulated genes (**fig.38B**). Strikingly, we identified 533 genes that result commonly deregulated by TAZ and TAZ-AS202 silencing, corroborating the hypothesis of a functional interplay between TAZ and its cognate lncRNA (**fig.38C**). Then, we performed Reactome pathways enrichment analysis, to identify biological processes affected by downregulation of the two genes (**fig.38D-E**). As expected, genes deregulated by TAZ silencing belong to pathways involved in cell proliferation, apoptosis, migration, EMT and metastasis (**fig.38D**). Genes deregulated by TAZ-AS202 silencing belong to EPH-ephrin pathway, membrane trafficking and to tRNA aminoacylation (**fig.38E**). To further characterize the interplay between TAZ and TAZ-AS202, we performed Reactome pathway enrichment analysis on the 533 genes commonly regulated by TAZ and TAZ-AS202. Strikingly, this analysis underlines the potential overlapping function of TAZ and TAZ-AS202 in the regulation of signal transduction pathways related to cancer progression, including WNT-signalling and EPH-Ephrin pathway (**fig.38F**).

Figure 38

A

B

Exp. Condition	numb.of DEG*	numb. of UPreg	numb. of DOWNreg	0<log2(FC)<1	1≤log2(FC)<2	Log2(FC)>=2
siTAZ_vs_siCT	**3,335**	1673	1662	3086	238	11
siAS-202_vs_siCT	**1,182**	487	695	1,094	87	1

C

TAZ DEGs   AS-202 DEGs

2802   533   649

significativity threshold: adj_pv < 0.05

D

Si TAZ vs SiCT   Reactome analysis

E

Si TAZ-AS202 vs SiCT   Reactome analysis

F

Int SiTAZ Si TAZ-AS202   Reactome analysis
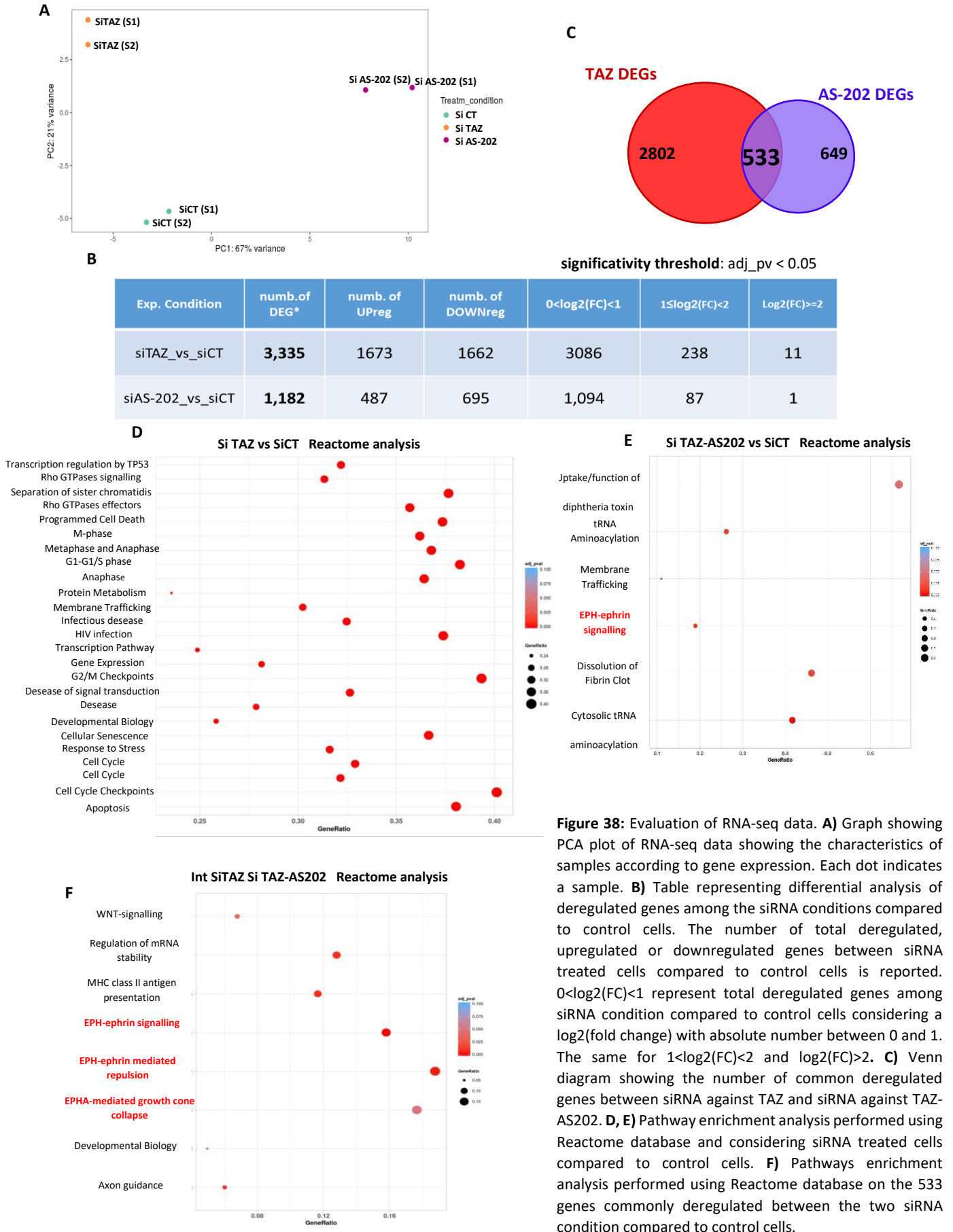
Figure 38: Evaluation of RNA-seq data. **A)** Graph showing PCA plot of RNA-seq data showing the characteristics of samples according to gene expression. Each dot indicates a sample. **B)** Table representing differential analysis of deregulated genes among the siRNA conditions compared to control cells. The number of total deregulated, upregulated or downregulated genes between siRNA treated cells compared to control cells is reported. 0<log2(FC)<1 represent total deregulated genes among siRNA condition compared to control cells considering a log2(fold change) with absolute number between 0 and 1. The same for 1<log2(FC)<2 and log2(FC)>2. **C)** Venn diagram showing the number of common deregulated genes between siRNA against TAZ and siRNA against TAZ-AS202. **D, E)** Pathway enrichment analysis performed using Reactome database and considering siRNA treated cells compared to control cells. **F)** Pathways enrichment analysis performed using Reactome database on the 533 genes commonly deregulated between the two siRNA condition compared to control cells.

TAZ and TAZ-AS202 promote migration and proliferation by controlling the expression of EPHB2
(B-type EPH receptor 2)

By RNA-seq analysis, we found a significant enrichment of EPH-ephrin signalling and WNT signalling between genes commonly regulated by TAZ and TAZ-AS202 (**fig.38F**): both these pathways are related to cancer cells proliferation, migration and Epithelial to Mesenchymal Transition (EMT). Intriguingly, while TAZ interplay with WNT signalling is well characterized, TAZ role in regulating EPH-ephrin pathway has never been reported. EPH-ephrin pathway has been a matter of intensive investigation because of its role in physiology and cancer. Interaction between ephrin ligands and EPH receptors generally regulates cell-cell interactions, promoting or inhibiting cell proliferation and/or migration, depending on the context. Members of this pathway have been described either as pro-oncogenic or tumor suppressive factors.

In lung cancer cells, we observed that TAZ or TAZ-AS202 silencing results in deregulation of several members of EPH-ephrin pathway, possibly explaining proliferation and migration deficiency observed in these conditions. First, we validated RNA-seq results, by measuring the expression of a list of genes belonging to EPH-ephrin signalling, including EPHB2, MYH10, DNM1, AP2M1, CLTCL1, ROCK2, SRC and VAV2 in NSCLC cells transfected with siRNA against TAZ or TAZ-AS202, compared to control (**fig.39A-C**). As expected, the majority of these genes are downregulated upon TAZ or TAZ-AS202 silencing in A549, NCI-H23 and NCI-H1299 cells. Among these, EPHB2 is one of the most deregulated in all cell lines. EPHB2 is a central node in EPH-ephrin pathway, encoding one of the three B-type EPH receptors, which initiates EPH forward signalling upon binding to ephrins ligands (**fig.39A-D**). Furthermore, its expression is upregulated in many cancer tissues and correlates with bad prognosis in lung cancer, even if few in vitro data are available in the lung cancer context *(Zhao, C., 2017)*. For these reasons, we selected EPHB2 for further experiments. To determine if TAZ and TAZ-AS202 pro-oncogenic activity may be due to EPHB2 regulation, we silenced EPHB2 through siRNA transfection in A549, NCI-H23 and H1299 NSCLC cells, obtaining a significative downregulation of specific mRNA and protein (**fig.39E**). Growth curves demonstrated that, as for TAZ and TAZ-AS202 downregulation, EPHB2 silencing impairs A549 and H1299 cells proliferation (**fig.39F**). Next, wound-healing assay was performed to determine the effect of EPHB2 silencing on migratory ability of NSCLC cells (**fig.40**). The results of wound-healing assay indicated that A549 and NCI-H23 cells silenced for EPHB2 migrate slower than control cells, as observed for TAZ and TAZ-AS202 silenced cells (**fig.40A-B**). A minor effect was also seen in NCI-H1299 cells (**fig.40C**). Furthermore, invasion assay through Matrigel matrix was conducted to evaluate the effect of EPHB2 silencing on the invasive ability of A549 cells. The results demonstrated that the ability to invade

through matrigel matrix was significantly decreased in EPHB2-silenced cells **(fig.41A-B)**. Overall, our results suggest that TAZ, TAZ-AS202 and EPHB2 control proliferative, migratory and invasive properties of NSCLC cells *in vitro*. Nevertheless, EPHB2 overexpression should be performed to rescue the phenotype resulting from TAZ and TAZ-AS202 downregulation and to demonstrate that TAZ/TAZ-AS202/EPHB2 axis is relevant during lung cancer progression.
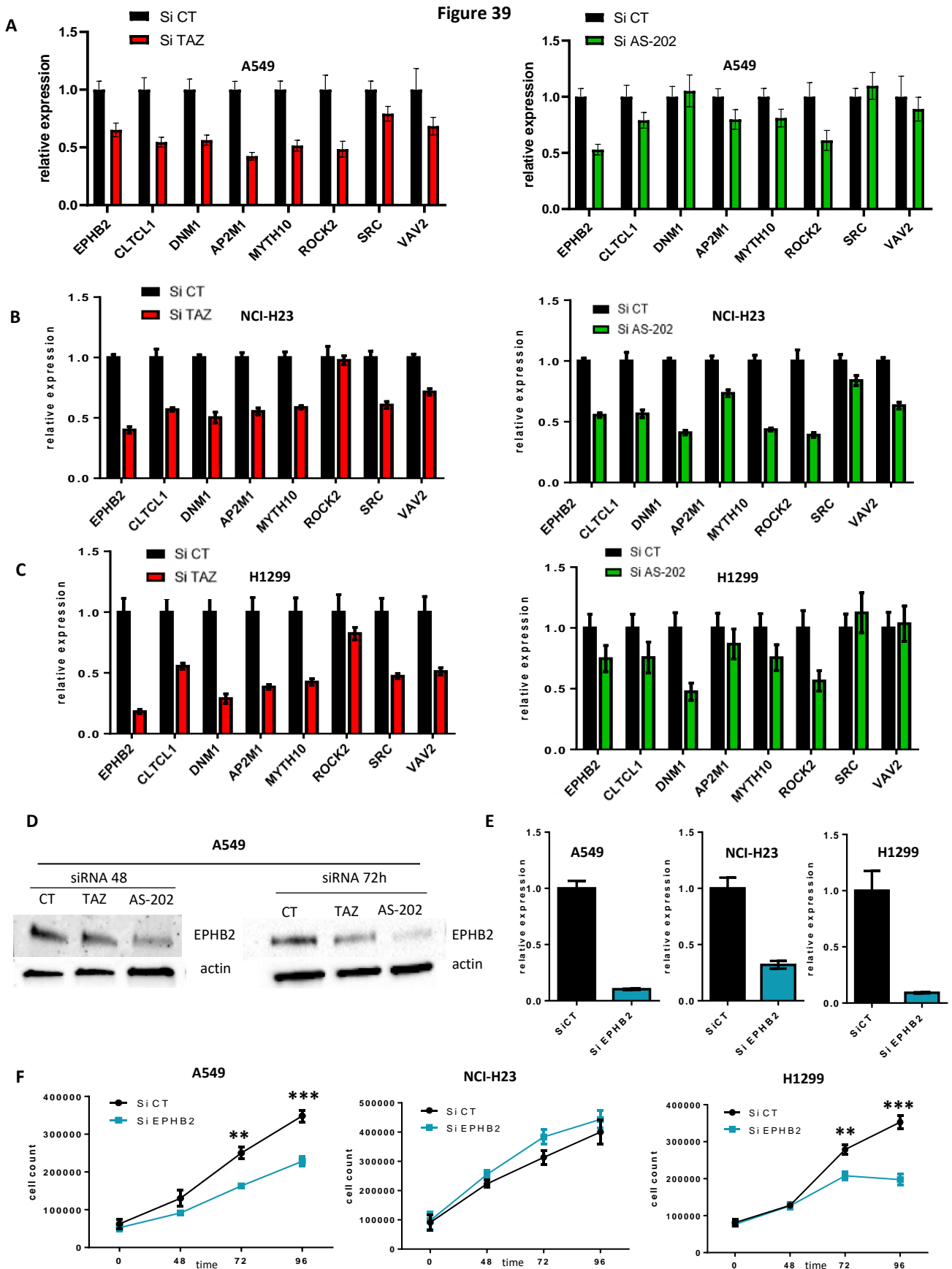
Figure 39: A, B, C) RT-qPCR showing the expression of EPH-ephrin genes upon transfection with siRNA against TAZ and TAZ-AS202 for 48 hours compared to CT siRNA in **A)** A549, **B)** NCI-H23 and **C)** H1299 cells. Data are expressed as mean +/- SEM. **D)** Western blot showing EPHB2 protein levels upon transfection with siRNA against TAZ and TAZ-AS202 for 48 or 72 hours in A549 cells compared to control cells. **E)** RT-qPCR showing EPHB2 mRNA downregulation upon 48h of siRNA transfection against EPHB2 in A549, NCI-H23 and H1299 cells. Data are expressed as mean +/- SEM. **F)** Growth curves generated by Trypan blue count of viable cells at different time points after transfection with siRNA against EPHB2, on A549, NCI-H23 and H1299 cells. Statistical significance was calculated between SiRNA treated cells and CT cells. Data are expressed as mean ± SEM. N = 6, *p < 0.05, **p< 0.01, ***p<0.001.

Figure 40
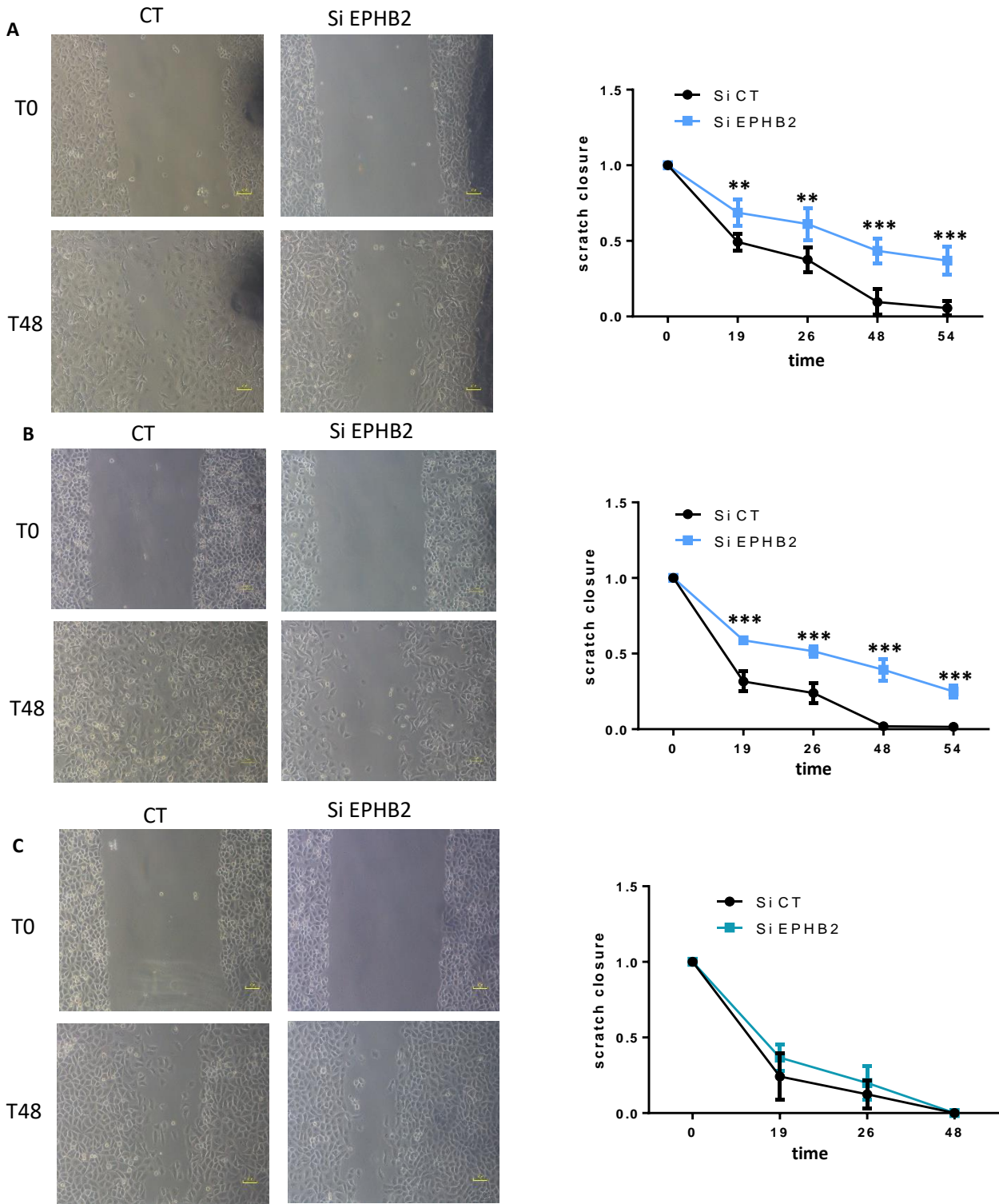
Figure 40: Migration ability of **A)** A549 cells, **B)** NCI-H23 cells and **C)** H1299 cells transfected with siRNA against EPHB2 compared to control cells, measured by scratch wound-healing assay. On the left, the wound closure 48 hours after the scratch is reported. On the right, wound closure rate. The area of the scratch was measured at different time points from the scratch in **A)** A549, **B)** NCI-H23 and **C)** H1299 cells. The area of the scratch was measured using ImageJ software. The area at each time point was normalized to the area at T0 and statistical significance was calculated between CT treated cells and siRNA treated cells. Data are expressed as mean ± SEM. N = 6, *p < 0.05, **p< 0.01, ***p<0.001.

Figure 41

A

B
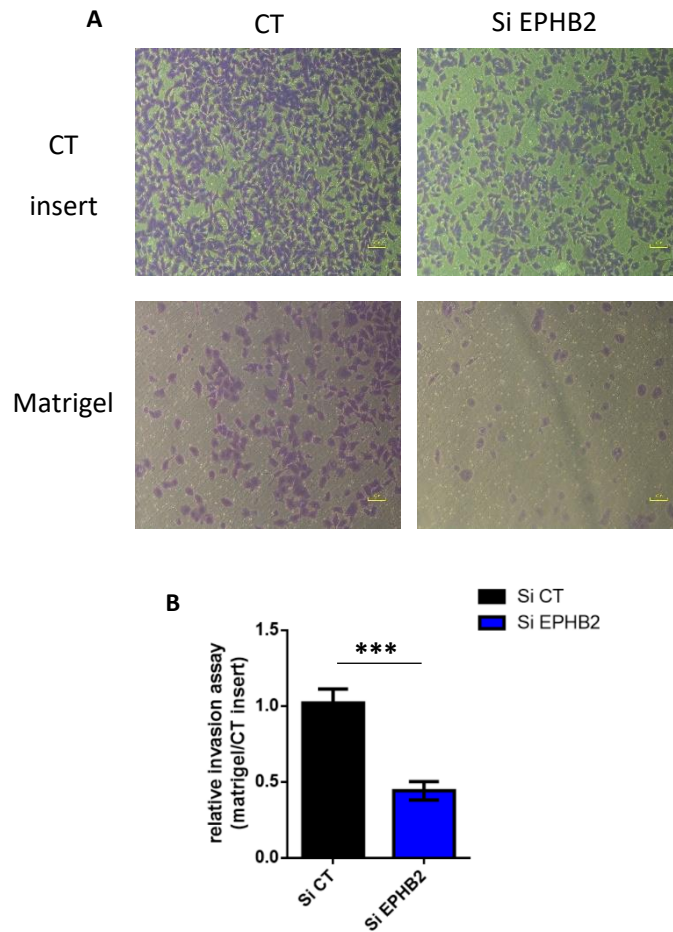
Figure 41: Invasion ability of A549 cells. **A)** Cells were transfected with siRNA against EPHB2 or control. Images of invading cells were taken 72h from transfection. **B)** Graph showing the rate of invasion. Cells were counted using ImageJ software and the number of cells for each condition was normalized on the number of cells in the control insert conditions. Data are expressed as mean ± SEM. N = 8, *p < 0.05, **p< 0.01, ***p<0.001.

TAZ-AS202 controls EPHB2 expression through a transcriptional and indirect mechanism

Our data indicate for the first time that TAZ and TAZ-AS202 have a role in regulating EPH-ephrin signalling. Next, we started to dissect the mechanism through which TAZ-AS202 regulates EPHB2 expression. To this end, we downregulated TAZ-AS202 through siRNA transfection and we treated cells with the transcription inhibitor Actinomycin D or DMSO (MOCK). As shown in **fig.42A**, actinomycin D blocks the effect of TAZ-AS202 silencing on EPHB2, demonstrating that this lncRNA regulates EPHB2 through a transcriptional mechanism. Next, to verify whether this mechanism is direct, we treated A549 cells with the protein synthesis inhibitor cycloheximide or DMSO (MOCK). As shown in **fig.42B**, cycloheximide blocks the effect of TAZ-AS202 silencing, demonstrating that this lncRNA regulates EPHB2 through an indirect mechanism. These data suggest that TAZ-AS202 may regulate EPHB2 through the regulation of another unknown transcriptional or co-transcriptional factor which in turn directly regulates EPHB2 expression.

Figure 42

Figure 42: A) RT-qPCR showing the expression of EPHB2 upon transfection with siRNA against TAZ-AS202 and treatment with DMSO (MOCK) or actinomycin D. 24 hours after transfection with siRNA against TAZ-AS202 or control siRNA, cells were treated with DMSO (MOCK) or actinomycin D at the concentration of 5µg/ml and RNA was collected after 8 hours. Data are expressed as mean ± SEM. N = 3, *p < 0.05, **p< 0.01, ***p<0.001. **B)** RT-qPCR showing the expression of EPHB2 upon transfection with siRNA against TAZ-AS202 and treatment with DMSO or cycloheximide. 24 hours after transfection with siRNA against TAZ-AS202, cells were treated with DMSO (MOCK) or cycloheximide at the concentration of 50µg/ml and RNA was collected after 24 hours. Data are expressed as mean ± SEM. N = 3, *p < 0.05, **p< 0.01, ***p<0.001.

TAZ-AS202 controls the transcription and the stability of mRNAs for several transcription factors

Since we observed that TAZ-AS202 regulates EPHB2 expression through an indirect transcriptional mechanism, we reasoned that TAZ-AS202 may control the expression of transcription factors that in turn may induce or repress EPHB2 expression.

From our RNA-Seq analysis, we identified several transcriptional factors whose expression is deregulated by TAZ-AS202 silencing, including: KLF2, FOSL2, JUNB, KLF4, SMAD7, SP6 and TCF7. Strikingly, all these factors have been reported to have a role in cancer development and progression and may be involved in EPHB2 regulation as well.

To explore this hypothesis, we verified if lncRNA-dependent regulatory activity on these genes is transcriptional, direct/indirect. To this end we downregulated TAZ-AS202 in A549 cells through siRNA transfection. 24 hours after siRNA transfection, we treated cells for 24 hours with protein synthesis inhibitor cycloheximide or DMSO (MOCK). As seen in **fig.43B-G**, cycloheximide is able to block the effect of TAZ-AS202 silencing on FOSL2, JUNB, SMAD7, SP6 and TCF, implying that the lncRNA regulates these transcriptional factors through an indirect mechanism. On the contrary, cycloheximide does not block the effect of TAZ-AS202 silencing on KLF2 (**fig.43A**), implying that the lncRNA regulates this gene through a direct mechanism.

Next, to evaluate if the direct regulatory activity of TAZ-AS202 on KLF2 is transcriptional, we downregulated TAZ-AS202 in A549 cells through siRNA transfection. 24 hours after siRNA transfection, we treated cells for 8 hours with the transcription inhibitor actinomycin D or DMSO (MOCK). As expected, actinomycin D is able to block the effect of TAZ-AS202 silencing on FOSL2, JUNB, SMAD7, SP6 and TCF, implying that this lncRNA regulates these transcriptional factors through a transcriptional and indirect mechanism **(fig44B-G)**. Strikingly, actinomycin D does not block the effect of TAZ-AS202 silencing on KLF2 (**fig.44A**), implying that this lncRNA directly regulates the stability of KLF2 mRNA.

Figure 43
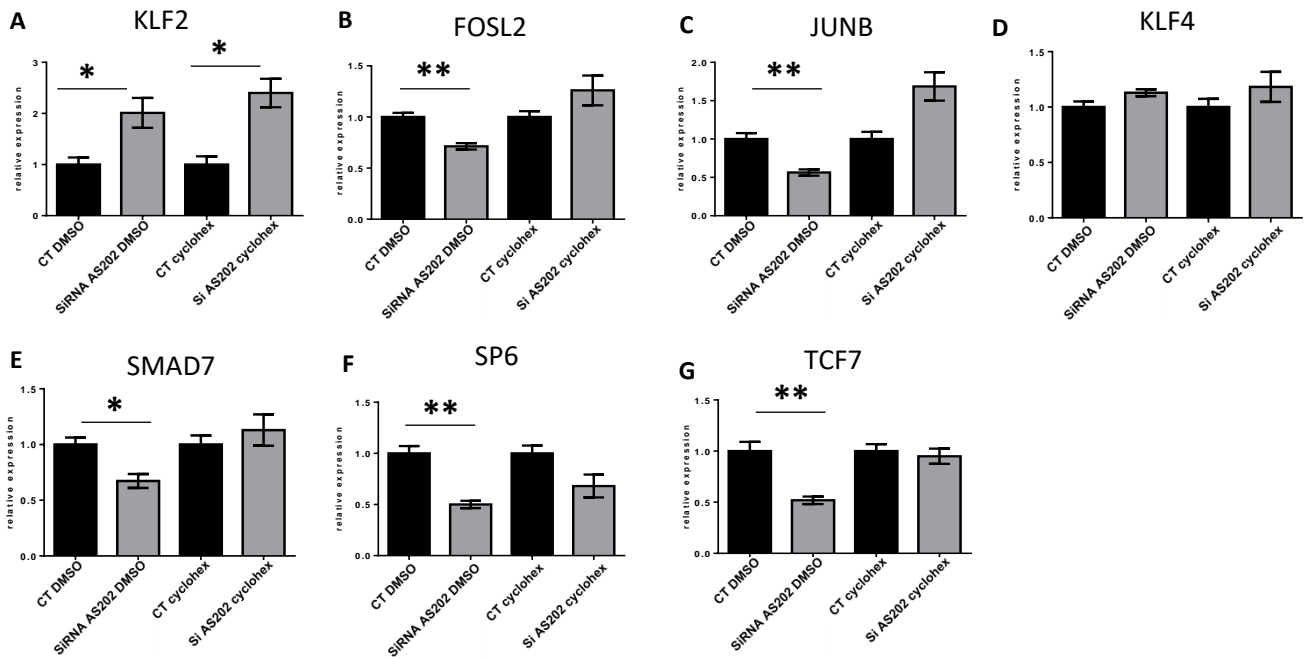
Figure 43: A-G) RT-qPCR showing the level of expression of TAZ-AS202 target genes upon SiRNA transfection against TAZ-AS202 with DMSO (MOCK) or cycloheximide. After 24h of siRNA treatment, cells were treated with cycloheximide and RNA pellet were collected 24h after. Statistical significance was calculated between CT treated cells and siRNA treated cells. Data are expressed as mean ± SEM. N = 3, *p < 0.05, **p< 0.01, ***p<0.001.
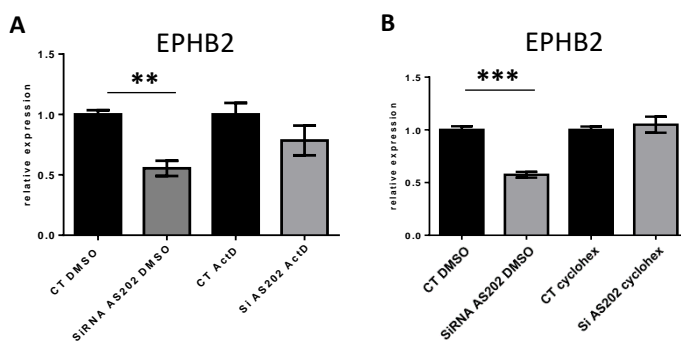
Figure 44
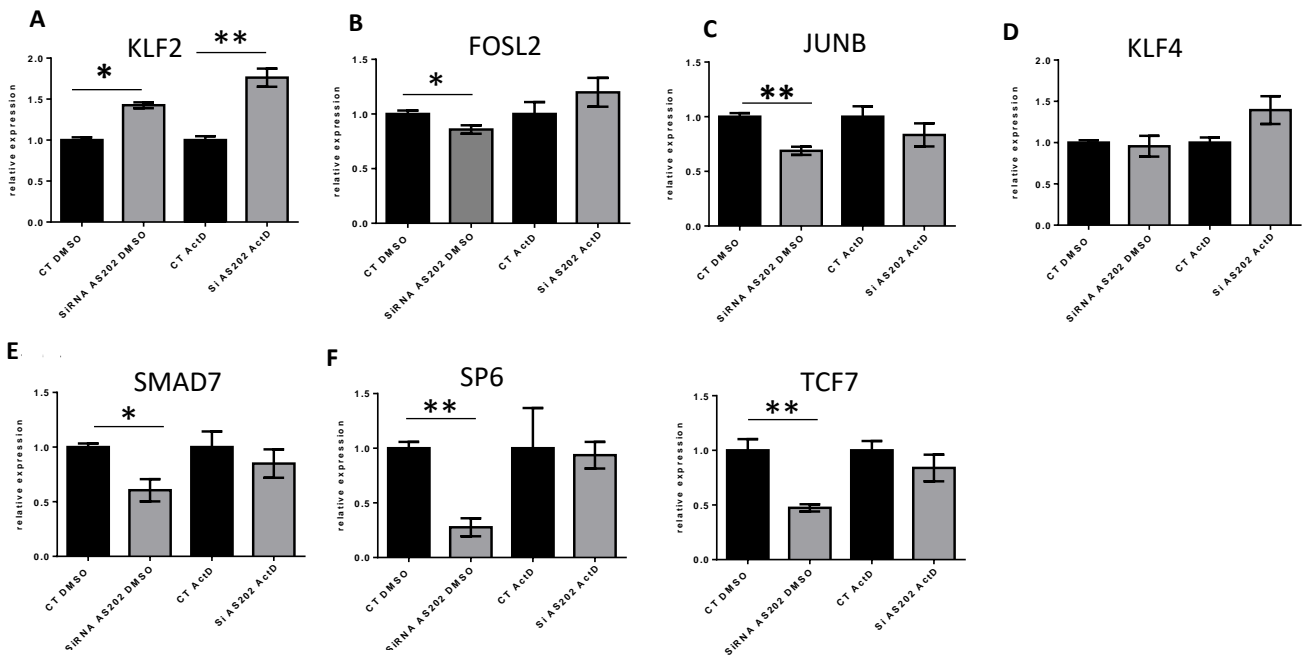
Figure 44: A-G) RT-qPCR showing the level of expression of TAZ-AS202 target transcriptional factors upon siRNA transfection against TAZ-AS202 with DMSO (MOCK) or actinomycin D (ActD). After 24h of SiRNA treatment, cells were treated with actinomycin D and RNA pellet were collected 8h after. Statistical significance was calculated between CT treated cells and siRNA treated cells. Data are expressed as mean ± SEM. N = 3, *p < 0.05, **p< 0.01, ***p<0.001.

DISCUSSION

In the first part of this work, we performed a genome-scale CRISPR/Cas9 screening on A549 NSCLC cells with the intent to identify genes and discover new mechanisms of resistance to BETi. This technique employed a large redundant library targeting virtually all genes in the human genome, holding the possibility to screen the whole genome for resistance and/or sensitivity genes to a given drug. With this approach, we showed for the first time that the increased TAZ activation, caused by independent loss of function of Hippo pathway genes LATS2, TAOK1 and NF2, causes resistance of lung cancer cells to BETi. In the proposed model, BRD4 binds to YAP, TAZ and TEAD promoters enhancing their expression and, treatment of lung cancer cells with BETi, causes BRD4 detachment from promoter regions; resulting in YAP, TAZ and TEAD downregulation. We showed for the first time that the downregulation of these genes is, at least in part, responsible of BETi cytotoxic effect in lung cancer cells. Loss of function of LATS2, TAOK1 and NF2 promotes TAZ nuclear localization and transcriptional activity, compensating the repression induced by BETi and sustaining resistance to this drug (**fig.45**).
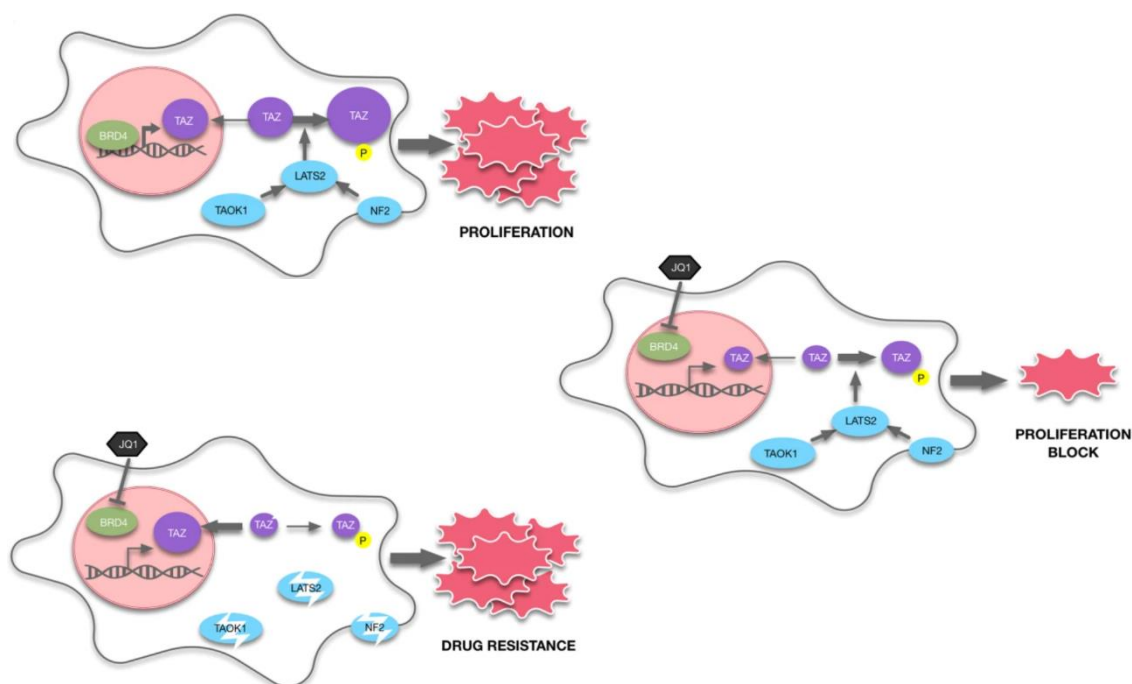
Figure 45: Proposed model of Hippo regulatory role on response to BETi drugs. **A)** TAZ transcription is enhanced through BRD4 binding on TAZ promoter regions, while TAZ protein activity is regulated by Hippo pathway that controls TAZ correct balancing between nucleus and cytosol. **B)** Treatment of lung cancer cells with JQ1 results in BRD4 detachment from TAZ promoter regions and TAZ downregulation at transcriptional level, thus causing proliferation block. **C)** In a context in which LATS2, TAOK1 and NF2 are inactivated, TAZ is more nuclear and more active, thus compensating BETi effects and inducing resistance. *This picture is from Gobbi et al, 2019.*

BETi have shown efficacy on pre-clinical models and entered in the first phases of clinical trials for both hematological and solid tumors, including lung cancer (see for example NCT04309968, NCT03205176, NCT03936465; source www.clinicaltrial.gov). However, early results of clinical trials showed limited efficacy on unselected groups of patients affected by solid tumors *(Postel-Vinay, S. et al, 2019)*. These results highlight the need to provide biomarkers that can be used to select patients that may benefit from the therapy. Our work is the first presenting the involvement of the Hippo signaling in regulating response to BETi in lung cancer.

In lung cancer context, it has been shown that inactivating mutations of LKB1 (STK11) in KRAS-mutated NSCLC increased resistance to the BETi JQ1 *(Shimamura, T. et al, 2013)*. LKB1 is a tumor suppressor gene encoding a protein with kinase activity able to control AMPK and mTOR signaling. This protein is mutated in a high percentage of NSCLC patients, approximately 15-30%. We observed that LKB1 is not present in the list of sensibility genes from our RNA-seq. This is expected, since LKB1 is mutated and hence inactive in A549 cells. However, our data confirm the existence of a link between LKB1 and BETi response. Indeed, LKB1 is also an upstream regulator of YAP and TAZ activity: LKB1 phosphorylates MARK kinases that, in turn, phosphorylate and activate MST1/2 and LATS1/2 Hippo pathway kinases *(Mohseni, M. et al, 2014)*. These findings, together with our data, support the existence of an LKB1-Hippo-YAP/TAZ signaling that modulates response to BETi and suggest that mutations and/or alteration in this axis may be considered biomarkers to predict BETi response in NSCLC patients.

Strikingly, our findings expand the comprehension on the cytotoxic effect of BETi treatment on cells. BETi are epigenetic drugs which cause the block of cancer cells proliferation and enhance apoptosis through the downregulation of known oncogenes to which cancer cells are addicted. The main genes downregulated upon BETi treatment are c-MYC, FOSL1, BCL2, WNT5A, RUNX2 and KIT *(Donati, B. et al, 2018; Dawson, M. et al, 2011; Lockwood, W.W. et al, 2012; Loven, J. et al, 2013; Sancisi, V. et al, 2017)*. Specifically, in lung cancer, BETi have been shown to exert anti-oncogenic properties through c-MYC and FOSL1 repression. In this study, we showed, for the first time, that BRD4 regulates YAP, TAZ and TEAD and BETi attenuate cancer cells proliferation, at least in part, through the repression of these oncogenes at transcriptional level, with consequent loss of downstream oncogenic program activation. Importantly, our model does not exclude the other mechanisms described, but could be concomitant, adding a new mechanism explaining BETi anti-cancer activity.

YAP and TAZ are paralogues, often considered as functionally redundant in cellular functions. Strikingly, our data are not in agreement with this conception. We observed an important difference between YAP and TAZ in our model of NSCLC: TAZ KO attenuates cell proliferation and sensitizes cells to BETi treatment while YAP KO does not attenuate cell proliferation and does not sensitize cells to BETi treatment. Moreover, alteration in these genes seems to exert different effects also on patient's prognosis, being overexpression or amplification of TAZ, but not of YAP, associated with a worse prognosis. These data are in line with the emerging literature considering TAZ and YAP function not completely overlapping. Indeed, structural differences, differential expression, different post-translational modifications and distinct interacting partners support the existence of a different role for YAP and TAZ in specific contexts, from morphogenesis to diseases *(Reggiani, F. et al, 2020)*.

Hippo Pathway is described as a well-conserved signalling cascade which consists in several proteins equally inhibiting both TAZ and YAP activity. On the contrary, we found that, in lung cancer context, the inactivation of LATS2, TAOK1 or NF2 significatively change only TAZ localization, resulting in TAZ, but not YAP, nuclear accumulation. We may speculate that, given the redundancy of Hippo Pathway, the different Hippo Pathway members selectively or preferentially regulate TAZ or YAP. This selective regulation may be context-dependent and may rely on the distinct structural features of these two proteins, including specific post-translational modifications, or on the interaction with different partners.

In the breast cancer context, it has been reported that BETi specifically suppress YAP/TAZ-dependent transcription (*Zanconato, F. et al, 2018*). However, the molecular mechanism proposed is different: BRD4 directly associates to YAP and TAZ to form a complex that activates the expression of target genes. Treatment of breast cancer cells with BETi disrupts this association, leading to downregulation of YAP/TAZ target genes. The model proposed in our study is slightly different but not entirely in contrast with the mechanism proposed by Zanconato F et al. It may be hypothesized that these two different mechanisms occur in different cancer contexts or that they are concomitant, at least in some cases, reinforcing the inhibitory effect of BETi treatment on YAP and TAZ transcriptional program.

Although limited to in vitro experiments, our data are in line with other studies which report that YAP and TAZ are modulators of response to different anti-cancer drugs as, cisplatin, gemcitabine and TKi. Overall, our data support a general role for Hippo Pathway and YAP/TAZ in modulating the response to various anti-cancer compounds. Moreover, since YAP and TAZ overexpression in tumors

has been associated with aggressive features, shorter patient's survival and resistance to anti-cancer drugs, our data suggest that BETi may be used in combination therapy to downregulate YAP and TAZ expression, counter-acting their pro-oncogenic activity and re-sensitizing cancer cells to other treatments. Giving that TAZ is a master transcriptional regulator, controlling the expression of a large number of target genes, it would be interesting, as a future prospect, to characterize which TAZ downstream specific effectors are directly involved in modulating response to BETi.

In the second part of this thesis, we studied the link between TAZ and its associated lncRNA TAZ-AS202 in lung cancer. TAZ expression is upregulated in 66% of NSCLC patients and our data show that lung cancer patients with high TAZ expression have worse prognosis. However, few mutations in the TAZ gene have been described, suggesting the existence of not fully characterized mechanisms regulating TAZ activity. TAZ-AS202 is a NAT whose transcription starts upstream TAZ promoter in antisense orientation. Its expression correlates with TAZ and exert a strong pro-oncogenic activity in vitro, being its silencing directly associated with a reduction of lung cancer cells proliferation, migration and invasion. Moreover, some main TAZ target genes are also regulated by TAZ-AS202 and 45% of TAZ-AS202 target genes are also regulated by TAZ. Based on these data and on well-characterized function of NATs in regulating neighbour genes *in cis*, our first hypothesis was that TAZ-AS202 regulated TAZ expression. Contrary to our hypothesis, our data demonstrated that TAZ-AS202 do not influence TAZ mRNA or protein levels. In addition, we demonstrated that TAZ-AS202 is not implicated either in regulating TAZ at post-translational level, since its expression does not influence TAZ phosphorylation or nucleo/cytoplasmic localization. Finally, we also showed that TAZ-AS202 do not influence YAP expression, phosphorylation or nucleo/cytoplasmic localization. These results suggest that TAZ-AS202 regulatory function on TAZ target genes is exerted through a different, still unknown mechanism. On the other hand, the interplay between TAZ and TAZ-AS202 is supported also by TAZ regulation on TAZ-AS202 expression. We hypothesize that TAZ controls the activity of its own promoter through direct binding. Indeed, binding sites for TEAD and SMAD factors are present on the promoter region shared between TAZ and TAZ-AS202. Based on observed influence of TAZ-AS202 on TAZ target genes and on influence of TAZ on TAZ-AS02 expression, we may speculate the existence of a positive autoregulatory crosstalk between TAZ and its cognate lncRNA in lung cancer (**fig.46**).
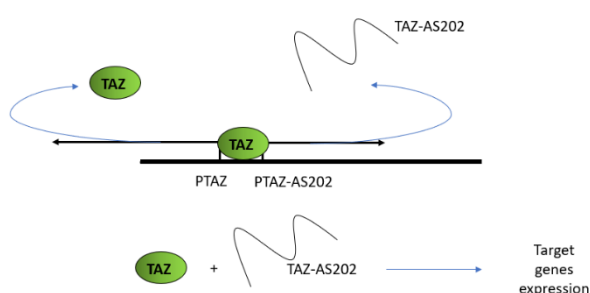
Figure 46: Proposed model of the crosstalk between TAZ and lncRNA in lung cancer. TAZ silencing downregulates TAZ-AS202 RNA suggesting that TAZ protein is required for lncRNA transcription. Subsequently, TAZ and TAZ-AS202 functionally cooperate to direct the transcription of target genes through a molecular mechanism yet to be characterized. In the graph, PTAZ and PTAZ-AS202 are TAZ and lncRNA promoter region, respectively.

71

Strikingly, in A549 cells, TAZ-AS202 silencing impairs cells migration more strongly than TAZ silencing, implying a more prominent role for this lncRNA in regulating migration capacity. This can be explained by the ability of TAZ-AS202 to regulate EPH-ephrin signalling. In particular, we demonstrated that TAZ-AS202 regulates the expression of the EPHB2 receptor, a central node of this pathway, through an indirect and transcriptional mechanism.

EPHB2 encodes a member of the B-type receptors belonging to EPH-ephrin signalling, a biological process with a key role during both embryogenesis and cancer progression. The main function of this pathway is the perception of cell-cell contacts which results in the control of migratory ability of cells. In lung cancer patients, EPHB2 overexpression correlates with a worse prognosis *(Zhao, C., 2017)*, but the molecular mechanism that regulates EPHB2 transcription and activity had never been described.

Downregulation of EPHB2 expression and, in general, attenuation of EPH-ephrin signaling upon TAZ-AS202 silencing might explain the phenotypic changes observed in lung cancer cell lines.

Confirming this hypothesis, we showed that EPHB2 silencing results in the attenuation of cell migration, proliferation and invasion. In our proposed model, TAZ and TAZ-AS202 functionally cooperate for EPHB2 expression, while EPHB2 supports lung cancer cells features, implying the relevance of EPHB2 as fundamental downstream effector of both TAZ and TAZ-AS202. Even if further experiments are required, we can speculate that the presence of EPHB2 supports lung pro-oncogenic features through the interaction with ephrins ligands and the activation of downstream EPH-ephrin signalling. Interestingly, increasing literature on EPH-ephrin signalling role in cancer prompted the development of monoclonal antibodies against EPH receptors that already entered in the first phases of clinical trials for glioblastoma, glioma and different solid tumors (see for example NCT03374943 and NCT02252211; source http://www.clinicaltrial.gov). Such treatments may be considered a further tool to blunt TAZ and TAZ-AS202 pro-oncogenic activity at the level of their downstream target EPHB2.

The characterization of the molecular mechanism through which TAZ-AS202 regulates EPHB2 expression is object of our ongoing study. Our data show that the lncRNA regulates EPHB2 through a transcriptional and indirect mechanism. Thus, we suppose that TAZ-AS202 may regulates a transcriptional factor, which in turn regulates EPHB2. RNA-seq analysis revealed the presence of several transcriptional factors positively or negatively regulated by the lncRNA. The relevance of each of these transcription factors has been well characterized in cancer progression, EMT and

metastasis. Among these, KLF2 particularly attracted our attention. Indeed, while TAZ-AS202 regulates the expression of the others transcriptional factors through an indirect mechanism, its silencing induces an increase of KLF2 mRNA, through a direct post-transcriptional mechanism, suggesting that its function may be to negatively regulates KLF2 mRNA stability. The KLF (Kruppel-like) factor family of proteins, consists of a set of transcription factors that are present in various organisms and are involved in differentiation and proliferation (*Black, A.R. et al, 2001*). KLF2 is a member of this family and exerts onco-suppressive functions in various cancer settings by enhancing apoptosis, differentiation and inhibiting cells growth. The anti-cancer functions exerted by KLF2 are explained by both inducing the expression of onco-suppressors and repressing the expression of oncogenes (*Wang, F. et al., 2005; Yuedi, D. et al. 2020*), among which EPHB2 may be included.

Even if several further experiments are needed to demonstrate this hypothesis, we can speculate that the presence of TAZ-AS202 may destabilize the mRNA of the onco-suppressor KLF2, which, on turn, may regulate EPHB2 expression through a molecular mechanism yet to be determined. On the contrary, lncRNA downregulation stabilizes KLF2 mRNA, leading to EPHB2 downregulation. In this proposed model, KLF2 may function as EPHB2 direct repressor or suppress EPHB2 expression through an indirect mechanism. Even if to date we still not have enough experimental evidences supporting this model, it has just been demonstrated that the stability of KLF2 mRNA is influenced by the TINCR lncRNA (terminal differentiation-induced non-coding RNA) in gastric cancer *(Xu, T.-P. et al. S, 2015)*. In addition, we observed the presence of putative KLF2 binding sites on EPHB2 promoter region and on two enhancer regions located in the first and the third introns of EPHB2 gene. This observation suggests that KLF2 may directly bind to EPHB2 regulatory regions to control its transcription.

Overall, even if limited by in vitro experiments, our data suggest for the first time the relevance of lncRNA TAZ-AS202 activity in controlling lung cancer cells proliferation, motility and invasion. Although the molecular mechanism underlying this role is still object of further studies, we showed that the EPH-ephrin signaling receptor EPHB2 is an important effector downstream TAZ and TAZ-AS202 activity. In future, the possibility to develop anti-cancer drugs against EPHB2, may be used to counteract TAZ and TAZ-AS202 downstream pro-oncogenic transcriptional program in lung cancer.

MATERIALS and METHODS

Cell cultures

A549, NCI-H23, H1299, NCI-H1975, MCF7, LNCAP and DU145 cell lines were obtained from Dr. Massimo Broggini (IRCCS-Istituto di Ricerche Farmacologiche Mario Negri Milan, Italy). BCPAP and TPC1 cells lines were obtained from Prof. Massimo Santoro (University of Naples, Naples, Italy). A375, SK-Mel28 and MDA-MB-231 cells lines were obtained from Dr. Adriana Albini (Institute for Reaserch and Treatment (IRCCS) MultiMedica, Milan, Italy). HEK293T cells lines were obtained from ATCC (LGC Standards, Sesto San Giovanni, Italy). All cell lines were authenticated by SNP profiling at Multiplexion GmbH. All cell lines were grown at 37°C and 5% CO2. A549, NCI-H23, NCI-H1975, H1299, LNCAP and DU145 were grown in RPMI medium supplemented with 10% fetal bovine serum and antibiotics (penicillin and streptomycin). The remaining cell lines were grown in DMEM medium supplemented with 10% fetal bovine serum and antibiotics.

Lentiviral Infection

For each lentiviral infection, lentiviral particles were obtained from HEK-293T cell line. Approximately 150000 HEK-293T cells were seeded in a 24-well plate in transfection culture medium (complete medium without Penicillin/Streptomicin). The day after, HEK-293T cells were transfected with a mix of the transfer plasmid of interest and the packaging/envelope plasmids: pRSV-Rev, pMDLg/pRRE and pMDG.2. pRSV-Rev, pMDLg/pRRE and pMD2.G were a gift from Didier Trono (Addgene plasmid # 12253, # 12251, # 12259) *(Dull, T. et al, 1998)*. For each transfection we used 500 ng of total DNA: 125ng of pRSV-Rev, 125ng of pMDLg/pRRE, 50ng of pMDG.2 and 200ng of the plasmid of interest, using the following protocol: The plasmid mix was diluted in 50 ul of OptiMEM. In parallel, we diluted 1.5ul of Lipofectamine2000 (Thermo Fischer Scientific) in 50ul of OptiMEM and incubated for 5 minutes. The two solutions were mixed and incubated for 25 minutes at room temperature. Finally, the final mix of plasmids was added on HEK-293T. Viral surnatant was collected 48 hours after transfection. It has been filtered through 0.45µm filters and polybrene was added at a final concentration of 2µg/ml. Viral suspension was added to cells and, then, centrifugated at 1800 rpm for 45' at 32°C. Cells were incubated at 37°C in the incubator. 4 hours after, the medium was replaced with normal medium. The day after, antibiotic selection started for one week. We used blasticidin 12,5µg/ml (Invivogen, Toulouse, France) or Puromycin 1µg/ml (Life Thecnologies, Monza, Italy).

Generation of A549, NCI-H23 and NCI-H1975 stably expressing CAS9

For Cas9 expression, cells were infected with lentiviral particles containing lentiCas9-Blast (gifted from Feng Zhang; Addgene plasmid #52962) (*Sanjana et al, 2014*). For A549, cells were infected in 24 wells and, the day after, blasticidin selection started. After selection, cells were seeded in 96 wells at the concentration of 1 cell for well for isolating clones. We tested each clone by Western blotting with anti-Flag antibodies (F1804, Sigma Aldrich) and we choose the clones with the highest Cas9 expression (clone #19) to perform the screening and the subsequent experiments. For NCI-H23 and NCI-H1975, Cas9 expression was verified in the pool of blasticidin resistant cells by Western blotting. The pool was used for subsequent experiments.

Generation of LATS2, TAOK1, NF2, YAP and TAZ knockout pools

Sequences of 3 sgRNAs for each target gene have been cloned in LentiGuide-Puro plasmid (sequences below) into BsmBI site (*Sanjana NE, 2014*). For lentiviral particles production, HEK-293T were transfected with a mix of the transfer plasmid of interest (LentiGuide-Puro + sgRNA) and the packaging/envelope plasmids (see *Lentiviral infection section)*. A549/Cas9, NCI-H23/Cas9 or NCI-H1975/Cas9 were infected as previously described (see *Lentiviral infection paragraph*). The day after the infection, puromycin selection started. Puromycin was used 1μg/ml for 1 week. After puromycin selection, the presence of the mutation at genomic level (indel) was verified by T7 endonuclease I cleavage assay (ALT-R kit, Integrated DNA Technologies, Skokie, Illinois, USA), following instructions described in the next paragraph.

Alt-R Genome Editing Detection Kit

After 1 week of antibiotic selection, sgRNA infected cells were washed with 100ul of PBS1X and lysed with 50ul of QuickExtract DNA Extraxtion Solution (Lucigen, Wisconsin, USA). Lysed cells were incubated for 10 minutes at 65°C and for 5 minutes at 98°C. Total lysed cells were diluted in 100ul of Nuclease-Free Water. The PCR mixes were prepared as follows: 4ul of genomic DNA, 300nm of specific primers pairs reported in the **table4**, 0.3mM of dNTPs (Promega, Milan, Italy), 0.3ul of Phusion High-Fidelity DNA Polymerase (Thermo-Fisher, Monza, Italy), 5X of Phusion Polymerase HF-Buffer (Thermo-Fisher, Monza, Italy) and Nuclease-Free Water up to a final volume of 25ul. The PCR reactions were performed on Thermal-Cycler (BioRad, Segrate, Italy) following the reported protocol: 95°C for 3 minutes, 95°C for 30 seconds, 68°C for 30 seconds, 72°C for 1 minute. Next, we repeated these last three steps decreasing from 68°C to 58°C. Finally, we performed 28 cycles as follows: 95°C for 30 seconds, 58°C for 30 seconds, 72°C for 1 minute. After amplifying the specific genomic regions, we formed homo/heteroduplex in a final volume of 18ul using 10 ul of PCR sample, 6ul of Nuclease-Free Water and 2ul of T7E1 Reaction Buffer (10X). For homo/heteroduplex

formation we used the following protocol: 95°C for 10 minutes, from 95°C to 85°C with a decrease of 2°C for second, from 85°C to 25°C with a decrease of 0,3°C for second. Next, homo/heteroduplex were digested with 2 ul of T7 endonuclease 1 (1U/μl) for 1h at 37°C. The digestion products were visualized using 1% agarose gel. After 30 minutes of the run of the gel, the digestion was analyzed with BioRad GelDoc EZ Imaging System. The two digested bands for each lane (band1 and band2) were quantified and the percentage of INDEL was calculated as follows: 100*{1-RADQ [1-((band1+band2)/100)]}.

Off-target frequencies determination

To evaluate the extend of off-target sites mutations, a NGS custom panel of amplicons was designed, comprising for each sgRNA, the 9 highest-scoring off-target sites. Libraries were generated starting from 10ng of DNA extracted from each sgRNA infected cell line and control cell line infected with a non-targeting sgRNA, using AmpliSeq Custom DNA Panel for Illumina. The total pool was loaded into MiSeq Reagent Kit v2 (500 cycles) cartridge and 2X250 pair-end sequenced using Illumina MiSeq sequencer. FastQ files were generated by MiSeq Reported Software and loaded on Basespace Software (Illumina). The alignment of the reads was checked by Basespace using DNA Amplicon App. We included the indels that were present in sgRNA infected cells with a coverage of at least 2000X and a frequency higher than 0.5%. The frequency of genetic modification in off-target sites is reported in **Table 2** of the *Results section.*

SiRNA transfection

For RNA Interference transfections, silencer select siRNA oligos (Thermo Fisher Scientific, Monza, Italy) targeting TAZ, AS-202, AS-203, EphB2, BRD4 **(table4)** or control oligos were transfected using RNAiMax Lipofectamine (Thermo Fisher Scientific, Monza, Italy). 20 nM oligos targeting BRD4 and 25 nM oligos targeting the other genes were transfected following a reverse transfection protocol, in T25 6 wells or 24 wells culture plates. For reverse transfection in 24 well culture plates, a mix containing the selected siRNA (20 or 25 nM), 1.5 ul of RNAimax (Thermo Fisher Scientific) and 100ul OptiMEM was prepared. For reverse transfection in the other culture plates, each mix was added in the correct proportion. After 20 minutes incubation, cells were trypsinized and added to transfection mixes. For 24-well culture plates we used 80000/100000 cells per well. The cell number for the other containers was scaled proportionally to container area. For RT-qPCR and Western blot analyses of transfected cells, cells were harvested 48 hours after transfection; for proliferation, scratch wound-healing and invasion assays, cells were harvested and seeded in the respective culture plates 24 hours after transfection.

RNA extraction, Reverse Transcriptase Reaction and quantitative real time-PCR

Total RNA was extracted and purified with RNAesy Mini kit (Qiagen, Milan, Italy). RNA was quantified with Nanodrop 2000/2000c Spectrophotometer (Thermo Fisher Scientific, Monza, Italy) and 250/500 ng RNA was retrotranscribed using iScript cDNA kit (Biorad, Segrate, Italy). Total RNA was mixed with 1ul of RT enzyme, 5X iScript Buffer (dNTPs, oligo (dt), random hexamers, RNAse inhibitors, MGCl2) and Nuclease free water to 20ul of final volume. The reaction was performed in thermal cycler with the following protocol: 25°C for 5 minutes (priming), 45°C 1 hour (RT reaction) and 95°C for 1 minute (RT inactivation). The obtained cDNA was diluted with Nuclease Free Water for qPCR and used for qPCR reactions. To perform qPCR, we used Sso Fast EvaGreen Super Mix (BioRad, Segrate, Italy), containing Taq polymerase, dNTPs, buffer and EvaGreen staining reagent for detection. We added 300nM of each primer and water up to 10ul. qPCR was performed in specific 96-well plates and the detection was performed using CFX96 Real Time PCR Detection System (BioRad, Segrate, Italy). The protocol is as follows: 95°C for 30 seconds, 95°C for 5 seconds, 59°C for 5 seconds. Repeated for 40 cycles.

For relative target gene expression, we applied the $2^{-\Delta\Delta Ct}$ method, using cyclophilinA (*CYPA*) as reference gene.

Western blot

Total proteins were extracted using Passive Lysis Buffer (PLB) (Promega, Milan, Italy). PLB was diluted to 1x concentration and supplemented with Protease Inhibitor Cocktail (Roche, Monza, Italy). Protein extracts were incubated on ice for 20 minutes and quantified using Bradford Reagent (BioRad, Segrate, Italy). SDS-PAGE was performed using BioRad apparatus and Mini-Protean TGX pre-cast gels (BioRad, Segrate, Italy). After the run of the gel, proteins were transferred on a nitrocellulose membrane using Turbo Blot protocol (BioRad, Segrate, Italy). The nitrocellulose membrane was washed 5 minutes with a solution containing PBS1X and Tween 0,01% (Sigma-Aldrich, Milan, Italy). Next, the membrane was incubated in blocking solution (PBS1X, Tween 0,01% and milk 5%). For specific protein detection, we used the following primary antibody diluted 1:1000 in PBS1X, Tween 0,01% and milk 2,5%: rabbit anti-EphB2 (BioRad, Segrate, Italy), anti-NF2 (D3S3W, Cell Signaling Technologies), rabbit anti-AMOTL2 (ab182177, Abcam), rabbit anti-LATS2 (D83D6, Cell Signaling Technologies), rabbit anti-SPOP (ab1375371, Abcam), rabbit anti-TAOK1 (A300-524A, Bethyl), rabbit anti-BRD4 (A301-985A50, Bethyl), mouse anti-β-actin (AC-15; Sigma-Aldrich), mouse anti-α-tubulin (sc-8035, Santa Cruz), mouse anti-RNA-PolII (ab817, Abcam), rabbit anti-TEAD2

(orb382464, Biorbyt); for TAZ detection we used rabbit anti-YAP1/TAZ (D24E4; Cell Signaling Technologies). Anti-YAP1/TAZ detects only a faint staining for YAP1, thus, YAP1 staining was obtained with rabbit anti-YAP (D8H1Z, Cell Signaling Thecnologies). As secondary antibodies, diluted 1:5000 in PBS1X, Tween 0,01% and milk 2,5%, we used horseradish peroxidase-conjugated anti-rabbit, anti-mouse and anti-goat (GE Healthcare, Piscataway, NJ) and Clarity ECL Substrate (BioRad, Segrate, Italy). Before and after adding the solution containing secondary antibody, the membrane was washed with PBS1X and Tween 0,01%. Finally, the protein signal was acquired using ChemiDoc Imaging System (BioRad, Segrate, Italy).

Immunofluorescence

Immunofluorescence analysis was performed seeding each pool of cells at the concentration of 200000 cells per well in a 4-Chamber Cell Imaging Slide (Eppendorf, Hamburg, Germany). The day after, cells were fixed in 4% of paraformaldehyde (in PBS 1X) for 15 minutes at room temperature. Cells were then washed and permeabilized with triton at the concentration of 0.1% (in PBS 1X) for 2 minutes. The blocking of the unspecific sites was performed with 20% FBS (fetal bovine serum) and 2% BSA (bovine serum albumine) diluted in PBS 1X for 1h. Cells were stained with the primary antibody diluted 1:200 in PBS1X and 2% BSA and incubated for 1 hour. Secondary anti-rabbit Alexa 594 conjugated antibody (Thermo Fischer Scientific, Monza, Italy) was diluted 1:1000 in PBS 1X and 2% BSA and incubated on cells for 1 hour. For specific protein detection, we used the following primary antibody: for Immunofluorescence of TAZ, we used rabbit anti-YAP1/TAZ (D24E4; Cell Signaling Technologies) and for the Immunofluorescence of YAP1 we used rabbit anti-YAP (D8H1Z, Cell Signaling Thecnologies). DAPI staining was performed by incubating cells with DAPI dye at 300nM concentration for 5 minutes. Images were acquired using fluorescent microscope (200X magnification in Nikon Eclipse NI microscope). We counted about 200 cells per condition.

Chromatin Immunoprecipitation (ChIP)

To perform ChIP experiments, 5 million of cells were seeded in two 150 cm plates. The day after we treated one plate with JQ1 1 μM and the other plate with DMSO. 24 hours after treatment, ChIP experiment was performed. Cells were crosslinked with 1% formaldehyde for 15 minutes at room temperature. Then, external membrane of cells was lysed with Cell Lysis Buffer (Tris 10mM pH 8; KCl 85mM; NP40 % and Protease Inhibitor Cocktail). Nuclei were lysed using Nuclei Lysis Buffer (Tris 50 mM pH 8; EDTA 10mM; SDS 1% and Protease Inhibitor Cocktail). The obtained lysates were sonicated for 2 cycles (30 seconds ON and 30 seconds OFF) to obtain chromatin fragments of mean length of 500 bp, using Bioruptor Pico sonicator (Diagenode, Milan, Italy). The obtained chromatin was diluted in Chip Dilution Buffer (SDS 0.01%; Triton X-100 1,1%; EDTA 1,2 mM; Tris 16,7 mM pH

8; NaCl 167 nM and Protease Inhibitor Cocktail). Diluted chromatin was immunoprecipitated at 4°C overnight in agitation using 20ul Magna ChIP protein G Magnetic Beads (Merck Millipore, Milan, Italy). We used 1µg of the following antibody rabbit anti-BRD4 (A301-985A50, Bethyl), 1µg of rabbit anti-acetyl-K27-histone H3 (ab4729; Abcam), 1µg of normal rabbit igG (Cell Signaling Technologies), 1µg of rabbit anti-YAP1/TAZ (D24E4; Cell Signaling Technologies) for TAZ detection and 1µg of rabbit anti-YAP (D8H1Z, Cell Signaling Thecnologies) for YAP detection. For each experiment, 10% of chromatin was kept before immunoprecipitation as input control. The day after, magnetic beads were precipitated using magnetic rack and the immunocomplex bound to the beads were washed using four different specific buffers. The beads were washed 1X with Low Salt buffer (SDS 0,1%, Triton 1%, EDTA pH8 2mM, Tris pH8 20mM, NaCl 150mM and water), 1X with High Salt Buffer (SDS 0.1%, Triton 1%, EDTA pH8 2mM, TrispH8 20mM, NaCl 500mM and water), 1X in LiCl Buffer (LiCl 250mM, NP40 1%, EDTA 1mM, Trisp pH8 1mM, Nadeoxicolato 1% and water) and 2X in TE Buffer (Tris pH8 10mM, EDTA 1mM). We used 300ul of Elution Buffer (NaHCO3 0.1M, SDS 1%) to elute the immunocomplexes and to dilute input samples. Reverse crosslink was performed adding to IP and input 12ul NaCl 5M and incubating over-night at 65°C. The day after, we performed Proteinase K treatment adding to IP and input 19ul Proteinase K solution (6ul EDTA 0.5M, 12ul Tris 1M pH 6.5 and 1ul Proteinase K 20mg/ml) and incubating for 1 hour at 45°C. After Proteinase K treatment, DNA was extracted with *QUIAquick PCR-purification Kit (*Qiagen, Milan, Italy) following manufacturer's instructions.

RNA-sequencing (RNA-seq)

RNA-seq was performed on A549 cells transfected with siRNA against TAZ, TAZ-AS202 and control siRNA in two independent biological replicates. For each experimental condition, cell pellets were collected 48 hours after transfection. The total RNA was extracted and the downregulation of TAZ, TAZ-AS202 was verified by RT-qPCR compared to control cells. Samples were quantified at Qubit (Thermo Fisher Scientific, Milan, Italy) and loaded on Bioanalyzer-RNA 6000 nano kit (Agilent Technologies, Santa Clara, California, USA) for purity and quality assessment. Libraries were prepared starting from 1 µg RNA, using TruSeq Stranded total RNA kit (Illumina, San Diego, California, USA). Next generation sequencing was conducted by NextSeq 500 platform (Illumina, San Diego, California, USA) on high-output cartridge (2X75) and a minimum of 30 million of reads for each replicate was expected. The graph of RNA-seq pipeline is reported in **fig.47**. Sequencing quality was assessed using FastQC v0.11.8 software (www.bioinformatics.babraham.ac.uk/projects/fastqc/), showing on average a Phred score per base >34 in each sample. Raw sequences were then aligned to the human reference transcriptome

(GRCh38, Gencode release 30) using STAR version 2.7 and gene abundances were estimated with RSEM algorithm (v1.3.1). Differential expression analysis was performed using DESeq2 R package, considering a False Discovery Rate (FDR) of 5% and excluding genes with low read counts. Significant genes underwent to enrichment analysis, performed on Reactome pathways databases via enrichR package, using a significance threshold of 0.05 on p-value adjusted by Benjamini-Hochberg correction for multiple testing.

Figure 47
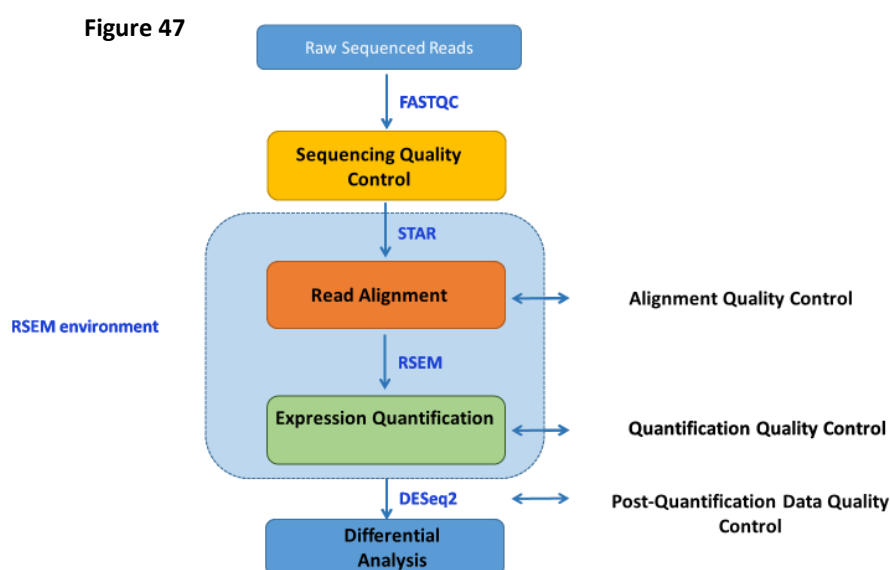
Luciferase Assay

For luciferase assay, cells were co-transfected with 8XGTIIC-luciferase vector, containing 8 TEAD binding sites upstream a firefly luciferase gene, and pRL-TK vector, containing a constitutive thymidine kinase promoter upstream a renilla luciferase gene, using Lipofectamine2000 (Life Thecnologies, Monza, Italy) in triplicates for each pool of cells in 96 wells. As control, we used PGL3-Empty Vector and pRL-TK vector. 24 hours after transfection, cells were harvested and luciferase activity was measured using the Dual-Luciferase Reporter Assay System (Promega) with a GloMax Discovery Luminometer (Promega), according to the protocol. For each sample, firefly luciferase activity was normalized on renilla luciferase activity.

Generation of A549 and NCI-H23 resistant cells line

To generate A549 and NCI-H23 cells resistant to JQ1, we treated cells with increasing doses of JQ1, starting with 0.1µM and ending with 2µM. Drug concentration was changed every 1-2 weeks.

Generation of TAZ overexpressing A549, NCI-H23 and NCI-H1975 cells lines

To generate TAZ overexpressing cells, we infected A549/Cas9, NCI-H23/Cas9 or NCI-H1975/Cas9 cells with pLL3.7 K122 FH-TAZ-ires-GFP-TEAD-responsive-H2B mCherry plasmid or with pLL3.7 K122 -ires-GFP-TEAD-responsive-H2B mCherry, as an empty vector control; using the protocol reported in *Lentiviral Production* paragraph. The plasmids were a gift from Yutaka Hata (Addgene plasmid #68713 and Addgene plasmid #68714). Infected cells were selected for GFP expression through FACSMelody cell sorter (BD).

TCGA data analysis

NSCLC patients were analyzed for mutational profile using TCGA dataset available through the cBioportal portal (http://www.cbioportal.org) *(Cerami, E. et al, 2012).* Survival analysis and Kaplan-Meier representations were performed using R version 3.5.1 and package "survival". Log rank test was applied to compare survival curves and calculate p values.

Cytoplasmic and Nuclear extract

For cytoplasmic and nuclear extract, 1 million of cells per pool were seeded in two T25 culture flask. To obtain total lysates we added the Passive Lysis Buffer (PLB) 5X (Promega) supplemented with protease inhibitor to cells for 15 minutes in ice and, then, we centrifuged for 15 minutes at @14500 rpm. For cytoplasmic fraction, cells were lysed in Cytoplasmic Buffer (10mM Hepes pH 7,9; 1,5mM MgCl2; 100mM KCl and protease inhibitor) for 15 minutes on ice. 0,05% NP40 for A549 and 0,025% NP40 for NCI-H23 was added to obtain lysate and centrifuged at @3000 rpm for 2 minutes. The surnatant, representing the cytoplasmic, was further centrifuged for 15 minutes at @3000 rpm. Nuclei pellet was washed twice with Cytoplasmic Buffer. For Nuclei lysis, the obtained pellet was lysed in Nuclei Lysis Buffer (20mM hepes pH 7.9; 25% Glycerol; 0.42M NaCl; 1,5mM MgCl2; 0,2mM EDTA and Protease inhibitor) on ice for 30 minutes. The lysate was centrifuged for 10 minutes at @14500 rpm. Surnatant represents nuclear extract while the pellet represents chromatin insoluble fraction. All centrifugations were performed at 4°C and all buffers were supplemented with Protease Inhibitor Cocktail (Bimake, Munich Germany) and SUPERase Rnase-Inhibitor (Thermo-Fisher, Monza, Italy) to evaluate nuclear/cytoplasmic localization of RNA and proteins.

Cell Viability Assay

Cell proliferation was evaluated using Real-Time-Glo Cell viability assay (Promega). For this assay, 400 cells were seeded per well in a 96 well culture plate, in triplicate. The following day, cells were treated with JQ1 at the concentration of 0.5, 1 or 2 µM and DMSO. At the same time, we added NanoLuc Luciferase substrate (1000X) and a cell permeant substrate (1000X). The luminescent signal was read with Glomax Discover Luminometer (Promega), 48, 72 and 96 hours after cell plating.

Trypan blue cell counting

Cell proliferation was evaluated also performing manual cell counting. For the evaluation of cell proliferation after JQ1 treatment, 3500 cells per well in a 96 well culture plate were seeded in triplicate. The day after, cells were treated with JQ1 at the concentration of 0.5, 1 or 2 µM, or DMSO. 72 hours after treatment, viable cells were counted in each well using Trypan blue staining (Sigma-Aldrich, Milan, Italy) and automated cell counter (Countess, Life Technologies). For the evaluation of cell proliferation after siRNA transfection: the first day cells were transfected in a 6-well culture plate. The day after, cells were harvested and seeded at the concentration of 3500 cells per well in a 96 well culture plates. 48, 72 and 96 hours after transfection, cells were counted in each well using Trypan blue (Sigma-Aldrich, Milan, Italy) and automated cell counter (Countess, Life Technologies).

Colony forming assay

For colony forming assay, A549 cells were seeded in 10cm culture dishes at the concentration of 1000 cells per dish while NCI-H23 were seeded in 10cm culture dishes at the concentration of 300 cells per dish. 24 hours after seeding, cells were treated with different concentration of JQ1 (0,5-1µM). Medium was freshly added every 2 days for 10 days for A549 cells and for 15 days for NCI-H23 cells. Next, the dishes were fixed with cold methanol and the colonies were stained with a solution containing Crystal Violet (0,2% w/v). The colonies were finally counted using ImageJ software.

Scratch Wound Healing Assay

24 hours after transfection with specific siRNAs, 1 million of cells were seeded in a 6-well culture plate. The day after, cells were treated with mytomicin (Sigma Aldrich, Milan, Italy) at the concentration of 2 µg/ml for A549, 10 µg/ml for H1299 and 1 µg/ml for NCI-H23, for 1 hour and 30 minutes. Then, cell medium was replaced with normal complete culture medium. Scratches were applied using a pipette tip. Healing areas were captured at 0, 19, 26 and 48 hours after the scratch using a Nikon Ti-E inverted microscope (Nikon Instruments, Florence, Italy). Three images per condition were taken. The area of the scratch was calculated at each time point using ImageJ software and each time point was normalized on the specific area of T0.

Invasion Chamber Assay

A549 cells were transfected the first day with siRNA against TAZ, TAZ-AS202, EPHB2 or control siRNA in a T25 flask. 24 hours after transfection, the RNA downregulation of the specific targets was checked by RT-qPCR. 48 hours after transfection, $3X10^4$ cells were seeded in a Matrigel Invasion Chamber or control chambers (CT insert) (BD Biosciences, San Jose, CA) in triplicate. Complete medium containing 10% FBS was used as chemo-attractant. The day after, invading cells were fixed

with methanol, stained with crystal violet and pictures were obtained using a Nikon Ti-E inverted microscope. Three fields for each well were captured and invading cells were manually counted. To obtain the graph, we divided the cells in the Matrigel Invasion Chamber with the cells in the control insert for each condition.

Actinomycin D and cycloheximide treatments

For actinomycin treatment: cells were transfected with the specific siRNA and, 24 hours after, were treated for 8 hours with actinomycin D (Sigma- Aldrich, Milan, Italy) at the concentration of 5µg/ml or DMSO (MOCK) as control. During the treatment, the RNA downregulation of the specific targets was checked by RT-qPCR. After actinomycin D treatment, RNA pellets were collected and the differences of the expression of genes between actinomycin D treated cells and DMSO treated cells was checked with RT-qPCR.

For cycloheximide treatment: cells were transfected with the specific siRNA and, 24 hours after, were treated for 24 hours with cycloheximide at the concentration of 50µg/ml or DMSO (MOCK) as control. During the treatment, the RNA downregulation of the specific target was controlled with RT-qPCR. After cycloheximide treatment, RNA pellets were collected and the differences of the expression of genes between cycloheximide treated cells ad DMSO treated cells was checked by RT-qPCR.

Statistical Analysis

Statistical analysis was performed using GraphPad Prism Software (GraphPad Software, San Diego, California, USA). Statistical significance was determined using the Student's t-test. Each experiment was replicated two to 6 times. Threshold for significance was considered P-value <0.05.

Table4

CTGF	CTGF_F	ATTCTGTCACTTCGGCTCCC
	CTGF_R	GCTGCTTGGAAGGACTCTC
CYR61	CYR61_F	CTGGAATGCAACTTCGGCG
	CYR61_R	CCGTTTTGGTAGATTCTGGAGT
AXL	AXL_F	CTGCGGACTGTCTGGATGG
	AXL_R	GGCCTTCAGTGTGTTCTTCCA
ANKRD1	ANKRD1_F	AGACCTTCAACGCCAAAGACA
	ANKRD1_R	CTTGATGTTGAGATCCGCGC
Ciclophilin A	Ciclophilin A_F	GACCCAACACAAATGGTTCC
	Ciclophilin A_R	TTTCACTTTGCCAAACACCA
YAP1	YAP1_F	GCAGGTTGGGAGATGGCAAA
	YAP1_R	GCTGTGACGTTCATCTGGGA
TAZ	TAZ_F	GGCTGGGAGATGACCTTCAC
	TAZ_R	GCTGATTCATCGCCTTCCTAG
TEAD1	TEAD1_F	CCACAAGCTCAAACACTTACCA
	TEAD1_R	ACACAGGCCATGCAGAGTAG
TEAD2	TEAD2_F	GCCTCTGAGCTTTTCCAGTT
	TEAD2_R	CGGTGTCTGTGAGAATGGCT
TEAD3	TEAD3_F	CAGCCTACCCCATCCAGC
	TEAD3_R	GAGGAGGCAATGGTACGGTC
TEAD4	TEAD4_F	GAAGACCCGCACCAGGAA
	TEAD4_R	TTAGCTTGGCCTGGATCTCG
BRD4	BRD4_F	ATGCCGTCAAGCTGAACCTC
	BRD4_R	GATACATTCCTGAGCATTCCAGT
TAZ-AS202	TAZ-AS202_F	ATGAAAACTTGAGGCCAGCC
	TAZ-AS202_R	GCCTTTCCTTCTCCATGTGG
TAZ-AS203	TAZ-AS203_F	GGCCGGATTCATCTTCTGC
	TAZ-AS203_R	GTCGAGACGTGGTGGAGTTG
ROCK2	ROCK2_F	TGGGCGAGAATGTGATTGGT
	ROCK2_R	TGTTCCTACAAGTGAATCCGCA
SRC	SRC_F	TGAGGCATGAGAAGCTGGTG
	SRC_R	CCCCTTGAGAAAGTCCAGCA
VAV2	VAV2_F	ATCGCGCAGAACAAAGGGAT
	VAV2_R	CCTCCAGGCTGCGGTAGA
DNM1	DNM1_F	GATGGACGAGGGCACAGATG
	DNM1_R	TCAATGTCCTTCTGGCTCCG
CLTCL1	CLTCL1_F	TGCTGTGCTCACCATGATGA
	CLTCL1_R	TAACAGAGCTCGACGTTGGC
EPHB2	EPHB2_F	TGGACTCCACTACAGCGACT
	EPHB2_R	GTGCGGATCGTGTTCATGTT
MYH10	MYH10_F	CCATCAGACAACCAGAGCCA
	MYH10	AGTTCTCTGCGCCATTGTAA
AP2M1	AP2M1_F	GACGTGATGGCTGCCTACTT
	AP2M1_R	CGGAATTCTGTGGGTAGCCA
TCF7	TCF7_F	CTCATGCATTACCCACCCC
	TCF7_R	TCGTAGAGAGAGAGTTGGGG
RUNX1	RUNX1_F	CCTCAGGTTTGTCGGTCGAA
	RUNX1_R	GATGGCTCTGTGGTAGGTGG
JUNB	JUNB_F	ACACCAACCTCAGCAGCTAC
	JUNB_R	GAGGTAGCTGATGGTGGTCG
FOSL2	FOSL2_F	GCGTGATCAAGACCATTGGC
	FOSL2_R	CGACGCTTCTCCTCCTCTTC
SP6	SP6_F	TCCAAACTTACCAGGGCCAC
	SP6_R	CATAGCCCTGCGAGAAGTCC
KLF2	KLF2_F	GAAGCCCTACCACTGCAACT
	KLF2_R	TGTGCTTTCGGTAGTGGCG
KLF4	KLF4_F	TTCCCATCTCAAGGCACACC
	KLF4_R	GCGAATTTCCATCCACAGCC
SMAD7	SMAD7_F	CCTCCTTACTCCAGATACCCGA
	SMAD7_R	CCCAGGGGCCAGATAATTCG
OIP5-AS1	OIP5-AS1_F	TTTCCTTGACCTTTAGGTGCTTT
	OIP5-AS1_R	GAAGCAGGACTACCCACTCTAGG
KCNQ1OT1	KCNQ1OT1_F	GGCTACGACCACAGGTGAAA
	KCNQ1OT1_R	GTCTGCTGGCTTGTGTGTTG

U1	U1_F	GGGAGATACCATGATCACGAAGGT
	U1_R	CCACAAATTATGCAGTCGAGTTTCCC

Chromatin Immunoprecipitation primers

YAP1	YAP1_CH_F	AGAACTTCCTGCAGCCAAGG
	YAP1_CH_R	GTATTCTGCCCCGCGAACC
TAZ	TAZ_CH_F	CCCAGACACTCAGCGGTAAG
	TAZ_CH_R	CCCTCGCCCTATCTTCTCCT
TEAD2	TEAD2_CH_F	TCTACAGGCGCTAGTGGACT
	TEAD2_CH_R	ACGCAGCCTTTCACCCTTAA
NEG CTRL	NegCtrl_F	TCTCAAGGTGCCTGTCTGC
	NegCtrl_R	TGAAGTTTGGCCTCTGGTCT

Alt-R primers

AMOTL2	A01819/21_F	AGTGTTGGGCATACAGTGGG
AMOTL2	A01819/21_R	CCTGTTTGGTGGCCTCTCAT
AMOTL2	A01820_F	AGGAAGAGTGGAGGGAGCTT
AMOTL2	A01820_R	AAGCACAGAAGGATCCAGCC
SPOP	A46762/63/64_F	AGTGGAAAGCTGAGATGCCC
SPOP	A46762/63/64_R	TCTTCTATGGGGCCTGCATT
LATS2	A26066/67_F	CACACGCACGCTCTTCAC
LATS2	A26066/67_R	GTTCAAGACCCTCAGCCCC
TAOK1	A48305_F	ACTATGTTCTTGATCTACTGTGTGA
TAOK1	A48305_R	ATCCCTGAAGAGCACCATGT
TAOK1	A48306_F	AGTTGCATGTTCTTGTTAACTCTT
TAOK1	A48306_R	ACCAAGGAATCGTGATCAGCT
TAOK1	A48307_F	ACCTCACAACCTGTAATGCACT
TAOK1	A48307_R	CCCCAGCTAGTTATGAATGGCT
NF2	A31760_F	CCCTTAGAGCAGCACGTTGA
NF2	A31760_R	TCTTCAAGTCCACAAGTCCCA
NF2	A31761_F	TTAGCCATCGAGCCAGTGAC
NF2	A31761_R	GTTTCTCCCTGGCCAGTTGA
NF2	A31762_F	ATCCCTTCCCACACTCATGC
NF2	A31762_R	ACAGAAAGTATGCGCCAAGTG
WWTR1	br2-4_F	AGAGTTGGCTTCAGTCCTGC
WWTR1	br2-4_R	CCTCTTACCCACTTCCTCCG
WWTR1	br3_F	GCTAGATGAAGACAGGAGGCC
WWTR1	br4_R	CTGCTTGCAGAATCCCCAGT
YAP1	A54630_F	ACAGTTTTCTTGGTGTGAGCC
YAP1	A54630_R	GTGATTCTGGTTAGTCGGCCA
YAP1	A54631_F	TGACTTTTGGGGTTTTGTGGTG
YAP1	A54631_R	ACCCGCTTCAGAACCAAATCT
YAP1	A54632_F	CAGTCAGAGTGCTCCAGTGA
YAP1	A54632_R	TTGAGAAATGTCATATTGGTGTATCC

siRNA sequences

	sense	antisense
siRNA TAZ	AAACACCAUGAACAUCAAtt	UUGAUGUUCAUGGGUGUUUgt
siRNA TAZ-AS202	AAAAUAAAGUCGAAGUUAAtt	UUAACUUCGACUUUAUUUUac
siRNA TAZ-AS203	GAAUCAGGCUCCUUAAAGAtt	UCUUUAAGGAGCCUGAUUCgg
siRNA EPHB2	GCGUGAUCCUGGACUAUGAtt	UCAUAGUCCAGGAUCACGCca

BIBLIOGRAPHY

- Alipoor, Behnam, Seyedeh Nasrin Parvar, Zolfaghar Sabati, Hamid Ghaedi, e Hassan Ghasemi. 2020. «An Updated Review of the H19 LncRNA in Human Cancer: Molecular Mechanism and Diagnostic and Therapeutic Importance». *Molecular Biology Reports*
- Azzolin, Luca, Tito Panciera, Sandra Soligo, Elena Enzo, Silvio Bicciato, Sirio Dupont, Silvia Bresolin, et al. 2014. «YAP/TAZ Incorporation in the β-Catenin Destruction Complex Orchestrates the Wnt Response». *Cell*
- Bartucci, M., R. Dattilo, C. Moriconi, A. Pagliuca, M. Mottolese, G. Federici, A. Di Benedetto, et al. 2015. «TAZ Is Required for Metastatic Activity and Chemoresistance of Breast Cancer Stem Cells». *Oncogene*
- Basheer, Faisal, e Brian J. P. Huntly. 2015 «BET Bromodomain Inhibitors in Leukemia». *Experimental Hematology*
- Basu-Roy, Upal, N. Sumru Bayin, Kirk Rattanakorn, Eugenia Han, Dimitris G. Placantonakis, Alka Mansukhani, e Claudio Basilico. 2015. «Sox2 Antagonizes the Hippo Pathway to Maintain Stemness in Cancer Cells». *Nature Communications*
- Belkina, Anna C., e Gerald V. Denis. 2012. «BET Domain Co-Regulators in Obesity, Inflammation and Cancer». *Nature Reviews. Cancer*
- Black, A. R., J. D. Black, e J. Azizkhan-Clifford. 2001. «Sp1 and Krüppel-like Factor Family of Transcription Factors in Cell Growth Regulation and Cancer». *Journal of Cellular Physiology*
- Camargo, Fernando D., Sumita Gokhale, Jonathan B. Johnnidis, Dongdong Fu, George W. Bell, Rudolf Jaenisch, e Thijn R. Brummelkamp. 2007. «YAP1 Increases Organ Size and Expands Undifferentiated Progenitor Cells». *Current Biology*
- Campbell, Tessa N., Alice Davy, Yiping Liu, Mayi Arcellana-Panlilio, e Stephen M. Robbins. 2008. «Distinct Membrane Compartmentalization and Signaling of Ephrin-A5 and Ephrin-B1». *Biochemical and Biophysical Research Communications*
- Cancer Genome Atlas Research Network. 2014. «Comprehensive Molecular Profiling of Lung Adenocarcinoma». *Nature*
- Cao, X., S. L. Pfaff, e F. H. Gage. 2008. «YAP Regulates Neural Progenitor Cell Number via the TEA Domain Transcription Factor». *Genes & Development*
- Castaño, Julio, Veronica Davalos, Simo Schwartz, e Diego Arango. 2008. «EPH Receptors in Cancer». *Histology and Histopathology*
- Cerami E, Gao JJ, Dogrusoz U, Gross BE, Sumer SO, Aksoy BA, et al. The cBio cancer genomics portal: an open platform for exploring multidimensional cancer genomics data. Cancer Disco. 2012
- Chan, Eunice H. Y., Marjaana Nousiainen, Ravindra B. Chalamalasetty, Anja Schäfer, Erich A. Nigg, e Herman H. W. Silljé. 2005. «The Ste20-like Kinase Mst2 Activates the Human Large Tumor Suppressor Kinase Lats1». *Oncogene*
- Chan, PuiYee, Xiao Han, Baohui Zheng, Michael DeRan, Jianzhong Yu, Gopala K. Jarugumilli, Hua Deng, Duojia Pan, Xuelian Luo, e Xu Wu. 2016. «Autopalmitoylation of TEAD Proteins Regulates Transcriptional Output of the Hippo Pathway». *Nature Chemical Biology*
- Chang, Lei, Luca Azzolin, Daniele Di Biagio, Francesca Zanconato, Giusy Battilana, Romy Lucon Xiccato, Mariaceleste Aragona, et al. 2018. «The SWI/SNF Complex Is a Mechanoregulated Inhibitor of YAP and TAZ». *Nature*
- Chen, Jin, Wenqiang Song, e Katherine Amato. 2015. «Eph Receptor Tyrosine Kinases in Cancer Stem Cells». *Cytokine & Growth Factor Reviews*
- Chen, Q., N. Zhang, R. S. Gray, H. Li, A. J. Ewald, C. A. Zahnow, e D. Pan. 2014. «A Temporal Requirement for Hippo Signaling in Mammary Gland Differentiation, Growth, and Tumorigenesis».

Genes & Development

- Cortina, Carme, Sergio Palomo-Ponce, Mar Iglesias, Juan Luis Fernández-Masip, Ana Vivancos, Gavin Whissell, Mireia Humà, et al. 2007. «EphB-Ephrin-B Interactions Suppress Colorectal Cancer Progression by Compartmentalizing Tumor Cells». *Nature Genetics*

- Cui, Di, Cai-Hua Yu, Min Liu, Qing-Qing Xia, Yu-Feng Zhang, e Wei-Long Jiang. 2016. «Long Non-Coding RNA PVT1 as a Novel Biomarker for Diagnosis and Prognosis of Non-Small Cell Lung Cancer». *Tumour Biology: The Journal of the International Society for Oncodevelopmental Biology and Medicine*

- Cui, Jiandong, Juanmei Mo, Min Luo, Qitao Yu, Shaozhang Zhou, Tao Li, Yu Zhang, e Weiling Luo. 2015. «C-Myc-Activated Long Non-Coding RNA H19 Downregulates MiR-107 and Promotes Cell Cycle Progression of Non-Small Cell Lung Cancer». *International Journal of Clinical and Experimental Pathology*

- Day, B. W. *et al.* EphA3 Maintains Tumorigenicity and Is a Therapeutic Target in Glioblastoma Multiforme. *Cancer Cell*, 2013

- Day, Bryan W., Brett W. Stringer, Fares Al-Ejeh, Michael J. Ting, John Wilson, Kathleen S. Ensbey, Paul R. Jamieson, et al. 2013. «EphA3 Maintains Tumorigenicity and Is a Therapeutic Target in Glioblastoma Multiforme». *Cancer Cell*

- Dai, Xiangpeng, Wenjian Gan, Xiaoning Li, Shangqian Wang, Wei Zhang, Ling Huang, Shengwu Liu, et al. 2017. «Prostate Cancer-Associated SPOP Mutations Confer Resistance to BET Inhibitors through Stabilization of BRD4». *Nature Medicine*

- Dasgupta, Ishani, e Dannel McCollum. 2019. «Control of Cellular Responses to Mechanical Cues through YAP/TAZ Regulation». *Journal of Biological Chemistry*

- Davis, S., N. W. Gale, T. H. Aldrich, P. C. Maisonpierre, V. Lhotak, T. Pawson, M. Goldfarb, e G. D. Yancopoulos. 1994. «Ligands for EPH-Related Receptor Tyrosine Kinases That Require Membrane Attachment or Clustering for Activity». *Science (New York, N.Y.)*

- Dawson, Mark A., Rab K. Prinjha, Antje Dittmann, George Giotopoulos, Marcus Bantscheff, Wai-In Chan, Samuel C. Robson, et al. 2011. «Inhibition of BET Recruitment to Chromatin as an Effective Treatment for MLL-Fusion Leukaemia». *Nature*

- Devaiah, Ballachanda N., Brian A. Lewis, Natasha Cherman, Michael C. Hewitt, Brian K. Albrecht, Pamela G. Robey, Keiko Ozato, Robert J. Sims, e Dinah S. Singer. 2012. «BRD4 Is an Atypical Kinase That Phosphorylates Serine2 of the RNA Polymerase II Carboxy-Terminal Domain». *Proceedings of the National Academy of Sciences of the United States of America*

- Diamantopoulou, Zoi, Gavin White, Muhammad Z. H. Fadlullah, Marcel Dreger, Karen Pickering, Joe Maltas, Garry Ashton, et al. 2017. «TIAM1 Antagonizes TAZ/YAP Both in the Destruction Complex in the Cytoplasm and in the Nucleus to Inhibit Invasion of Intestinal Epithelial Cells». *Cancer Cell*

- Djebali, Sarah, Carrie A. Davis, Angelika Merkel, Alex Dobin, Timo Lassmann, Ali Mortazavi, Andrea Tanzer, et al. 2012. «Landscape of Transcription in Human Cells». *Nature*

- Donati, Benedetta, Eugenia Lorenzini, e Alessia Ciarrocchi. 2018. «BRD4 and Cancer: Going beyond Transcriptional Regulation». *Molecular Cancer*

- Dykes, Iain M., e Costanza Emanueli. 2017. «Transcriptional and Post-Transcriptional Gene Regulation by Long Non-Coding RNA». *Genomics, Proteomics & Bioinformatics*

- Dull T, Zufferey R, Kelly M, Mandel RJ, Nguyen M, Trono D, et al. A third-generation lentivirus vector with a conditional packaging system. J Virol. 1998

- Faghihi, Mohammad Ali, e Claes Wahlestedt. 2009. «Regulatory Roles of Natural Antisense Transcripts». *Nature Reviews. Molecular Cell Biology*

- Fu, Lei-lei, Mao Tian, Xiang Li, Jing-jing Li, Jian Huang, Liang Ouyang, Yonghui Zhang, e Bo Liu. 2015. «Inhibition of BET Bromodomains as a Therapeutic Strategy for Cancer Drug Discovery». *Oncotarget*

- Gao, Jian, Yingxue Rong, Yuxing Huang, Peng Shi, Xitao Wang, Xuan Meng, Jiahong Dong, e Congying

Wu. 2019. «Cirrhotic Stiffness Affects the Migration of Hepatocellular Carcinoma Cells and Induces Sorafenib Resistance through YAP». *Journal of Cellular Physiology*

- Gao, Qing, Wei Liu, Jiangyi Cai, Mu Li, Yane Gao, Wenjing Lin, e Zongfang Li. 2014. «EphB2 Promotes Cervical Cancer Progression by Inducing Epithelial-Mesenchymal Transition». *Human Pathology*

- Gao, Zhongyuan, Ting Yuan, Xiao Zhou, Ping Ni, Geng Sun, Ping Li, Zhixiang Cheng, e Xuerong Wang. 2018. «Targeting BRD4 Proteins Suppresses the Growth of NSCLC through Downregulation of EIF4E Expression». *Cancer Biology & Therapy*

- Gise, A. von, Z. Lin, K. Schlegelmilch, L. B. Honor, G. M. Pan, J. N. Buck, Q. Ma, et al. 2012. «YAP1, the Nuclear Target of Hippo Signaling, Stimulates Heart Growth through Cardiomyocyte Proliferation but Not Hypertrophy». *Proceedings of the National Academy of Sciences*

- Gobbi Giulia, Benedetta Donati, Italo Faria Do Valle, Francesca Reggiani, Federica Torricelli, Daniel Remondini, Gastone Castellani, Davide Carlo Ambrosetti, Alessia Ciarrocchi, Valentina, Sancisi 2019 «The Hippo pathway modulates resistance to BET proteins inhibitors in lung cancer cells». *Oncogene*

- Guo, Dong Li, Ji Zhang, Siu Tsan Yuen, Wai Yin Tsui, Annie S. Y. Chan, Coral Ho, Jiafu Ji, Suet Yi Leung, e Xin Chen. 2006. «Reduced Expression of EphB2 That Parallels Invasion and Metastasis in Colorectal Tumours». *Carcinogenesis*

- Guo, Liwen, Jiaping Zheng, Jing Zhang, Haohao Wang, Guoliang Shao, e Lisong Teng. 2016. «Knockdown of TAZ Modifies Triple-Negative Breast Cancer Cell Sensitivity to EGFR Inhibitors by Regulating YAP Expression». *Oncology Reports*

- Guo, Y., J. Cui, Z. Ji, C. Cheng, K. Zhang, C. Zhang, M. Chu, et al. 2017. «MiR-302/367/LATS2/YAP Pathway Is Essential for Prostate Tumor-Propagating Cells and Promotes the Development of Castration Resistance». *Oncogene*

- Halder, Georg, Sirio Dupont, e Stefano Piccolo. 2012. «Transduction of Mechanical and Cytoskeletal Cues by YAP and TAZ». *Nature Reviews Molecular Cell Biology*

- Hallin J, Engstrom LD, Hargis L, Calinisan A, Aranda R, Briere DM, et al. The KRAS(G12C) Inhibitor MRTX849 Provides Insight toward Therapeutic Susceptibility of KRAS-Mutant Cancers in Mouse Models and Patients. Cancer Discov. 2020

- Hashad, Doaa, Amany Elbanna, Abeer Ibrahim, e Gihan Khedr. 2016. «Evaluation of the Role of Circulating Long Non-Coding RNA H19 as a Promising Novel Biomarker in Plasma of Patients with Gastric Cancer». *Journal of Clinical Laboratory Analysis*

- He, Juan, Ke Wu, Chenglin Guo, Jian-Kang Zhou, Wenchen Pu, Yulan Deng, Yuanli Zuo, et al. 2018. «Long Non-Coding RNA AFAP1-AS1 Plays an Oncogenic Role in Promoting Cell Migration in Non-Small Cell Lung Cancer». *Cellular and Molecular Life Sciences: CMLS*

- Hon, Chung-Chau, Jordan A. Ramilowski, Jayson Harshbarger, Nicolas Bertin, Owen J. L. Rackham, Julian Gough, Elena Denisenko, et al. 2017. «An Atlas of Human Long Non-Coding RNAs with Accurate 5' Ends». *Nature*

- Hong, Soon Auck, Si-Hyong Jang, Mee-Hye Oh, Sung Joon Kim, Jin-Hyung Kang, e Sook-Hee Hong. 2018. «Overexpression of YAP1 in EGFR Mutant Lung Adenocarcinoma Prior to Tyrosine Kinase Inhibitor Therapy Is Associated with Poor Survival». *Pathology, Research and Practice*

- Horie, Masafumi, Akira Saito, Mitsuhiro Ohshima, Hiroshi I. Suzuki, e Takahide Nagase. 2016. «YAP and TAZ Modulate Cell Phenotype in a Subset of Small Cell Lung Cancer». *Cancer Science*

- Hossain, Zakir, Safiah Mohamed Ali, Hui Ling Ko, Jianliang Xu, Chee Peng Ng, Ke Guo, Zeng Qi, Sathivel Ponniah, Wanjin Hong, e Walter Hunziker. 2007. «Glomerulocystic Kidney Disease in Mice with a Targeted Inactivation of Wwtr1». *Proceedings of the National Academy of Sciences of the United States of America*

- Hsu, Ping-Chih, Jinbai Miao, Zhen Huang, Yi-Lin Yang, Zhidong Xu, Joanna You, Yuyuan Dai, et al. 2018. «Inhibition of Yes-Associated Protein Suppresses Brain Metastasis of Human Lung Adenocarcinoma in a Murine Model». *Journal of Cellular and Molecular Medicine*

- Hsu, Ping-Chih, Bin You, Yi-Lin Yang, Wen-Qian Zhang, Yu-Cheng Wang, Zhidong Xu, Yuyuan Dai, et al. 2016. «YAP Promotes Erlotinib Resistance in Human Non-Small Cell Lung Cancer Cells». *Oncotarget*

- Huang, Chengsuo, Shuguang Liu, Huijun Wang, Zicheng Zhang, Qing Yang, e Fang Gao. 2016. «LncRNA PVT1 Overexpression Is a Poor Prognostic Biomarker and Regulates Migration and Invasion in Small Cell Lung Cancer». *American Journal of Translational Research*

- Huang, Wei, Xianbo Lv, Chenying Liu, Zhengyu Zha, Heng Zhang, Ying Jiang, Yue Xiong, Qun-Ying Lei, e Kun-Liang Guan. 2012. «The N-Terminal Phosphodegron Targets TAZ/WWTR1 Protein for SCFβ-TrCP-Dependent Degradation in Response to Phosphatidylinositol 3-Kinase Inhibition». *The Journal of Biological Chemistry*

- Huusko, Pia, Damaris Ponciano-Jackson, Maija Wolf, Jeff A. Kiefer, David O. Azorsa, Sukru Tuzmen, Don Weaver, et al. 2004. «Nonsense-Mediated Decay Microarray Analysis Identifies Mutations of EPHB2 in Human Prostate Cancer». *Nature Genetics*

- Igolkina Anna A, Arsenii Zinkevich, Kristina O Karandasheva, Aleksey A Popov, Maria V Selifanova, Daria Nikolaeva, Victor Tkachev, Dmitry Penzar, Daniil M Nikitin, Anton Buzdin 2019«H3K4me3, H3K9ac, H3K27ac, H3K27me3 and H3K9me3 Histone Tags Suggest Distinct Regulatory Evolution of Open and Condensed Chromatin Landmarks» *Cells*

- Ireton, Reneé C., e Jin Chen. 2005. «EphA2 Receptor Tyrosine Kinase as a Promising Target for Cancer Therapeutics». *Current Cancer Drug Targets*

- Isago, Hideaki, Akihisa Mitani, Yu Mikami, Masafumi Horie, Hirokazu Urushiyama, Ryuji Hamamoto, Yasuhiro Terasaki, e Takahide Nagase. 2020. «Epithelial Expression of YAP and TAZ Is Sequentially Required in Lung Development». *American Journal of Respiratory Cell and Molecular Biology*

- Iyer, Matthew K., Yashar S. Niknafs, Rohit Malik, Udit Singhal, Anirban Sahu, Yasuyuki Hosono, Terrence R. Barrette, et al. 2015. «The Landscape of Long Noncoding RNAs in the Human Transcriptome». *Nature Genetics*

- Janes, Peter W., Mary E. Vail, Hui K. Gan, e Andrew M. Scott. 2020. «Antibody Targeting of Eph Receptors in Cancer». *Pharmaceuticals (Basel, Switzerland)*

- Jang, Eun Jung, Hana Jeong, Ki Hwan Han, Hyug Moo Kwon, Jeong-Ho Hong, e Eun Sook Hwang. 2012. «TAZ Suppresses NFAT5 Activity through Tyrosine Phosphorylation». *Molecular and Cellular Biology*

- Janouskova H, El Tekle G, Bellini E, Udeshi ND, Rinaldi A, Ulbricht A, et al. Opposing effects of cancer type-specific SPOP mutations on BET protein degradation and sensitivity to BET inhibitors. Mol Cell Proteom. 2017

- Ji, Ping, Sven Diederichs, Wenbing Wang, Sebastian Böing, Ralf Metzger, Paul M. Schneider, Nicola Tidow, et al. 2003. «MALAT-1, a Novel Noncoding RNA, and Thymosin Beta4 Predict Metastasis and Survival in Early-Stage Non-Small Cell Lung Cancer». *Oncogene*

- Jiao, Shi, Huizhen Wang, Zhubing Shi, Aimei Dong, Wenjing Zhang, Xiaomin Song, Feng He, et al. 2014. «A Peptide Mimicking VGLL4 Function Acts as a YAP Antagonist Therapy against Gastric Cancer». *Cancer Cell*

- Jubb, Adrian M., Fiona Zhong, Sheila Bheddah, Heike I. Grabsch, Gretchen D. Frantz, Wolfram Mueller, Vidya Kavi, Phil Quirke, Paul Polakis, e Hartmut Koeppen. 2005. «EphB2 Is a Prognostic Factor in Colorectal Cancer». *Clinical Cancer Research: An Official Journal of the American Association for Cancer Research*

- Kania, Artur, e Rüdiger Klein. 2016. «Mechanisms of Ephrin-Eph Signalling in Development, Physiology and Disease». *Nature Reviews. Molecular Cell Biology*

- Kanno Tomohiko, Kanno Yuka, Gary LeRoy, Eric Campos, Hong-Wei Sun, Stephen R Brooks, Golnaz Vahedi, Tom D Heightman, Benjamin A Garcia, Danny Reinberg, Ulrich Siebenlist, John J

O'Shea & Keiko Ozato BRD4 assists elongation of both coding and enhancer RNAs by interacting with acetylated histones *Nat Struct Mol Biol*, 21 (2014)

- Kegelman, Christopher D., Devon E. Mason, James H. Dawahare, Daniel J. Horan, Genevieve D. Vigil, Scott S. Howard, Alexander G. Robling, Teresita M. Bellido, e Joel D. Boerckel. 2018. «Skeletal Cell YAP and TAZ Combinatorially Promote Bone Development». *The FASEB Journal*

- Khandelwal, Akanksha, Albino Bacolla, Karen M. Vasquez, e Aklank Jain. 2015. «Long Non-Coding RNA: A New Paradigm for Lung Cancer». *Molecular Carcinogenesis*

- Kim, Min Hwan, Jongshin Kim, Hyowon Hong, Si-Hyung Lee, June-Koo Lee, Eunji Jung, e Joon Kim. 2016. «Actin Remodeling Confers BRAF Inhibitor Resistance to Melanoma Cells through YAP/TAZ Activation». *The EMBO Journal*

- Kim, Nam-Gyun, e Barry M. Gumbiner. 2015. «Adhesion to Fibronectin Regulates Hippo Signaling via the FAK-Src-PI3K Pathway». *The Journal of Cell Biology*

- Kim, Nam-Gyun, e Barry M. Gumbiner. 2019. «Cell Contact and Nf2/Merlin-Dependent Regulation of TEAD Palmitoylation and Activity». *Proceedings of the National Academy of Sciences of the United States of America*

- Koo, Ja Hyun, e Kun-Liang Guan. 2018. «Interplay between YAP/TAZ and Metabolism». *Cell Metabolism*

- Lau, Allison N., Stephen J. Curtis, Christine M. Fillmore, Samuel P. Rowbotham, Morvarid Mohseni, Darcy E. Wagner, Alexander M. Beede, et al. 2014. «Tumor-Propagating Cells and Yap/Taz Activity Contribute to Lung Tumor Progression and Metastasis». *The EMBO Journal*

- Lee, Jeong Eun, Hee Sun Park, Dahye Lee, Geon Yoo, Tackhoon Kim, Haeyon Jeon, Min-Kyung Yeo, et al. 2016. «Hippo Pathway Effector YAP Inhibition Restores the Sensitivity of EGFR-TKI in Lung Adenocarcinoma Having Primary or Acquired EGFR-TKI Resistance». *Biochemical and Biophysical Research Communications*

- Lee, Keun-Wook, Sung Sook Lee, Sang-Bae Kim, Bo Hwa Sohn, Hyun-Sung Lee, Hee-Jin Jang, Yun-Yong Park, et al. 2015. «Significant Association of Oncogene YAP1 with Poor Prognosis and Cetuximab Resistance in Colorectal Cancer Patients». *Clinical Cancer Research: An Official Journal of the American Association for Cancer Research*

- Lee, Ting-Fang, Yu-Chi Tseng, Phung Anh Nguyen, Yu-Chuan Li, Chao-Chi Ho, e Cheng-Wen Wu. 2018. «Enhanced YAP Expression Leads to EGFR TKI Resistance in Lung Adenocarcinomas». *Scientific Reports*

- Levy, Dan, Yaarit Adamovich, Nina Reuven, e Yosef Shaul. 2008. «Yap1 Phosphorylation by C-Abl Is a Critical Step in Selective Activation of Proapoptotic Genes in Response to DNA Damage». *Molecular Cell*

- Li, Jin, Zhongwu Li, Yaping Wu, Pengfei Diao, Wei Zhang, Yanling Wang, Jianrong Yang, e Jie Cheng. 2019. «Overexpression of LncRNA WWTR1-AS1 Associates with Tumor Aggressiveness and Unfavorable Survival in Head-Neck Squamous Cell Carcinoma». *Journal of Cellular Biochemistry*

- Li, Jin, Zhongwu Li, Yaping Wu, Yanling Wang, Dongmiao Wang, Wei Zhang, Hua Yuan, et al. 2019. «The Hippo Effector TAZ Promotes Cancer Stemness by Transcriptional Activation of SOX2 in Head Neck Squamous Cell Carcinoma». *Cell Death & Disease*

- Li, Jipeng, Jianhua Wang, Yin Chen, Shanfeng Li, Mingwei Jin, Huaying Wang, Zhe Chen, e Wanjun Yu. 2016. «LncRNA MALAT1 Exerts Oncogenic Functions in Lung Adenocarcinoma by Targeting MiR-204». *American Journal of Cancer Research*

- Li, Youjun, Hao Zhou, Fengzhi Li, Siew Wee Chan, Zhijie Lin, Zhiyi Wei, Zhou Yang, et al. 2015. «Angiomotin Binding-Induced Activation of Merlin/NF2 in the Hippo Pathway». *Cell Research*

- Li, Zhiqiang, Pedram Razavi, Qing Li, Weiyi Toy, Bo Liu, Christina Ping, Wilson Hsieh, et al. 2018. «Loss of the FAT1 Tumor Suppressor Promotes Resistance to CDK4/6 Inhibitors via the Hippo Pathway». *Cancer Cell*

- Lim, Sun Min, Min Hee Hong, e Hye Ryun Kim. 2020. «Immunotherapy for Non-Small Cell Lung Cancer: Current Landscape and Future Perspectives». *Immune Network*
- Lin, Chuwen, Erica Yao, Kuan Zhang, Xuan Jiang, Stacey Croll, Katherine Thompson-Peer, e Pao-Tien Chuang. 2017. «YAP Is Essential for Mechanical Force Production and Epithelial Cell Proliferation during Lung Branching Morphogenesis». *ELife*
- Lin, Kai-Ti, Slawomir Sloniowski, Douglas W. Ethell, e Iryna M. Ethell. 2008. «Ephrin-B2-Induced Cleavage of EphB2 Receptor Is Mediated by Matrix Metalloproteinases to Trigger Cell Repulsion». *The Journal of Biological Chemistry*
- Lin, Luping, Amit J. Sabnis, Elton Chan, Victor Olivas, Lindsay Cade, Evangelos Pazarentzos, Saurabh Asthana, et al. 2015. «The Hippo Effector YAP Promotes Resistance to RAF- and MEK-Targeted Cancer Therapies». *Nature Genetics*
- Liu, Chen-Ying, Zheng-Yu Zha, Xin Zhou, Heng Zhang, Wei Huang, Di Zhao, Tingting Li, et al. 2010. «The Hippo Tumor Pathway Promotes TAZ Degradation by Phosphorylating a Phosphodegron and Recruiting the SCF{beta}-TrCP E3 Ligase». *The Journal of Biological Chemistry*
- Liu, Jie, Juan Li, Pingping Li, Yina Jiang, He Chen, Ruiqi Wang, Fang Cao, e Peijun Liu. 2019. «DLG5 Suppresses Breast Cancer Stem Cell-like Characteristics to Restore Tamoxifen Sensitivity by Inhibiting TAZ Expression». *Journal of Cellular and Molecular Medicine*
- Liu, Li, James Greger, Hong Shi, Yuan Liu, Joel Greshock, Roland Annan, Wendy Halsey, Ganesh M. Sathe, Anne-Marie Martin, e Tona M. Gilmer. 2009. «Novel Mechanism of Lapatinib Resistance in HER2-Positive Breast Tumor Cells: Activation of AXL». *Cancer Research*
- Liu-Chittenden, Yi, Bo Huang, Joong Sup Shim, Qian Chen, Se-Jin Lee, Robert A. Anders, Jun O. Liu, e Duojia Pan. 2012. «Genetic and Pharmacological Disruption of the TEAD-YAP Complex Suppresses the Oncogenic Activity of YAP». *Genes & Development*
- Liu, X., Liu Z., Sun, M., Liu J., Wang Z. De W. The long non-coding RNA HOTAIR indicates a poor prognosis and promotes metastasis in non-small cell lung cancer. *BMC Cancer* **13**, 464 (2013).
- Lo Sardo, Federica, Sabrina Strano, e Giovanni Blandino. 2018. «YAP and TAZ in Lung Cancer: Oncogenic Role and Clinical Targeting». *Cancers*
- Lockwood, William W., Kreshnik Zejnullahu, James E. Bradner, e Harold Varmus. 2012. «Sensitivity of Human Lung Adenocarcinoma Cell Lines to Targeted Inhibition of BET Epigenetic Signaling Proteins». *Proceedings of the National Academy of Sciences of the United States of America*
- Lovén, Jakob, Heather A. Hoke, Charles Y. Lin, Ashley Lau, David A. Orlando, Christopher R. Vakoc, James E. Bradner, Tong Ihn Lee, e Richard A. Young. 2013a. «Selective Inhibition of Tumor Oncogenes by Disruption of Super-Enhancers». *Cell*
- Makita, Ryosuke, Yasunobu Uchijima, Koichi Nishiyama, Tomokazu Amano, Qin Chen, Takumi Takeuchi, Akihisa Mitani, et al. 2008. «Multiple Renal Cysts, Urinary Concentration Defects, and Pulmonary Emphysematous Changes in Mice Lacking TAZ». *American Journal of Physiology. Renal Physiology*
- Manzotti, Gloria, Alessia Ciarrocchi, e Valentina Sancisi. 2019. «Inhibition of BET Proteins and Histone Deacetylase (HDACs): Crossing Roads in Cancer Therapy». *Cancers*
- McCormick, F. 2015. «KRAS as a Therapeutic Target». *Clinical Cancer Research*
- Meng, Zhipeng, Toshiro Moroishi, e Kun-Liang Guan. 2016. «Mechanisms of Hippo Pathway Regulation». *Genes & Development*
- Mohseni, Morvarid, Jianlong Sun, Allison Lau, Stephen Curtis, Jeffrey Goldsmith, Victor L. Fox, Chongjuan Wei, et al. 2014. «A Genetic Screen Identifies an LKB1-MARK Signalling Axis Controlling the Hippo-YAP Pathway». *Nature Cell Biology*
- Morin-Kensicki, Elizabeth M., Brian N. Boone, Michael Howell, Jaclyn R. Stonebraker, Jeremy Teed, James G. Alb, Terry R. Magnuson, Wanda O'Neal, e Sharon L. Milgram. 2006. «Defects in Yolk Sac Vasculogenesis, Chorioallantoic Fusion, and Embryonic Axis Elongation in Mice with Targeted

Disruption of Yap65». *Molecular and Cellular Biology*

- Muranen, Taru, Laura M. Selfors, Julie Hwang, Lisa L. Gallegos, Jonathan L. Coloff, Carson C. Thoreen, Seong A. Kang, David M. Sabatini, Gordon B. Mills, e Joan S. Brugge. 2016. «ERK and P38 MAPK Activities Determine Sensitivity to PI3K/MTOR Inhibition via Regulation of MYC and YAP». *Cancer Research*
- Noguchi, Satoshi, Akira Saito, Masafumi Horie, Yu Mikami, Hiroshi I. Suzuki, Yasuyuki Morishita, Mitsuhiro Ohshima, et al. 2014. «An Integrative Analysis of the Tumorigenic Role of TAZ in Human Non-Small Cell Lung Cancer». *Clinical Cancer Research: An Official Journal of the American Association for Cancer Research*
- Noren, Nicole K., e Elena B. Pasquale. 2007. «Paradoxes of the EphB4 Receptor in Cancer». *Cancer Research*
- Oku, Yusuke, Naoyuki Nishiya, Takaaki Tazawa, Takaya Kobayashi, Nanami Umezawa, Yasuyo Sugawara, e Yoshimasa Uehara. 2018. «Augmentation of the Therapeutic Efficacy of WEE1 Kinase Inhibitor AZD1775 by Inhibiting the YAP-E2F1-DNA Damage Response Pathway Axis». *FEBS Open Bio*
- Park, Hyun Woo, Young Chul Kim, Bo Yu, Toshiro Moroishi, Jung-Soon Mo, Steven W. Plouffe, Zhipeng Meng, et al. 2015. «Alternative Wnt Signaling Activates YAP/TAZ». *Cell*
- Park, JinSeok, Deok-Ho Kim, Sagar R. Shah, Hong-Nam Kim, null Kshitiz, Peter Kim, Alfredo Quiñones-Hinojosa, e Andre Levchenko. 2019. «Switch-like Enhancement of Epithelial-Mesenchymal Transition by YAP through Feedback Regulation of WT1 and Rho-Family GTPases». *Nature Communications*
- Pasquale, Elena B. 2010. «Eph Receptors and Ephrins in Cancer: Bidirectional Signalling and Beyond». *Nature Reviews. Cancer*
- Patel, Mira C., Maxime Debrosse, Matthew Smith, Anup Dey, Walter Huynh, Naoyuki Sarai, Tom D. Heightman, Tomohiko Tamura, e Keiko Ozato. 2013. «BRD4 Coordinates Recruitment of Pause Release Factor P-TEFb and the Pausing Complex NELF/DSIF to Regulate Transcription Elongation of Interferon-Stimulated Genes». *Molecular and Cellular Biology*
- Patel, Sachin H., Fernando D. Camargo, e Dean Yimlamai. 2017. «Hippo Signaling in the Liver Regulates Organ Size, Cell Fate, and Carcinogenesis». *Gastroenterology*
- Peng, Fei, Ting-Ting Li, Kai-Li Wang, Guo-Qing Xiao, Ju-Hong Wang, Hai-Dong Zhao, Zhi-Jie Kang, et al. 2017. «H19/Let-7/LIN28 Reciprocal Negative Regulatory Circuit Promotes Breast Cancer Stem Cell Maintenance». *Cell Death & Disease*
- Peng, W.-X., P. Koirala, e Y.-Y. Mo. 2017. «LncRNA-Mediated Regulation of Cell Signaling in Cancer». *Oncogene* 36 (41): 5661–67. https://doi.org/10.1038/onc.2017.184.
- Plouffe, Steven W., Zhipeng Meng, Kimberly C. Lin, Brian Lin, Audrey W. Hong, Justin V. Chun, e Kun-Liang Guan. 2016. «Characterization of Hippo Pathway Components by Gene Inactivation». *Molecular Cell*
- Postel-Vinay, Sophie, Karin Herbschleb, Christophe Massard, Victoria Woodcock, Jean-Charles Soria, Annette O. Walter, Flavio Ewerton, et al. 2019a. «First-in-Human Phase I Study of the Bromodomain and Extraterminal Motif Inhibitor BAY 1238097: Emerging Pharmacokinetic/Pharmacodynamic Relationship and Early Termination Due to Unexpected Toxicity». *European Journal of Cancer (Oxford, England: 1990)*
- Qin, Zhiming, Xiangru Zheng, e Yu Fang. 2019. «Long Noncoding RNA TMPO-AS1 Promotes Progression of Non-Small Cell Lung Cancer through Regulating Its Natural Antisense Transcript TMPO». *Biochemical and Biophysical Research Communications*
- Reggiani, Francesca, Giulia Gobbi, Alessia Ciarrocchi, Davide Carlo Ambrosetti, e Valentina Sancisi. 2020. «Multiple Roles and Context-Specific Mechanisms Underlying YAP and TAZ-Mediated Resistance to Anti-Cancer Therapy». *Biochimica Et Biophysica Acta. Reviews on Cancer*
- Reggiani, Francesca, Giulia Gobbi, Alessia Ciarrocchi, e Valentina Sancisi. 2020. «YAP and TAZ Are

Not Identical Twins». *Trends in Biochemical Sciences*

- Ren, Aixia, Guijun Yan, Bei You, e Jianxin Sun. 2008. «Down-Regulation of Mammalian Sterile 20-like Kinase 1 by Heat Shock Protein 70 Mediates Cisplatin Resistance in Prostate Cancer Cells». *Cancer Research*

- Rinn, John L., e Howard Y. Chang. 2012. «Genome Regulation by Long Noncoding RNAs». *Annual Review of Biochemistry*

- Roberts, Thomas C., Usue Etxaniz, Alessandra Dall'Agnese, Shwu-Yuan Wu, Cheng-Ming Chiang, Paul E. Brennan, Matthew J. A. Wood, e Pier Lorenzo Puri. 2017. «BRD3 and BRD4 BET Bromodomain Proteins Differentially Regulate Skeletal Myogenesis». *Scientific Reports*

- Rosenbluh, Joseph, Deepak Nijhawan, Andrew G. Cox, Xingnan Li, James T. Neal, Eric J. Schafer, Travis I. Zack, et al. 2012. «β-Catenin-Driven Cancers Require a YAP1 Transcriptional Complex for Survival and Tumorigenesis». *Cell*

- Roth, Anna, e Sven Diederichs. 2016. «Long Noncoding RNAs in Lung Cancer». *Current Topics in Microbiology and Immunology*

- Rotow, Julia, e Trever G. Bivona. 2017. «Understanding and Targeting Resistance Mechanisms in NSCLC». *Nature Reviews Cancer*

- Sancisi, Valentina, Gloria Manzotti, Mila Gugnoni, Teresa Rossi, Greta Gandolfi, Giulia Gobbi, Federica Torricelli, et al. 2017. «RUNX2 Expression in Thyroid and Breast Cancer Requires the Cooperation of Three Non-Redundant Enhancers under the Control of BRD4 and c-JUN». *Nucleic Acids Research*

- Sanjana NE, Shalem O, Zhang F. 2014 «Improved vectors and genome-wide libraries for CRISPR screening. *Nat Methods*»

- Sato, Shinya, Suhas Vasaikar, Adel Eskaros, Young Kim, James S. Lewis, Bing Zhang, Andries Zijlstra, e Alissa M. Weaver. 2019. «EPHB2 Carried on Small Extracellular Vesicles Induces Tumor Angiogenesis via Activation of Ephrin Reverse Signaling». *JCI Insight*

- Shao, Diane D., Wen Xue, Elsa B. Krall, Arjun Bhutkar, Federica Piccioni, Xiaoxing Wang, Anna C. Schinzel, et al. 2014. «KRAS and YAP1 Converge to Regulate EMT and Tumor Survival». *Cell*

- Shen, Liqin, Lei Chen, Yongsheng Wang, Xiaochun Jiang, Hongping Xia, e Zhixiang Zhuang. 2015. «Long Noncoding RNA MALAT1 Promotes Brain Metastasis by Inducing Epithelial-Mesenchymal Transition in Lung Cancer». *Journal of Neuro-Oncology*

- Shi, Rongxing, Zichen Jiao, Ao Yu, e Tao Wang. 2019. «Long Noncoding Antisense RNA FAM83A-AS1 Promotes Lung Cancer Cell Progression by Increasing FAM83A». *Journal of Cellular Biochemistry*

- Shimamura, Takeshi, Zhao Chen, Margaret Soucheray, Julian Carretero, Eiki Kikuchi, Jeremy H. Tchaicha, Yandi Gao, et al. 2013. «Efficacy of BET Bromodomain Inhibition in Kras-Mutant Non-Small Cell Lung Cancer». *Clinical Cancer Research: An Official Journal of the American Association for Cancer Research*

- Solanas, Guiomar, e Eduard Batlle. 2011. «Control of Cell Adhesion and Compartmentalization in the Intestinal Epithelium». *Experimental Cell Research*

- S. Song, *et al.* The Hippo coactivator YAP1 mediates EGFR overexpression and confers Chemoresistance in esophageal Cancer Clin. Cancer Res, 2015

- Sorrentino, Giovanni, Naomi Ruggeri, Valeria Specchia, Michelangelo Cordenonsi, Miguel Mano, Sirio Dupont, Andrea Manfrin 2014. «Metabolic Control of YAP and TAZ by the Mevalonate Pathway». *Nature Cell Biology*

- Soudeh Ghafouri Farda, Sepideh Dashtia, Molood Farsib, Bashdar Mahmud Hussenc, Mohammad Taheri, 2021. « A review on the role of oncogenic lncRNA OIP5-AS1 in human malignancies». *Biomedicine & Pharmacotherapy*

- St Laurent, Georges, Claes Wahlestedt, e Philipp Kapranov. 2015. «The Landscape of Long Noncoding RNA Classification». *Trends in Genetics: TIG*

- Su, Li-li, Wei-xia Ma, Jian-feng Yuan, Yang Shao, Wei Xiao, e Shu-juan Jiang. 2012. «Expression of Yes-Associated Protein in Non-Small Cell Lung Cancer and Its Relationship with Clinical Pathological Factors». *Chinese Medical Journal*
- Surawska, Hanna, Patrick C. Ma, e Ravi Salgia. 2004. «The Role of Ephrins and Eph Receptors in Cancer». *Cytokine & Growth Factor Reviews*
- Sutherland, Kate D., e Anton Berns. 2010. «Cell of Origin of Lung Cancer». *Molecular Oncology*
- Tang, Yi, GaoMing Xiao, YueJun Chen, e Yu Deng. 2018. «LncRNA MALAT1 Promotes Migration and Invasion of Non-Small-Cell Lung Cancer by Targeting MiR-206 and Activating Akt/MTOR Signaling». *Anti-Cancer Drugs*
- Teixeira Loiola de Alencar, Viviane, Maria Nirvana Formiga, e Vladmir Cláudio Cordeiro de Lima. 2020. «Inherited lung cancer: a review». *ecancermedicalscience*
- Ulitsky, Igor. 2016. «Evolution to the Rescue: Using Comparative Genomics to Understand Long Non-Coding RNAs». *Nature Reviews. Genetics*
- Vail, Mary E., Carmel Murone, April Tan, Linda Hii, Degu Abebe, Peter W. Janes, Fook-Thean Lee, et al. 2014. «Targeting EphA3 Inhibits Cancer Growth by Disrupting the Tumor Stromal Microenvironment». *Cancer Research*
- Varelas, Xaralabos. 2014. «The Hippo Pathway Effectors TAZ and YAP in Development, Homeostasis and Disease». *Development (Cambridge, England)*
- Varelas, Xaralabos, Rui Sakuma, Payman Samavarchi-Tehrani, Raheem Peerani, Balaji M. Rao, Joanna Dembowy, Michael B. Yaffe, Peter W. Zandstra, e Jeffrey L. Wrana. 2008. «TAZ Controls Smad Nucleocytoplasmic Shuttling and Regulates Human Embryonic Stem-Cell Self-Renewal». *Nature Cell Biology*
- Varella-Garcia, Marileila. 2010. «Chromosomal and Genomic Changes in Lung Cancer». *Cell Adhesion & Migration*
- Vassilev, A., K. J. Kaneko, H. Shu, Y. Zhao, e M. L. DePamphilis. 2001. «TEAD/TEF Transcription Factors Utilize the Activation Domain of YAP65, a Src/Yes-Associated Protein Localized in the Cytoplasm». *Genes & Development*
- Vitiello, Marianna, Andrea Tuccoli, e Laura Poliseno. 2015. «Long Non-Coding RNAs in Cancer: Implications for Personalized Therapy». *Cellular Oncology (Dordrecht)*
- Wan, Li, Ming Sun, Guo-Jian Liu, Chen-Chen Wei, Er-Bao Zhang, Rong Kong, Tong-Peng Xu, Ming-De Huang, e Zhao-Xia Wang. 2016. «Long Noncoding RNA PVT1 Promotes Non-Small Cell Lung Cancer Cell Proliferation through Epigenetically Regulating LATS2 Expression». *Molecular Cancer Therapeutics*
- Wang, Chao, Xiaoyong Zhu, Weiwei Feng, Yinhua Yu, Kangjin Jeong, Wei Guo, Yiling Lu, e Gordon B. Mills. 2016. «Verteporfin Inhibits YAP Function through Up-Regulating 14-3-3σ Sequestering YAP in the Cytoplasm». *American Journal of Cancer Research*
- Wang, Fang, Yu Zhu, Yan Huang, Sarah McAvoy, William B. Johnson, Tak Hong Cheung, Tony Kwok Hung Chung, et al. 2005. «Transcriptional Repression of WEE1 by Kruppel-like Factor 2 Is Involved in DNA Damage-Induced Apoptosis». *Oncogene*
- Wang, F. Fang Wang[1], Yu Zhu, Yan Huang, Sarah McAvoy, William B Johnson, Tak Hong Cheung, Tony Kwok Hung Chung, Keith Wing Kit Lo, So Fan Yim, May M Y Yu, Hextan Y S Ngan, Yick Fu Wong, David I Smith Transcriptional repression of WEE1 by Kruppel-like factor 2 is involved in DNA damage-induced apoptosis. *Oncogene*
- Wang, Qi, Ningning Cheng, Xuefei Li, Hui Pan, Chunyu Li, Shengxiang Ren, Chunxia Su, et al. 2017. «Correlation of Long Non-Coding RNA H19 Expression with Cisplatin-Resistance and Clinical Outcome in Lung Adenocarcinoma». *Oncotarget*
- Wang Y, Dong QZ, Zhang QF, Li ZX, Wang EH, Qiu XS. Overexpression of yes-associated protein contributes to progression and poor prognosis of non-small-cell lung cancer. Cancer Sci.

- Wilkinson, David G. 2003. «How Attraction Turns to Repulsion». *Nature Cell Biology*
- Wong, Martin C. S., Xiang Qian Lao, Kin-Fai Ho, William B. Goggins, e Shelly L. A. Tse. 2017. «Incidence and Mortality of Lung Cancer: Global Trends and Association with Socioeconomic Status». *Scientific Reports*
- Wu, Dapeng, Yong Li, Huixiang Zhang, e Xigang Hu. 2017. «Knockdown of Lncrna PVT1 Enhances Radiosensitivity in Non-Small Cell Lung Cancer by Sponging Mir-195». *Cellular Physiology and Biochemistry: International Journal of Experimental Cellular Physiology, Biochemistry, and Pharmacology*
- Wu, Ke-Feng, Wei-Cheng Liang, Lu Feng, Jian-Xin Pang, Mary Miu-Yee Waye, Jin-Fang Zhang, e Wei-Ming Fu. 2017. «H19 Mediates Methotrexate Resistance in Colorectal Cancer through Activating Wnt/β-Catenin Pathway». *Experimental Cell Research*
- Wu, Shian, Jianbin Huang, Jixin Dong, e Duojia Pan. 2003. «Hippo Encodes a Ste-20 Family Protein Kinase That Restricts Cell Proliferation and Promotes Apoptosis in Conjunction with Salvador and Warts». *Cell*
- Wu, Shwu-Yuan, e Cheng-Ming Chiang. 2007. «The Double Bromodomain-Containing Chromatin Adaptor Brd4 and Transcriptional Regulation». *The Journal of Biological Chemistry*
- Xi, Hong-Qing, Xiao-Song Wu, Bo Wei, e Lin Chen. 2012. «Eph Receptors and Ephrins as Targets for Cancer Therapy». *Journal of Cellular and Molecular Medicine*
- Xie M, Zhang L, He CS, Hou JH, Lin SX, Hu ZH, et al. Prognostic significance of TAZ expression in resected non-small cell lung cancer. J Thorac Oncol.
- Xu, Michelle Z., Tzy-Jyun Yao, Nikki P. Y. Lee, Irene O. L. Ng, Yuk-Tat Chan, Lars Zender, Scott W. Lowe, Ronnie T. P. Poon, e John M. Luk. 2009. «Yes-Associated Protein Is an Independent Prognostic Marker in Hepatocellular Carcinoma». *Cancer*
- Xu, T.-P., X.-X. Liu, R. Xia, L. Yin, R. Kong, W.-M. Chen, M.-D. Huang, e Y.-Q. Shu. 2015. «SP1-Induced Upregulation of the Long Noncoding RNA TINCR Regulates Cell Proliferation and Apoptosis by Affecting KLF2 MRNA Stability in Gastric Cancer». *Oncogene*
- Xu, Wei, Yunyan Wei, Yue Li, Yuan Yin, Weiwei Yuan, Yan Yang, Weihong Zhao, e Jianqing Wu. 2017. «TAZ Inhibition Restores Sensitivity of Cisplatin via AKT/MTOR Signaling in Lung Adenocarcinoma». *Oncology Reports*
- Xu, Wei, Yunyan Wei, Shuangshuang Wu, Yun Wang, Zhen Wang, Yu Sun, Steven Y. Cheng, e Jianqing Wu. 2015. «Up-Regulation of the Hippo Pathway Effector TAZ Renders Lung Adenocarcinoma Cells Harboring EGFR-T790M Mutation Resistant to Gefitinib». *Cell & Bioscience*
- Xu, Yali, e Christopher R. Vakoc. 2017. «Targeting Cancer Cells with BET Bromodomain Inhibitors». *Cold Spring Harbor Perspectives in Medicine*
- Yin, Feng, Jianzhong Yu, Yonggang Zheng, Qian Chen, Nailing Zhang, e Duojia Pan. 2013. «Spatial Organization of Hippo Signaling at the Plasma Membrane Mediated by the Tumor Suppressor Merlin/NF2». *Cell*
- Yuedi, Dai, Liu Houbao, Lu Pinxiang, Wang Hui, Tao Min, e Zhang Dexiang. 2020. «KLF2 Induces the Senescence of Pancreatic Cancer Cells by Cooperating with FOXO4 to Upregulate P21». *Experimental Cell Research*
- Yunlei Bai and Sheng Li, 2019. «Long noncoding RNA OIP5-AS1 aggravates cell proliferation, migration in gastric cancer by epigenetically silencing NLRP6 expression via binding EZH2». *Journal of Cellular Biochemistry*
- Zaidi, Sayyed K., Andrew J. Sullivan, Ricardo Medina, Yoshiaki Ito, Andre J. van Wijnen, Janet L. Stein, Jane B. Lian, e Gary S. Stein. 2004. «Tyrosine Phosphorylation Controls Runx2-Mediated Subnuclear Targeting of YAP to Repress Transcription». *The EMBO Journal*
- Zanconato, Francesca, Giusy Battilana, Mattia Forcato, Letizia Filippi, Luca Azzolin, Andrea Manfrin, Erika Quaranta, et al. 2018. «Transcriptional Addiction in Cancer Cells Is Mediated by YAP/TAZ

through BRD4». *Nature Medicine*

- Zanconato, Francesca, Michelangelo Cordenonsi, e Stefano Piccolo. 2016. «YAP/TAZ at the Roots of Cancer». *Cancer Cell*
- Zanconato, Francesca, Mattia Forcato, Giusy Battilana, Luca Azzolin, Erika Quaranta, Beatrice Bodega, Antonio Rosato, Silvio Bicciato, Michelangelo Cordenonsi, e Stefano Piccolo. 2015. «Genome-Wide Association between YAP/TAZ/TEAD and AP-1 at Enhancers Drives Oncogenic Growth». *Nature Cell Biology*
- Zhan, Ting, Xiaodong Huang, Xia Tian, Xiaoli Chen, Yu Ding, Hesheng Luo, e Yadong Zhang. 2018. «Downregulation of MicroRNA-455-3p Links to Proliferation and Drug Resistance of Pancreatic Cancer Cells via Targeting TAZ». *Molecular Therapy. Nucleic Acids*
- Zhang, Chun-Lin, Kun-Peng Zhu, e Xiao-Long Ma. 2017. «Antisense LncRNA FOXC2-AS1 Promotes Doxorubicin Resistance in Osteosarcoma by Increasing the Expression of FOXC2». *Cancer Letters*
- Zhang, Peichen, Qiantong Dong, Hua Zhu, Shi Li, Lingyan Shi, e Xiangjian Chen. 2019. «Long Non-Coding Antisense RNA GAS6-AS1 Supports Gastric Cancer Progression via Increasing GAS6 Expression». *Gene*
- Zhang, Yi, e Liling Tang. 2018. «The Application of LncRNAs in Cancer Treatment and Diagnosis». *Recent Patents on Anti-Cancer Drug Discovery*
- Zhao, Bin, Li Li, Karen Tumaneng, Cun-Yu Wang, e Kun-Liang Guan. 2010. «A Coordinated Phosphorylation by Lats and CK1 Regulates YAP Stability through SCF(Beta-TRCP)». *Genes & Development*
- Zhao, Chen, Aili Wang, Funian Lu, Hongxia Chen, Pin Fu, Xianda Zhao, e Honglei Chen. 2017. «Overexpression of Junctional Adhesion Molecule-A and EphB2 Predicts Poor Survival in Lung Adenocarcinoma Patients». *Tumour Biology: The Journal of the International Society for Oncodevelopmental Biology and Medicine*
- Zhao, Yue, Qi Liu, Pankaj Acharya, Kristy R. Stengel, Quanhu Sheng, Xiaofan Zhou, Hojoong Kwak, et al. 2016. «High-Resolution Mapping of RNA Polymerases Identifies Mechanisms of Sensitivity and Resistance to BET Inhibitors in t(8;21) AML». *Cell Reports* 16
- Zhao, Yulei, Prem Khanal, Paul Savage, Yi-Min She, Terry D. Cyr, e Xiaolong Yang. 2014. «YAP-Induced Resistance of Cancer Cells to Antitubulin Drugs Is Modulated by a Hippo-Independent Pathway». *Cancer Research*
- Zhao, Yulei, e Xiaolong Yang. 2015a. «Regulation of Sensitivity of Tumor Cells to Antitubulin Drugs by Cdk1-TAZ Signalling». *Oncotarget*
- Zheng, Yonggang, e Duojia Pan. 2019. «The Hippo Signaling Pathway in Development and Disease». *Developmental Cell*
- Zhou Zheng, Taishan Hu, Zhiheng Xu, Zhaohu Lin, Zhisen Zhang, Teng Feng, Liangcheng Zhu, et al. 2015. «Targeting Hippo Pathway by Specific Interruption of YAP-TEAD Interaction Using Cyclic YAP-like Peptides». *FASEB Journal: Official Publication of the Federation of American Societies for Experimental Biology*
- Zimmer, Manuel, Amparo Palmer, Jenny Köhler, e Rüdiger Klein. 2003. «EphB-EphrinB Bi-Directional Endocytosis Terminates Adhesion Allowing Contact Mediated Repulsion». *Nature Cell Biology*
- Zito Marino, Federica, Roberto Bianco, Marina Accardo, Andrea Ronchi, Immacolata Cozzolino, Floriana Morgillo, Giulio Rossi, e Renato Franco. 2019. «Molecular Heterogeneity in Lung Cancer: From Mechanisms of Origin to Clinical Implications». *International Journal of Medical Sciences*